1983

A single equivalent representation of a group of induction motors using a reduced order model for power system studies

Farzan Roohparvar
Iowa State University

INFORMATION TO USERS

This reproduction was made from a copy of a document sent to us for microfilming. While the most advanced technology has been used to photograph and reproduce this document, the quality of the reproduction is heavily dependent upon the quality of the material submitted.

The following explanation of techniques is provided to help clarify markings or notations which may appear on this reproduction.

1. The sign or "target" for pages apparently lacking from the document photographed is "Missing Page(s)". If it was possible to obtain the missing page(s) or section, they are spliced into the film along with adjacent pages. This may have necessitated cutting through an image and duplicating adjacent pages to assure complete continuity.

2. When an image on the film is obliterated with a round black mark, it is an indication of either blurred copy because of movement during exposure, duplicate copy, or copyrighted materials that should not have been filmed. For blurred pages, a good image of the page can be found in the adjacent frame. If copyrighted materials were deleted, a target note will appear listing the pages in the adjacent frame.

3. When a map, drawing or chart, etc., is part of the material being photographed, a definite method of "sectioning" the material has been followed. It is customary to begin filming at the upper left hand corner of a large sheet and to continue from left to right in equal sections with small overlaps. If necessary, sectioning is continued again–beginning below the first row and continuing on until complete.

4. For illustrations that cannot be satisfactorily reproduced by xerographic means, photographic prints can be purchased at additional cost and inserted into your xerographic copy. These prints are available upon request from the Dissertations Customer Services Department.

5. Some pages in any document may have indistinct print. In all cases the best available copy has been filmed.

University Microfilms International
300 N. Zeeb Road
Ann Arbor, MI 48106

Roohparvar, Farzan

A SINGLE EQUIVALENT REPRESENTATION OF A GROUP OF INDUCTION MOTORS USING A REDUCED ORDER MODEL FOR POWER SYSTEM STUDIES

Iowa State University PH.D. 1983

PLEASE NOTE:

In all cases this material has been filmed in the best possible way from the available copy. Problems encountered with this document have been identified here with a check mark ✓.

1. Glossy photographs or pages _____
2. Colored illustrations, paper or print _____
3. Photographs with dark background _____
4. Illustrations are poor copy _____
5. Pages with black marks, not original copy ✓
6. Print shows through as there is text on both sides of page _____
7. Indistinct, broken or small print on several pages ✓
8. Print exceeds margin requirements _____
9. Tightly bound copy with print lost in spine _____
10. Computer printout pages with indistinct print ✓
11. Page(s) _____ lacking when material received, and not available from school or author.
12. Page(s) _____ seem to be missing in numbering only as text follows.
13. Two pages numbered _____. Text follows.
14. Curling and wrinkled pages ✓
15. Other Dissertation contains pages with print at a slant, filmed as received.

A single equivalent representation of a group of induction motors using a reduced order model for power system studies

by

Farzan Roohparvar

A Dissertation Submitted to the
Graduate Faculty in Partial Fulfillment of the
Requirements for the Degree of
DOCTOR OF PHILOSOPHY

Department: Electrical Engineering
Major: Electric Power

Approved:

Signature was redacted for privacy.

In Charge of Major Work

Signature was redacted for privacy.

For the Major Department

Signature was redacted for privacy.

For the Graduate College

Iowa State University
Ames, Iowa

1983

TABLE OF CONTENTS

CHAPTER I. INTRODUCTION

General Load Modeling

Two of the major functions involved in electric utilities are system planning and operation. These functions require extensive use of simulation tools such as loadflow, faulted system analysis, contingency analysis and dynamic stability. One of the elements that is required in the realistic simulation of power systems is the load. The characteristics of the load models used in these studies have been shown to significantly effect the behavior of the power systems [6]. For these system simulations to accurately reflect the actual power system, the proper load representation becomes very important. In order to represent the power system load, there have been a variety of load models suggested [6, 13]. One may divide power system loads into two classes: (1) static, and (2) rotating.

Static load models

The load representation in typical system studies is a static load model where the load is represented as constant MVA, constant current, constant impedance or some combination of the three [6]. These static models may be expressed by equations 1.1 and 1.2:

$$P(V) = P_o(aV^2 + bV + c) \tag{1.1}$$

$$Q(V) = Q_o(dV^2 + eV + g) \tag{1.2}$$

where constants "a" and "d" specify the per unit of real and reactive load that behaves as constant impedance, and constants "b" and "e"

specify the per unit of real and reactive load that behaves as constant current, and constant "c" and "g" specify the per unit of real and reactive load that behaves as constant MVA.

Rotating load models

Arthur D. Little [10] has analyzed and classified load in the United States. This study has shown that induction motors constitute over 66% of the total system load. This contribution to the load is large enough that one should examine the dynamic effects of induction motors on the various types of simulation studies.

Individual induction machines can be represented in a number of ways including:

(1) A single impedance;

(2) An equivalent steady-state circuit where the inertia transients are considered; and

(3) Full representation by the o.d.q. model where stator and rotor electrical transients and inertia transients are included.

All of these models have been used to represent a single induction machine in one or more types of power system studies.

Multi-Machine Starting of Rotating Loads

System studies have shown that modern network configurations are encountered in which the dynamic behavior of large industrial loads has a pronounced influence on transient studies [3].

Industrial plants typically have controlled and uncontrolled types

of loads. Controlled induction motor loads are those remotely controlled by an operator or which have a presequenced schedule of start-up. Uncontrolled induction motor loads are those with automatic restarters, motors that operate independently of the system voltage with limited or no built-in protection devices, or those that have an operator assigned to each motor.

A system designer tries to avoid simultaneous starting of a large number of induction motors either by remote control or by sequencing the motor start-up procedure. Starting motors one by one would be impractical in an industry large enough to warrant automatic starting control of induction motor loads. Therefore, a sequential starting procedure of small groups of motors is adopted. In these cases, the next group of motors is usually started before the previously started group of motors reaches normal steady-state conditions.

Uncontrolled motor loads include unintentional restarts that can occur where the motors' switching devices are independent of the system voltage, e.g. electrically operated water or oil pumps. Even though the industrial load may be temporarily disconnected from the power source, the motors are still electrically connected. Consequently, when the power is restored, a large number of motors will begin to start up simultaneously.

Another type of uncontrolled load is due to industrial plants' need for continuity of process. When a power outage occurs with a duration less than a preset length of time, the automatic restarters will start all motors that were in operation prior to the power outage. This is a

typical mode of operation in refineries.

One more type of uncontrolled induction motor load would be found in industries such as foundries or auto industries where a large number of induction motors are assigned to individual operators. These induction motors are switched on and off intermittently due to the nature of the work. While numerous motors are operating at normal condition, a random number of additional motors are being switched on and off.

No matter what type of motor load is used in industry (controlled or uncontrolled), multi-machine starting is one of the load features. A power system analysis for the purpose of voltage dip studies, design of industrial distribution systems, contingency analysis, or stability studies should examine the effect of multi-machine starting.

Review of Existing Induction Motor Load Models

The problem of induction machine modeling has been studied over many years starting with Stanley [18] and Maginnis and Schultz [11]. These researchers studied the interactive effects of machine loads and the power system. Stanley [18] and Krause and Thomas [9] have developed a number of equations for studying the steady state and transient behavior of induction machines. Brereton et al. [5] developed a method of representing an induction motor load for power system stability studies. In Sastry and Burridge's work [17], the performance of an induction machine predicted by a reduced order model is discussed. These authors made a comparison of the linearized version of the detailed and reduced order model for dynamic stability studies and showed the effects of ignoring stator electrical transients. Berg and

Subramaniam [4] discussed modeling of induction motor loads for the purpose of power system transient studies. A number of motor models were discussed and are presented in the following paragraphs.

Single machine two axis model

The assumptions made for the two axis model include neglecting core losses, saturation, and skin effects. The performance equations for three-phase squirrel cage motors may be expressed in terms of voltages and currents, rotor position θ, winding parameters, and time [18].

$$V_{abc}^{sr} = Z_{abc}^{sr}(\theta,p)\ I_{abc}^{sr} \tag{1.3}$$

where $p = d/t$, superscripts s and r denote stator and rotor, subscripts a, b and c denote the three phases.

For solution purposes, it is usually convenient to transform the variables to a two-phase equivalent. The orthogonal axes rotate at synchronous speed ω with respect to the stator and are designated d and q, where d is direct and q is quadrature. The following set of voltage-current relations results.

$$\begin{bmatrix} v_d^s \\ v_q^s \\ 0 \\ 0 \end{bmatrix} = \begin{bmatrix} R^s + L^s p & -\omega L^s & Mp & -\omega M \\ \omega L^s & R^s + L^s p & \omega M & Mp \\ Mp & -Ms\omega & R^r + L^r p & -L^r s\omega \\ Ms\omega & Mp & L^r s\omega & R^r + L^r p \end{bmatrix} \begin{bmatrix} i_d^s \\ i_q^s \\ i_d^r \\ i_q^r \end{bmatrix} \tag{1.4}$$

where R^s, R^r and L^s, L^r are the resistances and self inductances of the equivalent two-phase windings of the stator and rotor, M is the maximum mutual inductance between the stator and rotor windings in the two-phase

equivalent, ω is the angular frequency of the supply voltage, and s is per unit slip given by

$$s = 1 - \omega^{-1} p\theta \quad . \tag{1.5}$$

Assuming symmetrical, balanced supply voltages of amplitude V_m, angular frequency ω and, for the reference phase, an arbitrary phase angle ϕ, the power invariant transformation yields

$$v_d^s = \sqrt{\frac{3}{2}}\, V_m \cos\phi \quad ; \tag{1.6a}$$

$$v_q^s = \sqrt{\frac{3}{2}}\, V_m \sin\phi \tag{1.6b}$$

$$p\begin{bmatrix} i_d^s \\ i_q^s \\ i_d^r \\ i_q^r \end{bmatrix} = \frac{1}{\sigma}\begin{bmatrix} v_d^s/L^s \\ v_q^s/L^s \\ -K^2 v_d^s/M \\ -K^2 v_q^s/M \end{bmatrix} + \begin{bmatrix} -R^s/L^s & -\omega(\sigma+K^2(1-s)) & K^2R^r/M & \omega(1-s)M/L^s \\ -\omega(\sigma+K^2(1-s)) & -R^s/L^s & -\omega(1-s)M/L^s & K^2R^r/M \\ K^2R^s/M & -\omega(1-s)M/L^r & -R^r/L^r & \omega(\sigma-1+s) \\ \omega(1-s)M/L^r & K^2R^s/M & -\omega(\sigma-1+s) & -R^r/L^r \end{bmatrix}\begin{bmatrix} i_d^s \\ i_q^s \\ i_d^r \\ i_q^r \end{bmatrix} \tag{1.7}$$

ϕ can be set to zero, in which case v_d^s equals the line-to-line rms voltage, appearing as a dc quantity, and all other input voltage vector elements are zero.

The current derivatives required for numerical solution are obtained from equation 1.4 and are expressed by equation 1.7, where

$$K = M(L^s L^r)^{-1/2} \quad ; \tag{1.8a}$$

$$\sigma = 1 - K^2 \quad . \tag{1.8}$$

The developed torque can be written as

$$T_e = M[i_q^s i_d^r - i_d^r i_q^s] \tag{1.9}$$

and the shaft load torque is assumed to be of the form

$$T_m = T_o \, \omega_m^{\alpha} \tag{1.10}$$

where ω_m is the mechanical speed and α is a constant depending on the type of load connected. With inertia J, the equation of motion becomes

$$\frac{d\omega_m}{dt} = \frac{1}{J} (T_e - T_m) \quad . \tag{1.11}$$

Input active and reactive power to the motor can also be expressed conveniently in terms of the transformed variables as follows:

$$P = v_d^s i_d^s + v_q^s i_q^s \tag{1.12}$$

$$Q = v_q^s i_d^s - v_d^s i_q^s \quad . \tag{1.13}$$

In this method, all the above equations are evaluated numerically to determine P and Q, the total input power to the motor.

The transformation of a, b, c variables to o.d.q. variables is given in Appendix D.

Single induction machine model including mechanical and rotor electrical transients only

In this model, stator electrical transients are neglected [5]. Electrical rotor transients are governed by

$$\frac{de'}{dt} = \frac{1}{T'_{do}} (e'-j(x-x')i)+je' \frac{d\theta}{dt} s \qquad (1.14)$$

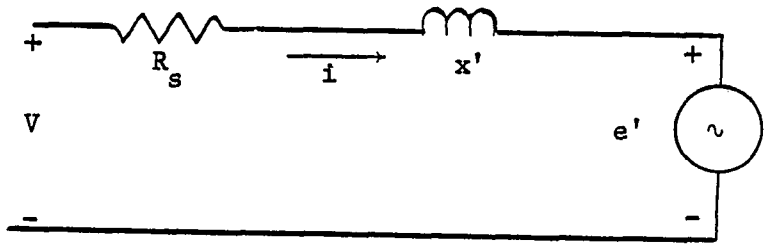

Figure 1.1. Induction machine model including rotor electrical transient

$$i = \frac{V - e'}{R_s+jx'} \qquad (1.15)$$

$$\frac{ds}{dt} = \frac{1}{2H} T_e \qquad (1.16)$$

$$T_e = \text{Real}(e'i^*) \qquad (1.17)$$

where:

i = phasor current

i^* = current conjugate

V = supply voltage

e' = complex internal emf, proportional to rotor flux linkages

x = input reactance at zero slip

x' = input reactance at 1 per unit slip

T'_{do} = rotor time constant, stator open circuit

θ = electrical angle of phase 1 of rotor referred to d axis rotating at synchronous speed.

Single machine model including mechanical transients only

This model uses conventional steady-state circuit equations with phasor representation of electrical variables along with the equation of mechanical motion.

The model has been utilized for the development of multi-machine models by Berg and Subramaniam [4].

Multi-machine modeling

Representing a group of induction motors by a single equivalent model was suggested by Akhtar [2]. His model is restricted to a relatively narrow operating range near full load speed due to the assumption of a fixed linear torque speed characteristic. Also, he assumed that all motors in the group run at the same p.u. speed.

Abdel-Hakim and Berg [1] derived a simple equivalent of a group of motors, neglecting stator copper losses. The equivalent circuit was used as the basis for the model. The motors' electrical transients are neglected. This model is also useful for only the running condition and not for starting.

More recently, Iliceto and Capasso [8] have studied the modeling of a number of induction machines when the supply voltage undergoes voltage dips and swings after the occurrence of system faults. In Iliceto and Capasso's model, the stator electrical transients were neglected. They

noted that two parameters can have a marked influence on the dynamic behavior of large induction motors, the inertia constant H, and the time constant of the rotor with open-circuited stator (T'_{do}). They developed a statistical approach to calculate the weighted mean of all time constants.

$$T'_{doeq} = \frac{\sum_{i=1}^{n} T'_{do,i} \times P_i}{\sum_{i=1}^{n} P_i} \tag{1.18}$$

where P_i is the individual motor power rating.

Their results showed such an equivalent model is acceptable only for motor groups containing motors whose inertia constant H does not differ widely in the group under study. For this condition, the dynamic equivalents were shown to have errors in the following ranges for different power ratings:

(i) Up to 20-25% error when the power rating of the largest motor is less than twice the rating of the smaller one.

(ii) From 25% to 45% error for power rating ratios between 2 and 10.

The results were even less favorable for motor groups having a common value of T'_{do} and different values of H. It was found that in such cases, the simulation of the complete group by a single "equivalent machine" is not proper.

The inertia constant to be assigned to the equivalent is calculated as a weighted mean.

$$H_{eq} = \frac{\sum_{i=1}^{n} H_i P_i}{\sum_{i=1}^{n} P_i} \tag{1.19}$$

The remaining parameters of the dynamic equivalents R_{seq}, X_{eq}, and X'_{eq} are calculated as weighted means in a like manner to T'_{doeq} and H_{eq}

where

R_{seq} = equivalent stator winding resistance;

X_{eq} = equivalent reactance at synchronous speed; and

X'_{eq} = equivalent reactance at blocked rotor.

This model is intended for motors in the running state and could not be applied directly to the condition of starting induction motors.

Summary of Literature Review

There have been a number of induction machine representations suggested. Most of the models are used to represent a single induction machine such as those suggested by Brereton et al. [5], Maginnis and Schultz [11], Krause and Thomas [9], and Stanley [18]. Early in the art, Brereton et al. [5] developed various simplified models for induction machines for use in transient stability studies and showed the limitation of some of the simplified models. Equations derived by Stanley [17] and Krause and Thomas [9] are widely used for studying steady-state and transient behavior of induction machines.

Another portion of induction machine modeling encompasses representing a group of induction motors. Akhtar [2] proposed a model using the

assumptions that the machines are all running at the same p.u. speed and that they have a linear torque speed relationship. Another method of grouping induction motors was proposed and formulated by Abdel-Hakim and Berg [1] for calculating the equivalent of a number of induction machines supplied from a common bus. In this method, all machines are represented by their equivalent circuit and the equation of mechanical motion. This model is applicable to running conditions only.

Another method of obtaining a single unit equivalent was developed by Iliceto and Capasso [8]. They used a third order model (which includes the rotor electrical and mechanical transients of the induction machines) in deriving the equivalent. The open circuit time constant, T'_{do}, and the inertia constant, H, of the rotor and connected mechanical load are important parameters which greatly affect the dynamic response of any motor. In their work, all the equivalent parameters of the single unit model are given by the weighted averages of all the individual machine parameters. The weighting factors are the motor power ratings. These authors found that not all motors could be combined into one equivalent, but only those satisfying the condition $H > (\frac{1}{2}) T'_{do}$.

All these proposed models for grouping induction machines are confined to machines running near their full load condition. To this researcher's knowledge, no published research which includes the starting effects of a group of induction motors exists.

Research Objective

The objective of this research includes the following points:

(1) Develop a single equivalent model of a group of induction

machines for starting as well as running conditions. This model can be used for different types of power system studies such as:

(a) Voltage dip due to starting one or more motors;

(b) Circuit protector rating and time current characteristics;

(c) Contingency analysis for system overload during the start-up of one or more induction motors; and

(d) System stability studies.

(2) Expand the equivalent model to include machines with deep bar rotors.

(3) Compare the proposed equivalent model with the superposition of all the machines represented by their equivalent circuit to verify the appropriateness of the equivalent model.

(4) Determine criteria for grouping similar induction machines into a single unit.

(5) Illustrate applications of the proposed dynamic load model.

The improvement areas to be examined are validity of the model over the whole speed range (zero to full load speed), effects of deep-bar rotor, accuracy, and computational and data requirements.

The representation which will be used as the basis for the model development is the induction motor steady-state equivalent circuit. This permits the calculation of electrical and mechanical input/output quantities while taking the mechanical transients into account, but assumes that all electrical transients are negligible. The validity of this assumption depends on the induction motor design and its connected load.

Research Outline

To develop a single equivalent unit for a group of induction motors, the equivalent circuit along with the equation of motion will be used. This research is subdivided into four parts.

Part I. Equivalent model behavior

In this part, the research will focus on developing an equivalent model of a group of induction motors where the parameters of the equivalent model are expressed as functions of the individual machines' parameters and speeds. A series of studies of the performance of a group of induction motors under various conditions will be conducted. These studies assume a prior knowledge of the separate characteristics (current, torque, speed vs. time) of each motor. Individual motor characteristics may be provided by the manufacturers or can simply be found by digital computer simulation of each motor knowing their equivalent circuit parameters. The following steps outline Part I.

(1) Find the electrical parameters of a single equivalent model by network reduction and the mechanical parameters using power invariance.

(2) Determine starting characteristics of the single-unit equivalent of two induction motors under the following conditions:

  (a) Simultaneous start under no load condition.

  (b) Simultaneous start under load condition.

  (c) Nonsimultaneous start under noload condition.

  (d) Nonsimultaneous start under load condition.

(3) Determine starting characteristics of the single-unit equivalent of two induction motors including deep-bar effects under the conditions specified in Step 2.

(4) Expand the modeling process to three or more motors.

Part II. Sensitivity analysis and mathematical development of the model

In this part, the goal is to establish a dynamic single equivalent model of a group of motors where the parameters of the model are independent of the individual motor speeds. The mathematical development of the dynamic single equivalent motor will be illustrated in the following steps:

(1) Analyze the variable leakage reactance coefficient (β) curves and determine the factors which effect the shapes, magnitudes and period of the curve variations for starting two induction motors under the conditions of Step 2 of Part I.

(2) Determine the effect of deep-bar rotor conductors on the β curve.

(3) Define an approximate curve to practically but accurately fit the β curve for more than two motors.

(4) Define an approximate β curve for more than two motors.

(5) Determine a criterion for grouping similar induction machines into a single unit.

Part III. Model verification

In this part, the single equivalent model will be simulated and compared against other modeling techniques in the following steps:

(1) Simulate the single equivalent model of two induction motors and compare against the summation of responses obtained from simulation of the two individual motors.

(2) Repeat step (1) for more than two induction motors.

(3) Compare with other models.

(4) Set up an experiment for starting two induction machines and compare the experimental results with results from the single equivalent model.

Part IV. Model application

A small power system which supplies a group of induction motors as part of the load will be specified. A three phase fault will be placed on one of the buses in this system. The voltage, power and reactive power at the induction motor load bus will be monitored and will be compared with the same system having the same prefault condition but using a different load representation.

Voltage dip simulation on a small distribution system will be performed and the results obtained from the reduced model will be compared with the results obtained from a detailed analysis of each machine.

CHAPTER II. INDUCTION MACHINE EQUIVALENT CIRCUIT AND RELATED PARAMETERS AND EQUATIONS IN THE DYNAMIC AND STEADY STATES

The development of the equivalent circuit for three-phase induction motors assumes that balanced alternating three-phase currents are supplied directly to the stator windings which induce currents in the rotor winding. These currents in the stator and rotor windings create a revolving magnetic field in the stator as well as in the rotor. Interactions of the stator and rotor MMF wave give rise to a unidirectional torque. The electromechanical performance can be modeled by an equivalent circuit for the machine.

Figure 2.1a shows the well-known equivalent circuit of the induction motor and Figure 2.1b is an approximate representation, where the magnetizing reactance is moved to the supply side of the stator parameters. R_1 and R_2 are the stator and rotor effective resistances respectively, and $X_{\ell 1}$ and $X_{\ell 2}$ are the stator and rotor leakage reactances respectively. X_m is defined as the megnetization reactance, and S is the slip. The equivalent circuit shows that total power P_{g1} transferred across the air-gap from the stator is given by equation 2.1:

$$P_{g1} = q_1 I_2^2 \frac{R_2}{S} \tag{2.1}$$

where q_1 is the number of stator phases, and I_2 is the rotor current.

The internal mechanical power P developed by the motor is given by

$$P = (1 - S)P_{g1} \quad . \tag{2.2}$$

The internal electromagnetic torque T corresponding to the internal

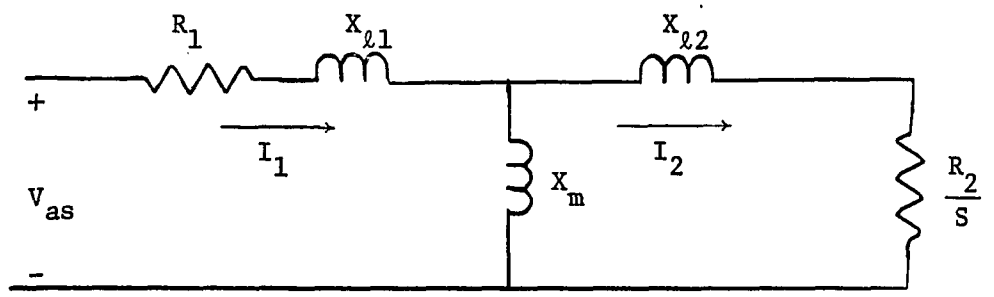

(a)

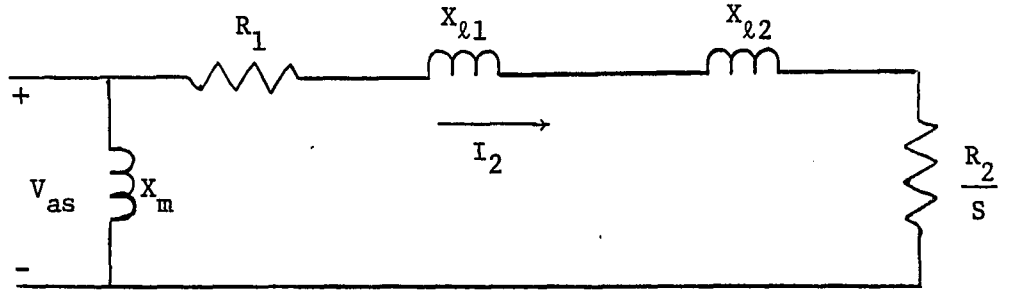

(b)

Figure 2.1. Steady-state equivalent circuit of a three-phase induction motor
(a) Circuit diagram of a three-phase induction motor
(b) Approximate circuit diagram of a three-phase induction motor

mechanical power P can be obtained by recalling that the mechanical power equals the torque times the angular velocity. ω_s is defined as the synchronous angular velocity of the rotor in mechanical radians per second.

$$P = (1 - S)\ \omega_s T \quad . \tag{2.3}$$

The internal electromagnetic torque T, the synchronous velocity ω_s and the rotor angular velocity ω, are expressed in the following equations:

$$T = \frac{1}{\omega_s}\ q_1\ I_2^2\ \frac{R_2}{S} \tag{2.4}$$

$$\omega_s = \frac{4\pi\ f_s}{\text{number of poles}} \tag{2.5a}$$

$$\omega = (1 - S)\omega_s \tag{2.5b}$$

where f_s = frequency of stator voltage and current.

Maximum Torque

Using the Thevenin's equivalent method, we can reduce the induction motor equivalent circuit of Figure 2.1a to a new configuration, as shown in Figure 2.2.

The Thevenin voltage V_{1a} and the Thevenin impedance $R_1'+jX_1'$, and the internal electromagnetic torque expressions are given in the following equations:

$$R_1' + jX_1' = (R_1 + jX_{\ell 1})\,||\,(jX_m) \tag{2.6}$$

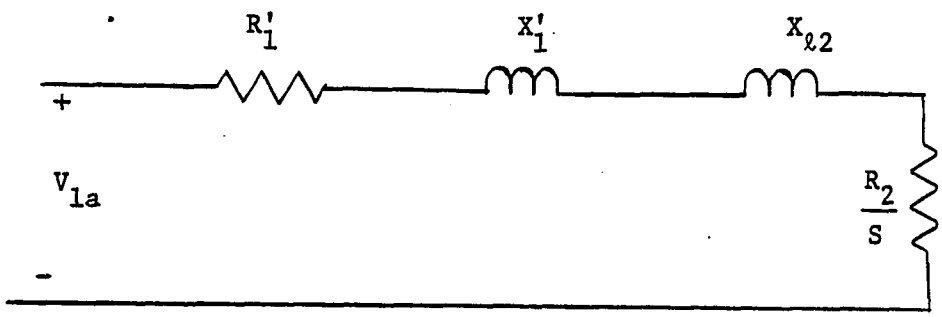

Figure 2.2. Thevenin equivalent of the induction machine equivalent circuit

$$V_{1a} = V_{as} \frac{jX_m}{R_1 + j(X_{\ell 1} + X_m)} \tag{2.7}$$

$$T = \frac{1}{\omega_s} \frac{q_1 V_{1a}^2 \frac{R_2}{S}}{(R_1' + \frac{R_2}{S})^2 + (X_1' + X_{\ell 2})^2} \tag{2.8}$$

By the impedance matching principle in circuit theory, this internal electromagnetic torque will be maximized when the impedance of $\frac{R_2}{S}$ equals the magnitude of the impedance between it and the constant voltage V_{1a}, or at a value S_{maxT} of slip for which

$$\frac{R_2}{S_{maxT}} = \sqrt{R_1'^2 + (X_1' + X_{\ell 2})^2} \tag{2.9}$$

The slip, S_{maxT}, at maximum torque is therefore

$$S_{maxT} = \frac{R_2}{\sqrt{R_1'^2 + (X_1' + X_{\ell 2})^2}} \tag{2.10}$$

and, from equation 2.8, the corresponding torque is

$$T_{max} = \frac{1}{\omega_s} \frac{.5q_1 V_{1a}^2}{R_1' + \sqrt{R_1'^2 + (X_1' + X_{\ell 2})^2}} \quad . \tag{2.11}$$

Normalizing torque by its maximum value, we will arrive at the following approximate relationship:

$$\frac{T}{T_{max}} = \frac{2}{\frac{S}{S_{maxT}} + \frac{S_{maxT}}{S}} \quad . \tag{2.12}$$

Deep Bar Induction Machines

Modified equivalent circuit

The starting torque of an induction motor is dependent on the rotor resistance. Starting torque normally increases with the rotor resistance when all other parameters are constant. To improve the starting torque of induction motors, the rotor bars on squirrel cage induction motors are often designed so that their effective resistance of 60 Hz is several times their resistance at 2 or 3 Hz. The rotor resistance varies with speed because at standstill, the rotor frequency equals the stator frequency and as the motor accelerates, the rotor frequency decreases to a very low value, about 2 or 3 Hz at full load in 60 Hz motors.

Because the effective rotor resistance of a deep-bar or double squirrel cage rotor varies with frequency, the parameter R_2, the referred effect of rotor resistance as viewed from the stator, is not constant. Therefore, the simple equivalent circuit shown in Figure 2.1a still

correctly represents the motor except that now the rotor resistance is a function of slip. A cage factor K_{db} can be included that approximates the variation of rotor resistance.

$$R_r = R_2(1 + K_{db}\ S) \tag{2.13}$$

where

R_2 = rotor dc resistance;

S = slip; and

R_r = rotor resistance.

The equivalent circuit of an induction motor with a deep-bar rotor is shown in Figure 2.3, where R_r denotes the variable rotor resistance and other symbols have their usual meanings.

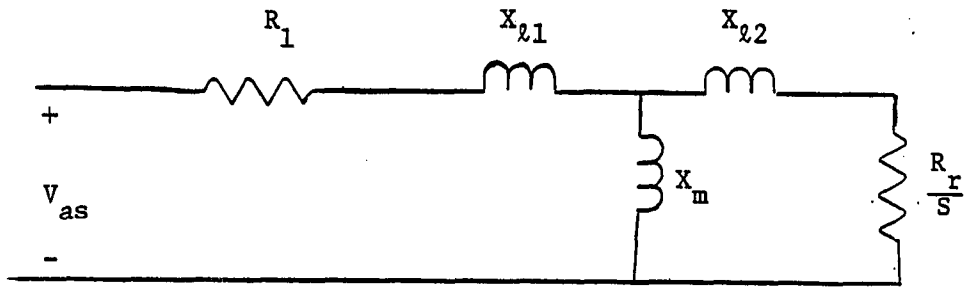

Figure 2.3. Induction motor with deep-bar rotor

Torque expression for the modified equivalent circuit

When torque and power relations for the induction motor are needed, considerable simplification results from the application of Thevenin's network theorem to the above equivalent circuit as was done before. Thevenin's impedance can be calculated to be

$$R_1' + jX_1' = (R_1 + jX_{\ell 1}) \,||\, jX_m \tag{2.14}$$

$$R_1' + jX_1' = \frac{(R_1 + jX_{\ell 1})(jX_m)}{R_1 + j(X_{\ell 1} + X_m)} \tag{2.15}$$

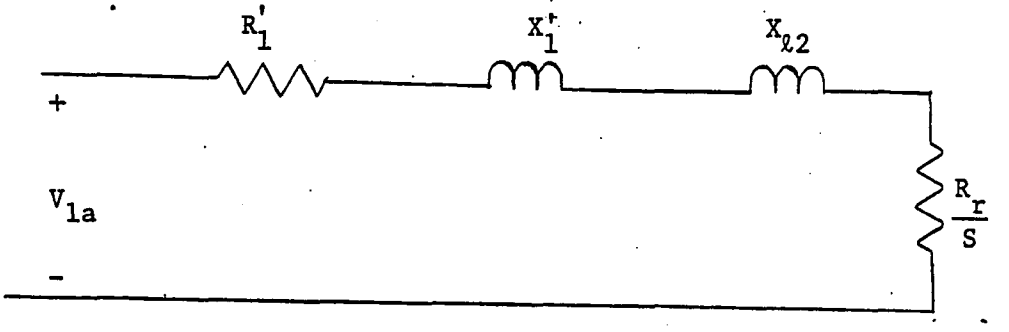

Figure 2.4. Thevenin equivalent circuit of a deep-bar induction motor

By the impedance matching principle between Thevenin's impedance and rotor resistance, we'll have

$$\frac{R_r}{S_{maxT}} = \sqrt{R_1'^2 + (X_1' + X_{\ell 2})^2} \tag{2.16}$$

Substituting R_r from equation 2.13 will result in

$$\frac{R_2(1 + K_{db} S_{maxT})}{S_{maxT}} = \sqrt{R_1'^2 + (X_1' + X_{\ell 2})^2} \tag{2.17}$$

Then S_{maxT} for a deep-bar rotor can be obtained by

$$S_{maxT} = \frac{R_2}{\sqrt{R_1'^2 + (X_1' + X_{\ell 2})^2} - K_{db} R_2} \tag{2.18}$$

To determine the value of maximum torque, we can write the equation

for torque as

$$T = \frac{V_{1a}^2 \left(\frac{R_r}{S}\right)}{\left(R_1' + \frac{R_r}{S}\right)^2 + \left(X_1' + X_{\ell 2}\right)^2} \frac{q_1}{\omega_s} \quad . \tag{2.19}$$

To find maximum torque, we can substitute the value of S_{maxT} into equation 2.19 and obtain the expression for maximum torque

$$T_{max} = \frac{.5\, V_{1a}^2}{R_1' + \sqrt{R_1'^2 + \left(X_1' + X_{\ell 2}\right)^2}} \frac{q_1}{\omega_s} \quad . \tag{2.20a}$$

The above equation shows that maximum torque will remain the same for any induction motor (i.e., squirrel cage or deep-bar rotor) because the value of maximum torque is independent of the rotor resistance. The maximum power expression can be found by substituting equation 2.20a into equation 2.3:

$$P_{max} = \frac{.5\, q_1 V_{1a}^2 (1 - S_{maxT})}{R_1' + \sqrt{R_1'^2 + \left(X_1' + X_{\ell 2}\right)^2}} \quad . \tag{2.20b}$$

Mechanical Considerations

The dynamic behavior of an induction machine is influenced by mechanical as well as electrical properties of such machines. The electromechanical equation of motion for an induction motor is given by equation 2.21:

$$2H \frac{d\omega}{dt} = T_a \quad . \tag{2.21}$$

In the above equation, all motor quantities are expressed in p.u. except the time (t).

H, the inertia constant in seconds, is the inertia of the rotor and the connected mechanical equipment. T_a, the accelerating torque, is given by equation 2.22:

$$T_a = T_e - T_m \tag{2.22}$$

$$T_m = T_o \omega^{\alpha} \tag{2.23}$$

where

T_e = electrical torque;

T_m = mechanical torque;

T_o = mechanical load torque at synchronous speed; and

α = exponent for mechanical load model.

Equation 2.21 can be written in the integral form as expressed in equation 2.24:

$$t = -2H \int_1^S \frac{ds}{T_e - T_m} \quad . \tag{2.24}$$

Run-up time calculations

In this part of the research, a series of expressions and equations to calculate the run-up time for an induction machine will be developed. To obtain these expressions, there are two cases to be considered:

(1) Machine start-up under noload.

(2) Machine start-up under load.

Machine start-up under no load In this case, the mechanical load torque is zero and equation 2.24 is reduced to

$$t = -2H \int_1^S \frac{ds}{T_e} \tag{2.25}$$

Substituting internal electromagnetic torque T for T_e from equation 2.12 and simplifying gives

$$t = -\frac{H}{2\,T_{max}} \left(\frac{1}{S_{maxT}} \int_1^S S\,ds + S_{maxT} \int_1^S \frac{ds}{S}\right)$$

$$t = -\frac{H}{2\,T_{max}} \left(\frac{1}{2\,S_{maxT}} (S^2 - 1) + S_{maxT}\,\ell nS\right) \tag{2.26}$$

where t is the time for the machine to reach a certain slip S.

Machine start-up under load The derivation of run-up times should also include consideration of the load. Referring to the electromechanical equation of motion, equation 2.21

$$-2H \frac{ds}{dt} = T_e - T_m \quad ,$$

T_m mechanical torque can be expressed as a function of slip by equation 2.27.

$$T_m = T_0(1 - S)^{\alpha} \quad . \tag{2.27}$$

Substituting equation 2.27 into equation 2.21 gives

$$-2H \frac{ds}{dt} = T_e - T_0(1 - S)^{\alpha}$$

$$-2H \frac{ds}{dt} = \frac{2\,T_{max}}{\frac{S_{maxT}}{S} + \frac{S}{S_{maxT}}} - T_0(1 - S)^{\alpha} \quad . \tag{2.28}$$

Simplifying equation 2.28 in the following steps results in

$$\frac{ds}{dt} = \frac{-1}{2H}\left[\frac{2\ T_{max}}{\frac{S_{maxT}}{S} + \frac{S}{S_{maxT}}} - T_0(1 - S)^{\alpha}\right]$$

$$\frac{ds}{dt} = -\frac{1}{2H}\left[\frac{2S_{maxT}\ T_{max}S}{S^2 + S^2_{maxT}} - T_0(1 - S)^{\alpha}\right]$$

$$\frac{ds}{dt} = -\frac{1}{2H}\left[\frac{2S_{maxT}\ T_{max}\ S - T_0(1 - S)^{\alpha}\ (S^2 + S^2_{maxT})}{S^2 + S^2_{maxT}}\right]$$

$$dt = +2Hds\left[\frac{S^2 + S^2_{maxT}}{T_0(1-S)^{\alpha}(S^2 + S^2_{maxT}) - 2T_{max}\ S_{maxT}\ S}\right] . \quad (2.29)$$

Integrating both sides of equation 2.29 will give the general integral form for calculating the explicit run-up time.

$$t = 2H \int_1^S \frac{(S^2 + S^2_{maxT})}{T_0(1-S)^{\alpha}(S^2 + S^2_{maxT}) - 2T_{max}\ S_{maxT}S}\ ds . \quad (2.30)$$

In order to find the time required for any induction motor to reach a slip of S, one has to integrate the expression given in equation 2.30. The method of solving such problems is partial fraction expansion. This requires calculating the roots of the denominator. In general, Newton's method (outlined in Appendix A) is the best available method to find these roots. In most practical cases, α can be approximated by one of the three values 0, 1, and 2. Therefore, an explicit expression to calculate the time to reach any speed for the above-mentioned practical cases (i.e., α = 0, 1, 2) will be developed.

Case I In this case, $\alpha = 0$. Substituting $\alpha = 0$ into equation 2.30 results in

$$t = 2H \int_1^S \frac{(S^2 + S_{maxT}^2)}{T_0(S^2 + S_{maxT}^2) - 2T_{max} S_{max} S} ds \quad . \tag{2.31}$$

Equation 2.31 can be rewritten in a new form as

$$t = \frac{2H}{T_0} \int_1^S \left(1 + \frac{2 \frac{T_{max} S_{maxT}}{T_0} S}{S^2 - 2 \frac{T_{max} S_{max}}{T_0} S + S_{maxT}^2}\right) ds \quad , \tag{2.32}$$

The denominator of equation 2.32 is a quadratic equation and its Δ is found to be

$$\Delta = 4 \frac{T_{max}^2}{T_0^2} S_{maxT}^2 - 4 S_{maxT}^2$$

$$\Delta = 4 S_{maxT}^2 \left(\frac{T_{max}^2}{T_0^2} - 1\right) > 0 \quad . \tag{2.33}$$

T_{max}, the maximum torque of an induction motor, is always greater than T_0. Therefore, Δ is always greater than zero. The roots of the quadratic equation are real numbers and can be calculated as follows:

$$S_1, S_2 = \frac{T_{max} S_{maxT}}{T_0} \pm \sqrt{S_{maxT}^2 \left(\frac{T_{max}^2}{T_0^2} - 1\right)} \quad . \tag{2.34}$$

To integrate equation 2.32, the partial fraction expansion method is used.

$$t = \frac{2H}{T_0} \int_1^S \left(1 + \frac{A}{S - S_1} + \frac{B}{S - S_2}\right) ds \tag{2.35}$$

where A and B are given in equations 2.36 and 2.37

$$A = \frac{\frac{2T_{max}S_{max}}{T_0} S_1}{S_1 - S_2} \tag{2.36}$$

$$B = \frac{\frac{2T_{max}S_{max}}{T_0} S_2}{S_2 - S_1} \quad . \tag{2.37}$$

The closed form equation for t is

$$t = \frac{2H}{T_0} \left[\frac{S^2}{2} + A\ell n(S - S_1) + B\ell n(S - S_2)\right]_1^S \tag{2.38}$$

or

$$t = \frac{2H}{T_0} \left[\frac{S^2}{2} + A\ell n(S - S_1) + B\ell n(S - S_2) - \frac{1}{2} + A\ell n(1 - S_1) + B\ell n(1 - S_2)\right] . \tag{2.39}$$

The time to reach any slip S can then be found by equation 2.40.

$$t = \frac{2H}{T_0} \left[\frac{1}{2}(S^2 - 1) + \ell n\left(\left(\frac{S - S_1}{1 - S_1}\right)^A \times \left(\frac{S - S_2}{1 - S_2}\right)^B\right)\right] \quad . \tag{2.40}$$

Equation 2.40 is an expression for the run-up time of an induction motor under constant mechanical load torque (i.e., $\alpha = 0$).

Case II In this case, α is equal to 1 and mechanical torque is

$$T_m = T_0(1 - S) \quad . \tag{2.41}$$

Substituting $\alpha = 1$ in equation 2.29 gives

$$dt = 2H\ ds\left[\frac{S^2 + S_{maxT}^2}{T_0(1-S)(S^2 + S_{maxT}^2) - 2T_{max}S_{maxT}S}\right] \quad . \qquad (2.42)$$

Integrating both sides of equation 2.42 and simplifying equation 2.42 results in

$$t = \frac{2H}{-T_0}\int_1^S \frac{(S^2 + S_{maxT}^2)}{S^3 - S^2 + (\frac{2T_{max}S_{maxT}}{T_0} + S_{maxT}^2)S - S_{maxT}^2}\ ds \quad . \qquad (2.43)$$

The denominator of equation 2.43 is a cubic function and has three real roots which can be found by Kardan's formula.

$$S^3 - S^2 + (2\frac{T_{max}S_{maxT}}{T_0} + S_{maxT}^2)\ S - S_{maxT}^2 = 0 \qquad (2.44)$$

$$p^3 = (2\frac{T_{max}S_{maxT}}{T_0} + S_{maxT}^2) - \frac{1}{3}$$

$$q = \frac{-2}{27} + (\frac{2T_{max}S_{maxT}}{3T_0}) - \frac{2}{3}S_{maxT}^2$$

$$M = \sqrt[3]{-q/2 + \sqrt{p^3/27 + q^2/4}}$$

$$N = \sqrt[3]{-q/2 - \sqrt{p^3/27 + q^2/4}}$$

Then, three roots of equation 2.44 can be calculated as follows:

$$S_1 = M + N \qquad (2.45)$$

$$S_2 = -\frac{M+N}{2} + \frac{M-N}{2}\sqrt{-3} \qquad (2.46)$$

$$S_3 = -\frac{M+N}{2} - \frac{M-N}{2}\sqrt{-3} \quad . \tag{2.47}$$

When $\frac{p^3}{27} + \frac{q^2}{4} < 0$, these will be three real roots. Equation 2.43 can be rewritten as

$$t = \frac{-2H}{T_0}\int_1^S \left(\frac{A}{S-S_1} + \frac{B}{S-S_2} + \frac{C}{S-S_3}\right) ds \tag{2.48}$$

where

$$A = \frac{S_1^2 + S_{maxT}^2}{(S_1-S_2)(S_1-S_3)} \tag{2.49}$$

$$B = \frac{S^2 + S_{maxT}^2}{(S_2-S_1)(S_2-S_3)} \tag{2.50}$$

$$C = \frac{S_3^2 + S_{maxT}^2}{(S_3-S_1)(S_3-S_2)} \quad . \tag{2.51}$$

Integrating equation 2.48 results in

$$t = \frac{-2H}{T_0}\left(A\ell n(S-S_1) + B\ell n(S-S_2) + C\ell n(S-S_3)\right)\Big|_1^S \quad . \tag{2.52}$$

The time for an induction motor to reach a certain slip S when the mechanical load is linear (i.e., $\alpha = 1$) is

$$t = \frac{-2H}{T_0}\ \ell n\left[\left(\frac{S-S_1}{1-S_1}\right)^A \times \left(\frac{S-S_2}{1-S_2}\right)^B \times \left(\frac{S-S_3}{1-S_3}\right)^C\right] \tag{2.53}$$

Case III ($\alpha = 2$) Mechanical torque T_m is represented as

$$T_m = T_0(1-S)^2 \quad . \tag{2.54}$$

Substituting $\alpha = 2$ in equation 2.29 results in

$$dt = 2Hds\left[\frac{(S^2 + S_{maxT}^2)}{T_0(1-S)^2(S^2+S_{maxT}^2) - 2T_{max}S_{maxT}S}\, ds\right] \quad . \qquad (2.55)$$

In this case, one can find the roots of a fourth order equation and use partial fraction expansion to develop an explicit time equation for the motor to reach any slip. But, with certain simplifications, this case could be converted to a cubic equation. For most induction motors, S_{maxT} is less than 0.1. When S_{maxT} is raised to the second power, one could neglect S_{maxT}^2 in equation 2.55. Integrating both sides of the equation results in

$$t = \frac{2H}{T_0}\int_1^S \frac{S^2}{(1-S^2)(S^2) - 2\frac{T_{max}S_{maxT}}{T_0}S}\, ds \qquad (2.56)$$

$$t = \frac{2H}{-T_0}\int_1^S \frac{S}{S^3 - S + 2\frac{T_{max}S_{maxT}}{T_0}}\, ds \quad . \qquad (2.57)$$

In this case, the denominator of equation 2.57 has three roots that can be found by the special case of the Kardan formula.

$$M = \sqrt[3]{-\frac{T_{max}S_{maxT}}{T_0} + \sqrt{\left(\frac{T_{max}S_{max}}{T_0}\right)^2 - \frac{1}{27}}} \qquad (2.58)$$

$$N = \sqrt[3]{-\frac{T_{max}S_{maxT}}{T_0} - \sqrt{\left(\frac{T_{max}S_{maxT}}{T_0}\right)^2 - \frac{1}{27}}} \qquad (2.59)$$

$$S_1 = M + N \qquad (2.60)$$

$$S_2 = \frac{-M+N}{2} + \frac{M-N}{2}\sqrt{-3} \tag{2.61}$$

$$S_3 = \frac{-M^2+N}{2} + \frac{M^2-N}{2}\sqrt{-3} \quad . \tag{2.62}$$

The condition to insure the existence of 3 real roots is satisfied when

$$\left(\frac{T_{max}S_{maxT}}{T_0}\right)^2 - \frac{1}{27} < 0 \quad . \tag{2.63}$$

Then the integral of equation 32 will be

$$t = \frac{2H}{-T_0}\int_1^S \left(\frac{A}{S-S_1} + \frac{B}{S-S_2} + \frac{C}{S-S_3}\right) ds \tag{2.64}$$

where

$$A = \frac{S_1}{(S_1-S_2)(S_1-S_3)} \tag{2.65}$$

$$B = \frac{S_2}{(S_2-S_1)(S_2-S_3)} \tag{2.66}$$

$$C = \frac{S_3}{(S_3-S_1)(S_3-S_2)} \quad . \tag{2.67}$$

From equation 2.64, the time to reach any slip s, when a motor starts under load with $\alpha = 2$, will be

$$t = \frac{2H}{T_0}\,\&n\left[\left(\frac{S-S_1}{1-S_1}\right)^A\left(\frac{S-S_2}{1-S_2}\right)^B\left(\frac{S-S_3}{1-S_3}\right)^C\right] \quad . \tag{2.68}$$

Equation 2.68 is an expression for the time required for an induction motor to reach any slip S when $\alpha = 2$.

Run-up time expressions for deep bar induction motors

All of the explicit time to reach any speed equations developed in the previous sections can be used for a motor with a deep-bar rotor. The only difference is that motors with deep bars will have different S_{maxT} values. By substituting the deep-bar motor S_{maxT} value calculated from equation 2.18, the time to reach any speed for an induction motor with a deep-bar rotor can be calculated.

Mathematical Developments for Calculation of Operating Speeds Under Different Load Conditions

In order to find the operating speed of an induction motor under a certain load, one must equate the electric torque to mechanical load torque as shown in Figure 2.5.

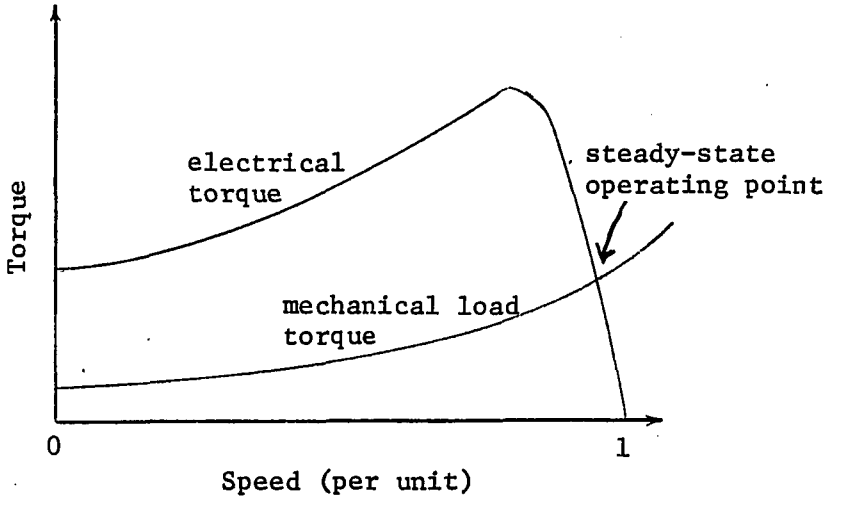

Figure 2.5. Electrical and mechanical torque characteristics

Recalling equations 2.12 and 2.23 and equating them results in

$$\frac{2T_{max}}{\frac{S}{S_{maxT}} + \frac{S_{maxT}}{S}} = T_0(1 - S)^{\alpha} \quad . \tag{2.69}$$

Equation 2.69 can be simplified to

$$(S^2 + S_{maxT}^2)(1-S)^{\alpha} - \frac{2T_{max}S_{maxT}}{T_0} S = 0 \quad . \tag{2.70}$$

Equation 2.70 is a general expression used to find the operating slip under any given mechanical load conditions. To find the root of equation 2.70, it should be noted that the only acceptable solution occurs when the S value is between zero and S_{maxT}. Using Newton's method to solve for S with an initial slip of $S_{maxT}/2$ will result in a very rapid convergence and the slip can be found with sufficient accuracy within five iterations. Application of Newton's method is outlined in Appendix A.

As previously discussed, in most practical cases α can be approximated by one of the values 0, 1 and 2. The following sections develop explicit expressions to find the operating speed for these three cases.

Case I ($\alpha = 0$)

By substituting $\alpha = 0$ in equation 2.70, S may be determined in the following steps.

$$S^2 - \frac{2T_{max}S_{maxT}}{T_0} S + S_{maxT}^2 = 0 \tag{2.71a}$$

$$S_{1,2} = \frac{+T_{max}S_{maxT}}{T_0} \pm \sqrt{\frac{(T_{max}S_{maxT})^2}{T_0^2} - S_{maxT}^2} \quad . \qquad (2.71b)$$

Only a positive root close to zero is acceptable.

Case II ($\alpha = 1$)

Substituting $\alpha = 1$ into equation 2.70 results in

$$(S^2 + S_{maxT}^2)(1 - S) - \frac{2T_{max}S_{maxT}}{T_0} S = 0 \qquad (2.72a)$$

Equation 2.72a can be simplified to

$$S^3 - S^2 + (\frac{2\ T_{max}S_{maxT}}{T_0} + S_{maxT}^2)S - S_{maxT}^2 = 0 \quad . \qquad (2.72b)$$

The above equation is the same as equation 2.44, and the method of calculating its roots has already been outlined. Again, the only acceptable root is positive and close to zero.

Case III ($\alpha = 2$)

Substituting $\alpha = 2$ into equation 2.70 and solving the equation results in

$$(S^2 + S_{maxT}^2)(1 - S)^2 - \frac{2T_{max}S_{maxT}}{T_0} S = 0$$

$$S^4 - 2S^3 + (1 + S_{maxT}^2)S^2 - (\frac{2T_{max}S_{maxT}}{T_0} + 2S_{maxT}^2)S + S_{maxT}^2 = 0 \ . \qquad (2.73a)$$

Equation 2.73a is in the form of

$$S^4 + aS^3 + bs^2 + cS + d = 0$$

where

$$a = -2$$

$$b = (1 + S_{maxT}^2)$$

$$c = -2\left(\frac{T_{max} S_{maxT}}{T_0} + S_{maxT}^2\right)$$

$$d = S_{maxT}^2$$

which has the resultant cubic equation

$$y^3 - by^2 + (ac-4d)\, y + 4bd-c^2 = 0 \quad . \tag{2.73b}$$

Let y be any root of this equation; then,

$$R \triangleq \sqrt{\frac{a^2}{4} - b + y} \quad . \tag{2.73c}$$

If $R \neq 0$, then

$$D = \sqrt{\frac{3a^2}{4} - R^2 - 2b + \frac{4ab-8c-a^3}{4R}} \tag{2.73d}$$

$$E = \sqrt{\frac{3a^2}{4} - R^2 - 2b - \frac{4ab-8c-a^3}{4R}} \quad . \tag{2.73e}$$

If $R = 0$,

$$D = \sqrt{\frac{3a^2}{4} - 2b + 2\sqrt{y^2 - 4d}} \tag{2.73f}$$

$$E = \sqrt{\frac{3a^2}{4} - 2b - 2\sqrt{y^2 - 4d}} \quad . \tag{2.73g}$$

Then

$$\begin{aligned} S_{1,2} &= -\frac{a}{4} + \frac{R}{2} \pm \frac{D}{2} \\ S_{3,4} &= \frac{a}{4} - \frac{R}{2} \pm \frac{E}{2} \end{aligned} \quad . \tag{2.73h}$$

Here again the only acceptable root is the positive root close to zero.

Summary

In this chapter, the equivalent circuit of an induction motor along with the mechanical equations of motion were reviewed. A modified induction machine equivalent circuit to include the effect of deep bar rotors was presented. A series of expressions to calculate the run-up time and the operating speed of any induction motor under different mechanical load torque conditions were derived. These expressions are also applicable for an induction motor with a deep bar rotor. In the following chapters, these equations will be recalled frequently for the development of the single equivalent representation of a group of induction motors.

CHAPTER III. EQUIVALENT MODEL BEHAVIOR

This chapter focuses on developing a single equivalent model of two induction motors where the parameters of the equivalent model are functions of the individual machines' speeds and electrical parameters. A series of studies on the performance of the two induction motors under various conditions will be shown. These studies assume prior knowledge of the separate characteristics (current, torque and speed vs. time) of each motor. Individual motor characteristics can be provided by the manufacturer or can be found by digital computer simulation of each motor with knowledge of their equivalent circuit parameters.

Methodology

The steady-state equivalent circuit of a single induction machine is widely used to predict the performance characteristics of induction motors and their impact on the power network. The equivalent circuit has also been used in studying the dynamic performance of induction motors [5]. Since it has been shown to be reasonable to use such a circuit representation of each individual motor, it is proposed to use this circuit as a basis to develop an equivalent model for a group of induction motors.

Two machine representations (electrical parameters)

Consider a set of two parallel induction motors that are supplied from the same infinite bus, as shown in Figure 3.1. Substituting an equivalent circuit for each individual motor of Figure 3.1 yields the

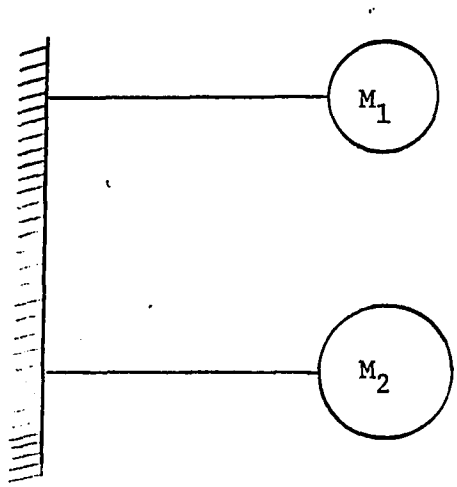

Figure 3.1. Two parallel induction motors

circuit shown in Figure 3.2. V_{as} is the bus voltage and all parameters of each motor equivalent circuit of Figure 3.2 are given in Table 3.1. The resistances representing core losses are neglected. The motor parameters are referred to a common base and the magnetizing branches are moved to the supply points to facilitate deriving an equivalent model, as shown in Figure 3.3. x_1 and x_2 represent the total leakage reactance of each motor.

Electrical parameters of the single equivalent model

The proposed model of two induction motors is shown in Figure 3.4, where R_s and R_r represent the equivalent stator and rotor resistance, respectively. In the equivalent model, the leakage reactance x/β and the equivalent slip are not constant and will vary as a function of the individual machines' speeds and electrical parameters.

The terms "stator" and "rotor" are used when referring to the equivalent model. Although the model is not an actual machine, referring to the "stator" and "rotor" of the equivalent model helps in the analysis and allows a straight forward derivation of the equivalent model's parameters. The equivalent magnetizing reactance is given by

$$X_m = \frac{X_{m1} X_{m2}}{X_{m1}+X_{m2}} \quad . \tag{3.1}$$

To obtain other equivalent model parameters, the circuits of Figures 3.3 and 3.4 must be electrically equivalent, for both standstill and running conditions. Under running conditions with individual

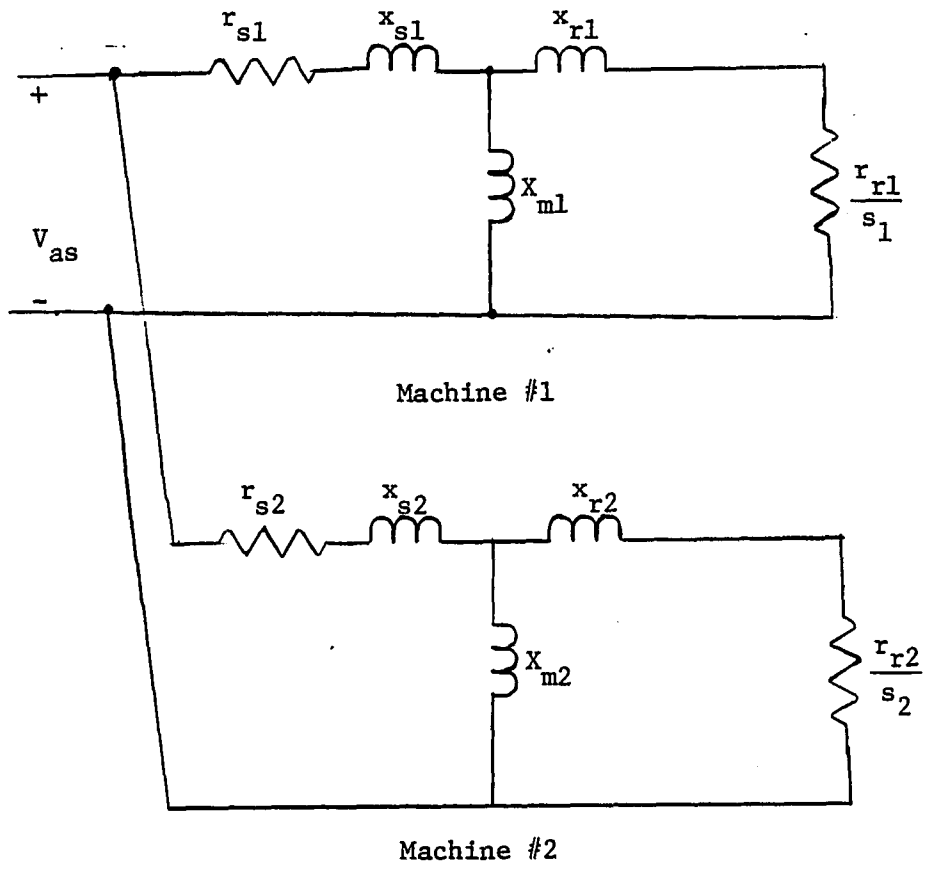

Figure 3.2. Two parallel induction motors represented by their equivalent circuits

Table 3.1. Electrical parameters of machines #1 and #2

Motor	Slip	Stator quantity		Rotor quantity		Magnetizing reactance
		Resistance	Leakage reactance	Resistance	Leakage reactance	
Motor #1	s_1	r_{s1}	x_{s1}	r_{r1}	x_{r1}	X_{m1}
Motor #2	s_2	r_{s2}	x_{s2}	r_{r2}	x_{r2}	X_{m2}

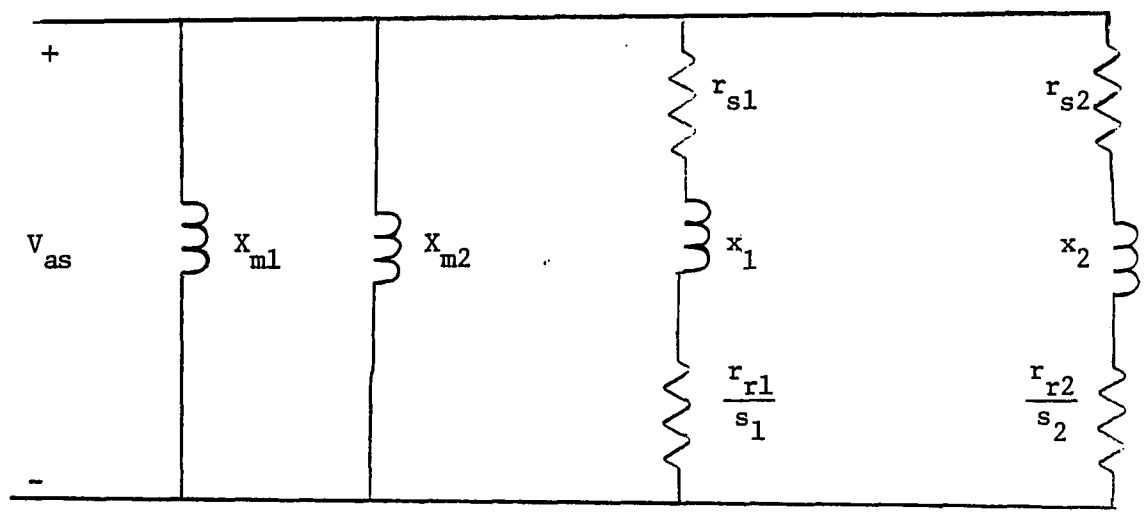

Figure 3.3. Two parallel induction motors represented by their approximate circuit equivalent

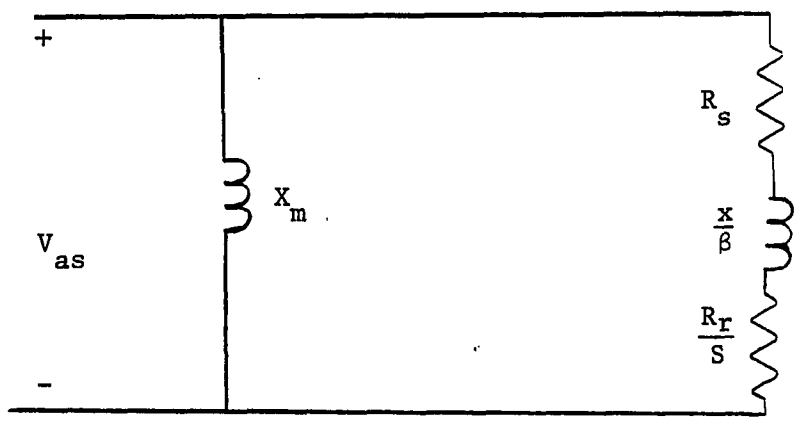

Figure 3.4. Single equivalent model of two induction motors

motor slips s_1 and s_2, equivalence of the circuits of Figures 3.3 and 3.4 leads to equation 3.2.

$$(R_s + \frac{R_r}{S}) + j\frac{x}{\beta} = \frac{[(r_{s1} + \frac{r_{r1}}{s_1}) + jx_1][(r_{s2} + \frac{r_{r2}}{s_2}) + jx_2]}{(r_{s1} + \frac{r_{r1}}{s_1} + r_{s2} + \frac{r_{r2}}{s_2}) + j(x_1 + x_2)} \tag{3.2}$$

where:

R_s = equivalent model stator resistance;

R_r = equivalent model rotor resistance;

x = equivalent model leakage reactance;

β = equivalent model leakage reactance coefficient; and

S = equivalent model slip.

Separating the real and imaginary components of both sides of equation 3.2 will result in equations 3.3a and 3.3b.

$$R_s + \frac{R_r}{S} =$$

$$\frac{(r_{s1} + \frac{r_{r1}}{s_1} + r_{s2} + \frac{r_{r2}}{s_2})(r_{s1} + \frac{r_{r1}}{s_1})(r_{s2} + \frac{r_{r2}}{s_2}) + x_2^2(r_{s1} + \frac{r_{r1}}{s_1}) + x_1^2(r_{s2} + \frac{r_{r2}}{s_2})}{(r_{s1} + \frac{r_{r1}}{s_1} + r_{s2} + \frac{r_{r2}}{s_2})^2 + (x_1 + x_2)^2} =$$

$$A(s_1, s_2) \tag{3.3a}$$

$$\frac{x}{\beta} = \frac{x_2(r_{s1}+\frac{r_{r1}}{s_1})^2 + x_1(r_{s2}+\frac{r_{r2}}{s_2})^2 + x_1x_2(x_1+x_2)}{(r_{s1}+\frac{r_{r1}}{s_1} + r_{s2} + \frac{r_{r2}}{s_2})^2+(x_1+x_2)^2} = B(s_1,s_2) \quad . \tag{3.3b}$$

For the standstill condition, substitute $s_1 = s_2 = S = \beta = 1$ in equations 3.3a and 3.3b. This results in

$$R = \frac{(r_{s1}+r_{r1}+r_{s2}+r_{r2})(r_{s1}+r_{r1})(r_{s2}+r_{r2}) + x_2^2(r_{s1}+r_{r1}) + x_1^2(r_{s2}+r_{r2})}{[(r_{s1}+r_{r1}+r_{s2}+r_{r2})^2 + (x_1+x_2)^2]} \tag{3.4}$$

$$x = \frac{(r_{s1}+r_{r1})^2x_2 + (r_{s2}+r_{r2})^2x_1 + x_1x_2(x_1+x_2)}{[(r_{s1}+r_{s2}+r_{r1}+r_{r2})^2 + (x_1+x_2)^2]} \tag{3.5}$$

where:

$R = R_s + R_r$.

An expression which approximates the relationship between R_s and R_r is given in equation 3.6. This expression divides the rotor and stator resistance according to the individual ratings of each motor.

$$\frac{R_r}{R_s} = \frac{\frac{r_{r1}}{r_{s1}} VA_1 + \frac{r_{r2}}{r_{s2}} VA_2}{VA_1 + VA_2} \tag{3.6}$$

where VA_1 and VA_2 are volt ampere ratings of machine #1 and machine #2, respectively.

Equations 3.1, 3.4, 3.5 and 3.6 will provide the electrical parameters of the equivalent model at standstill.

Comparing equations 3.3a and 3.3b with 3.4 and 3.5 leads to the following expressions for the equivalent slip S and the variable coefficient $1/\beta$ of the equivalent leakage reactance. The mathematical speed limit of the equivalent model is given in Appendix C.

$$S = \frac{R_r}{A(s_1,s_2) - R_s} \tag{3.7}$$

$$\beta = \frac{x}{B(s_1,s_2)} \quad . \tag{3.8}$$

Motor mechanical load representation

The concept of conservation of mechanical energy is used in finding the torque speed characteristics of the equivalent mechanical load. Assuming the usual exponential relationship between load torque T_m and speed ω gives

$$T_m = T_o \, \omega^{\alpha} \tag{3.9}$$

where:

T_o is a constant and is defined as the load torque at synchronous speed;

ω is the rotor speed; and

α is defined as the speed exponent of the load torque.

Since the output mechanical power of the equivalent model must be

equal to the sum of the output powers of the individual motors, the following expression may be written:

$$T_0\omega^{\alpha+1} = T_{01}\omega_1^{\alpha_1+1} + T_{02}\omega_2^{\alpha_2+1} \quad . \tag{3.10}$$

T_{01}, α_1, T_{02} and α_2 are known constants defining the individual motor loads and ω_1 and ω_2 are per unit motor speeds.

T_0, the load torque, and α, the speed exponent of the equivalent models, are given in equations 3.12 and 3.13.

$$T_0 = T_{01} + T_{02} \tag{3.12}$$

$$\alpha = \log_\omega \left[\frac{1}{T_{01}+T_{02}} \left(T_{01}\ \omega_1^{1+\alpha_1} + T_{02}\ \omega_2^{1+\alpha_2}\right)\right] - 1 \tag{3.13}$$

Qualitative Analysis of Variable Leakage Reactance

One of the characteristics of the equivalent model for a group of induction machines is its variable leakage reactance, $\frac{x}{\beta}$. In this part of the research, the variation of the leakage reactance coefficient β will be studied in order to determine the effects of individual machine parameters which influence this parameter.

There are two cases to be considered for such analysis: first, simultaneous starting; and second, nonsimultaneous starting.

Case I: Simultaneous starting

In this case, three sets of two parallel induction machines were selected. Each machine was separately simulated (the simulation method

is explained in Appendix E) and the slip, current, and torque vs. time of the individual machines were recorded and are shown in Figures 3.5-3.8.

It was shown previously that the equivalent model parameters of two induction motors are a function of each machine's individual electrical parameters as well as its slip. For each pair of machines to be grouped together, the equivalent electrical and mechanical parameters were calculated using the equations which were developed in this chapter. The equivalent parameters of each pair of motors along with recorded values of slips were used to obtain the equivalent model's characteristics (i.e., slip, leakage reactance coefficient, current and torque vs. time).

The current vs. time and torque vs. time graphs shown in the (b) and (c) parts of Figures 3.5-3.8 follow the expected pattern. The current drawn by the equivalent model is shown to be equal to the vector sum of the two individual motor currents. The current curve is a double stepped curve, with each step representing the attainment of steady-state speed by one machine after another. The torque curve of the equivalent model is also shown to be the sum of the two individual motor torques.

The leakage reactance coefficient β given by equation 3.8 was analyzed for a variety of conditions. The general characteristics of the β versus time curve can be seen in Figures 3.5-3.8 part (a). The value of β remains nearly constant for the initial part of the curve, then changes rapidly to a new value, and finally returns rapidly to a final value near 1.0. The parameters of the simulated machine are given in Table 5.1.

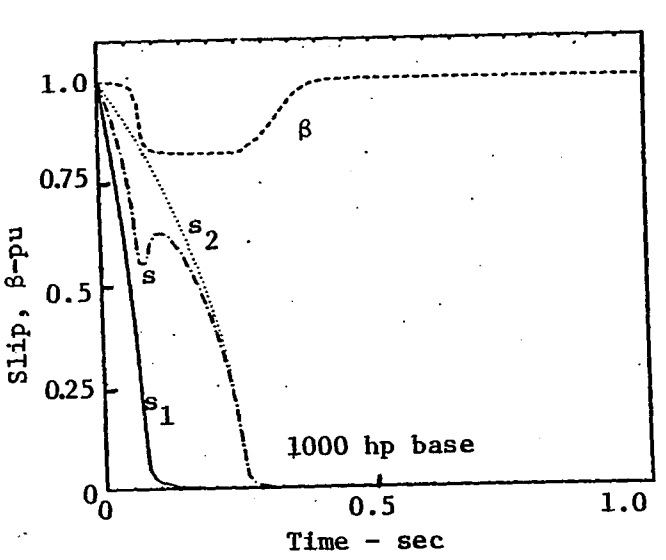

(a)

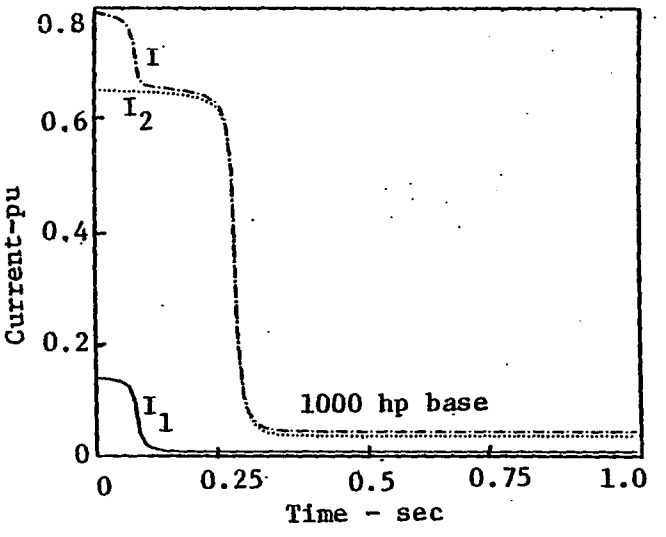

(b)

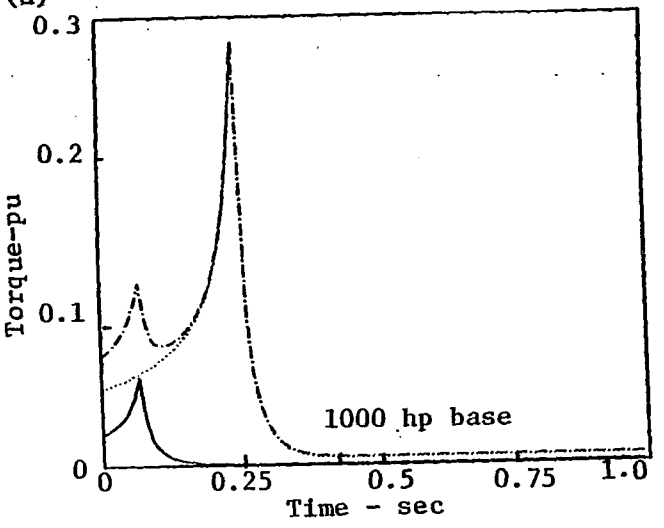

(c)

Figure 3.5. 20 hp.100 hp

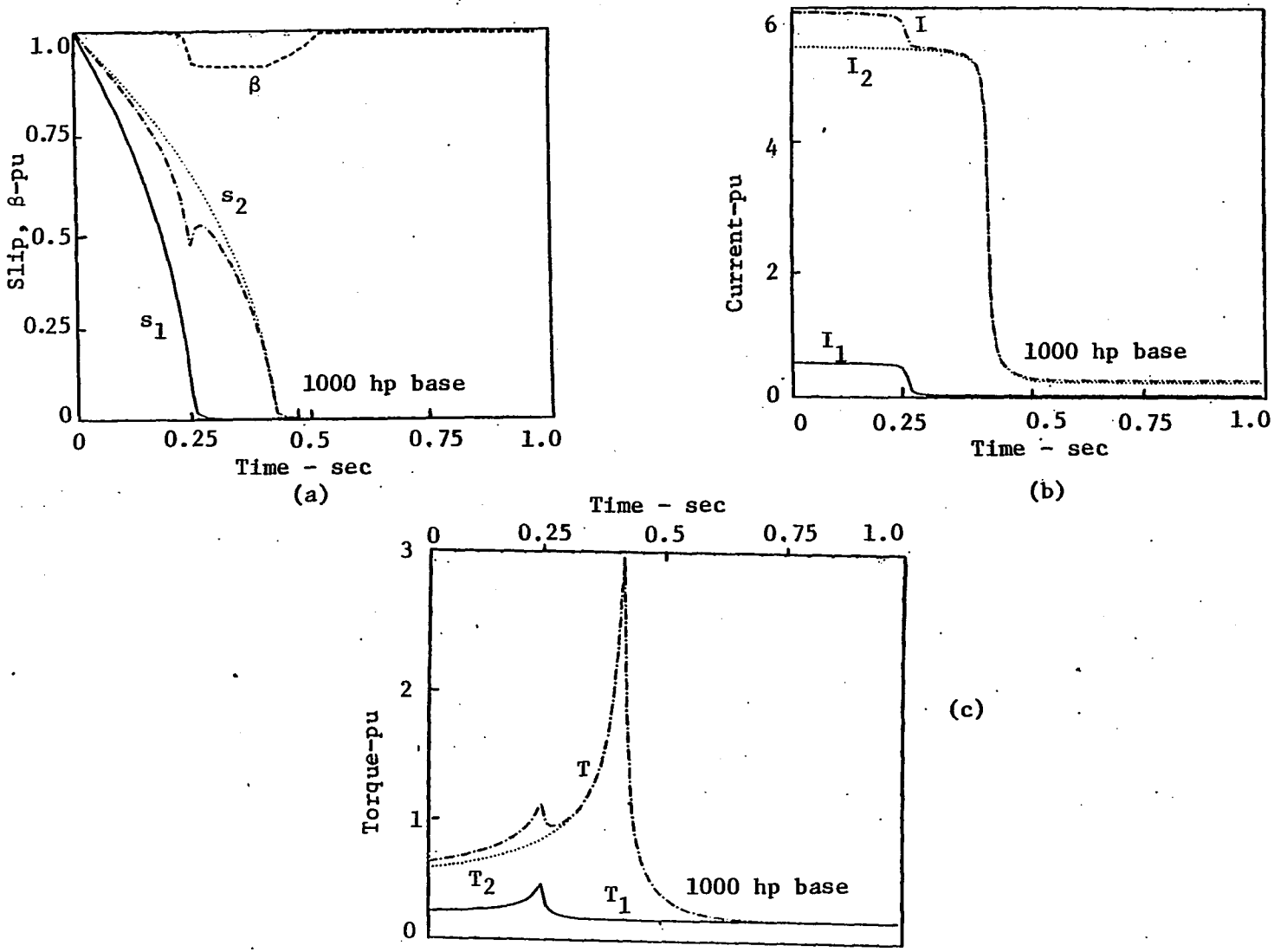

Figure 3.6. 100 hp/1000 hp

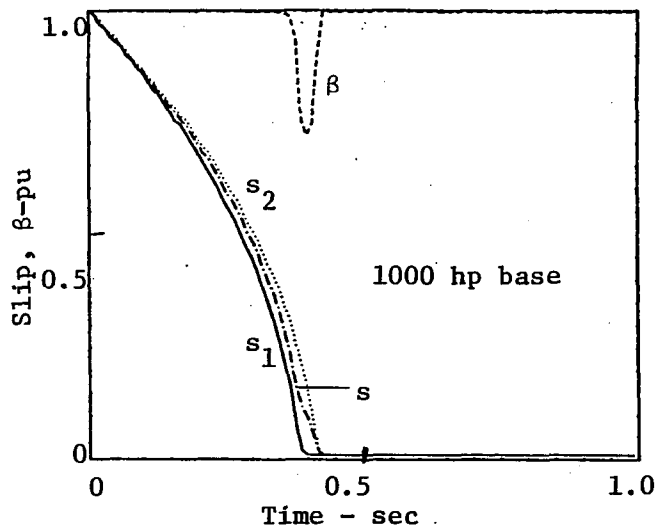

(a)

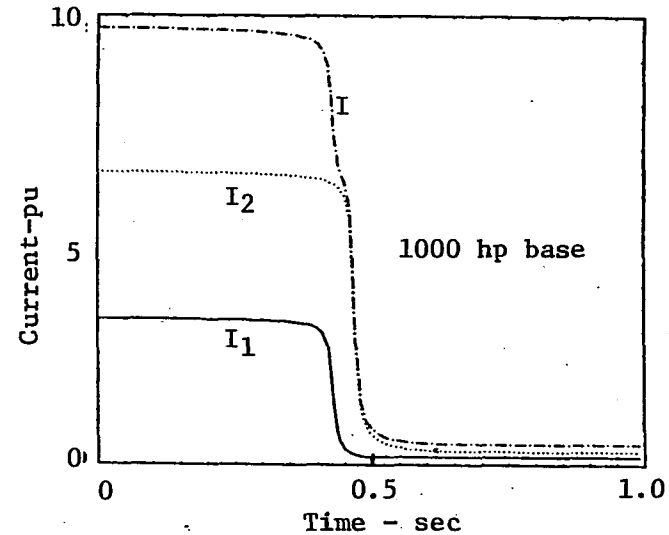

(b)

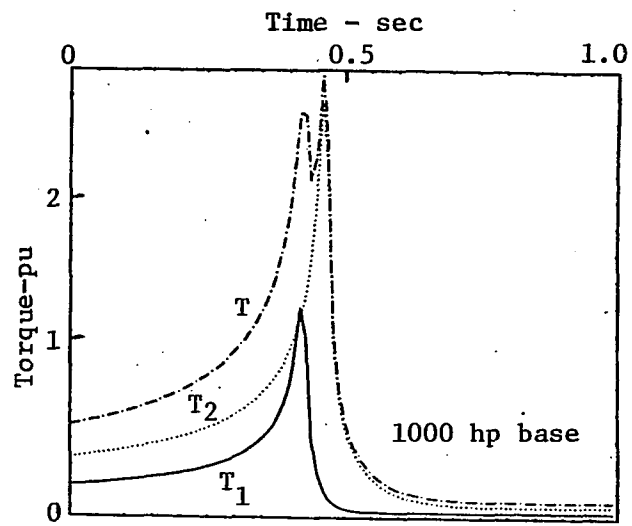

(c)

Figure 3.7. 500 hp/1000 hp

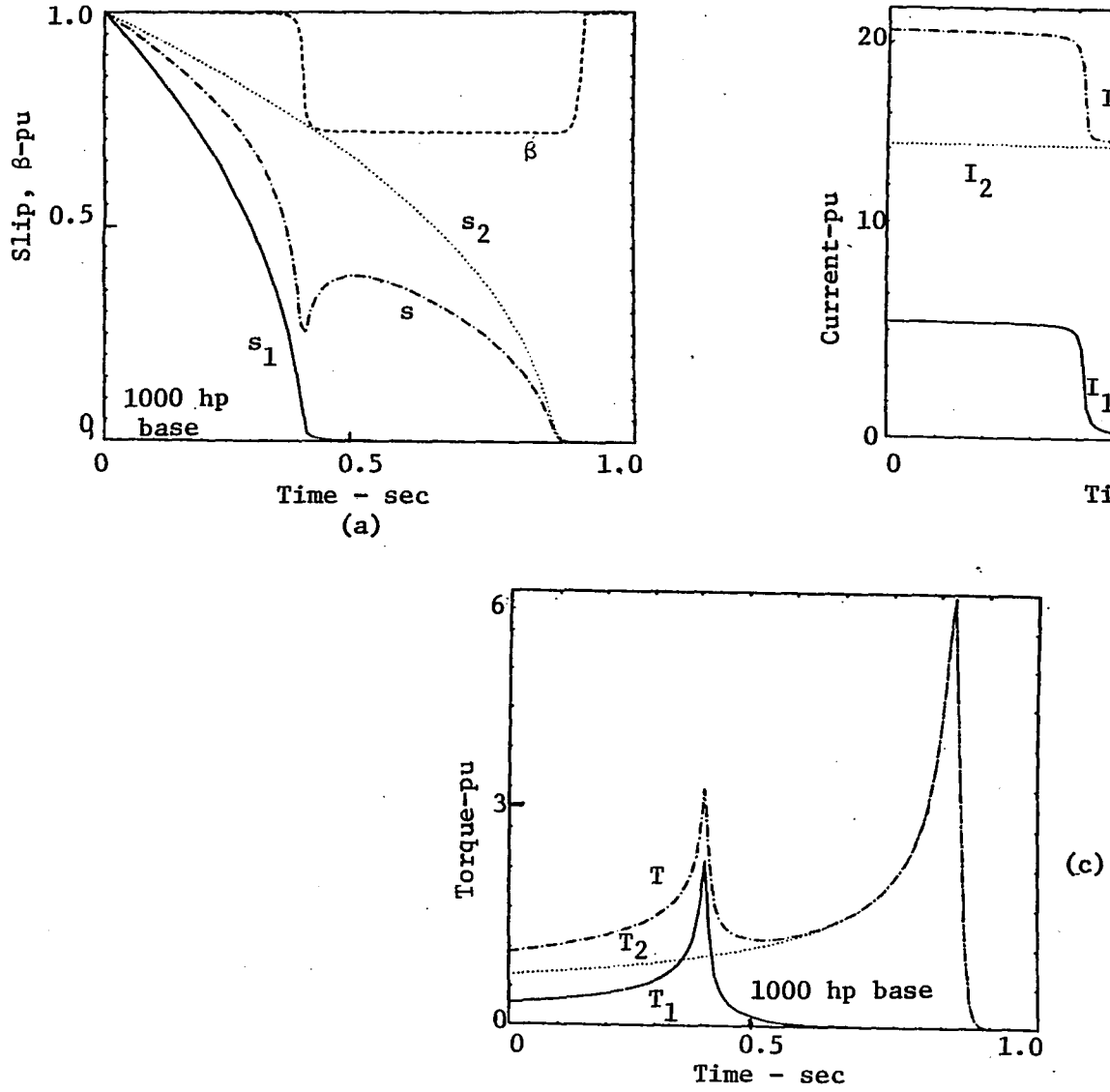

Figure 3.8. 1000 hp/2500 hp

The curves obtained from the 1000/2500 hp combination of motors are enlarged in Figure 3.9. The separate torque time relations are included because they throw light on the nature of the β coefficient. It should be stated here that the separate simulation of each machine is used only for analyzing the nature of the reactance coefficient and will not be needed once the model is developed. It will be shown that the reactance coefficient β can be defined by a relatively simple general expression, and two machines can be fully represented by the equivalent model.

Figure 3.9 shows the plot of the beta coefficient for two dissimilar machines as they start simultaneously under no load. The changes in β are related to the individual torque and slip variations, with the lower value of β being applicable from the time the first machine attains steady-state speed to the time that the second machine approaches its final speed. It is also seen that the first point of inflection in the curve occurs at or near the instant the first machine reaches breakdown torque. The rate of change of β is thus related to the interval from the time t_{m1} that machine one takes to reach maximum torque to the time t_{01} that machine one takes to reach steady-state speed. This interval is clearly related to the rotor resistance as the slip of maximum torque increases linearly with rotor resistance.

Figures 3.10 and 3.11 verify that, as the rotor resistance is increased, the beta coefficient variation becomes more trapezoidal than rectangular, but the correlation between the beta changes and t_{m1} and t_{01} indicated above remains essentially valid. As a direct consequence of the increased rotor resistance, the run-up times are reduced because of the

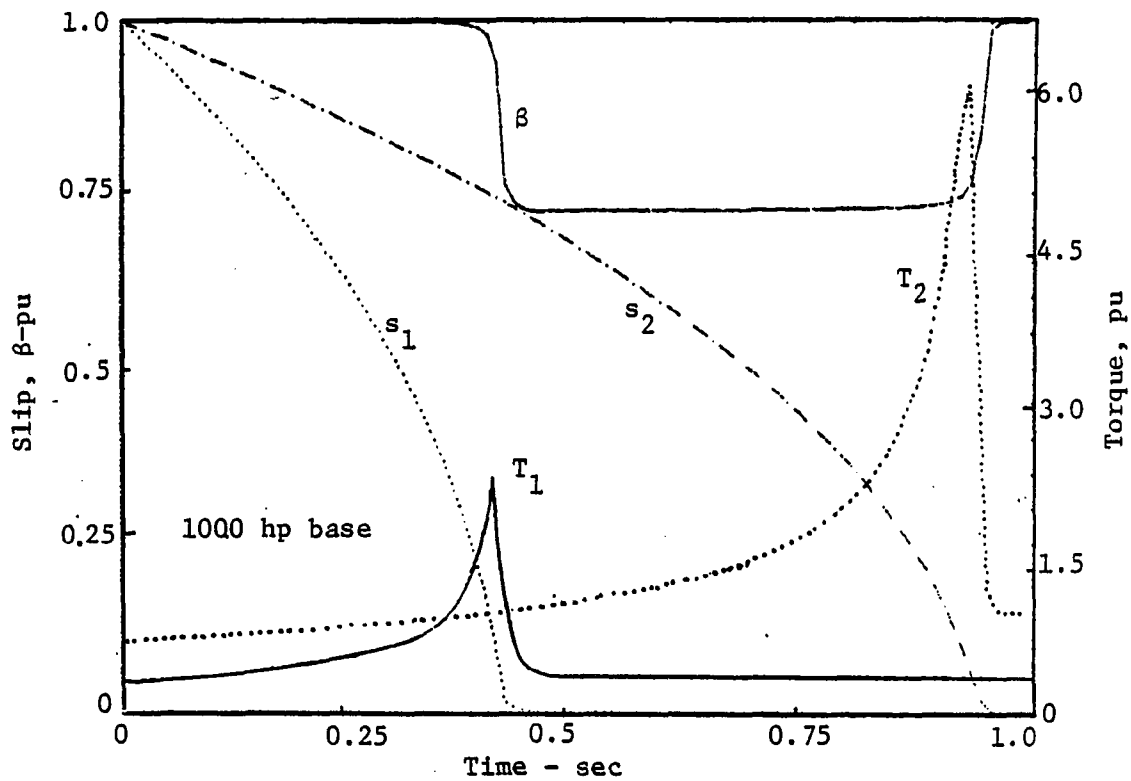

Figure 3.9. 1000 hp/2500 hp base case. Simultaneous starts. No load. Reactance coefficient β, slips and per unit torques on 1000 hp base

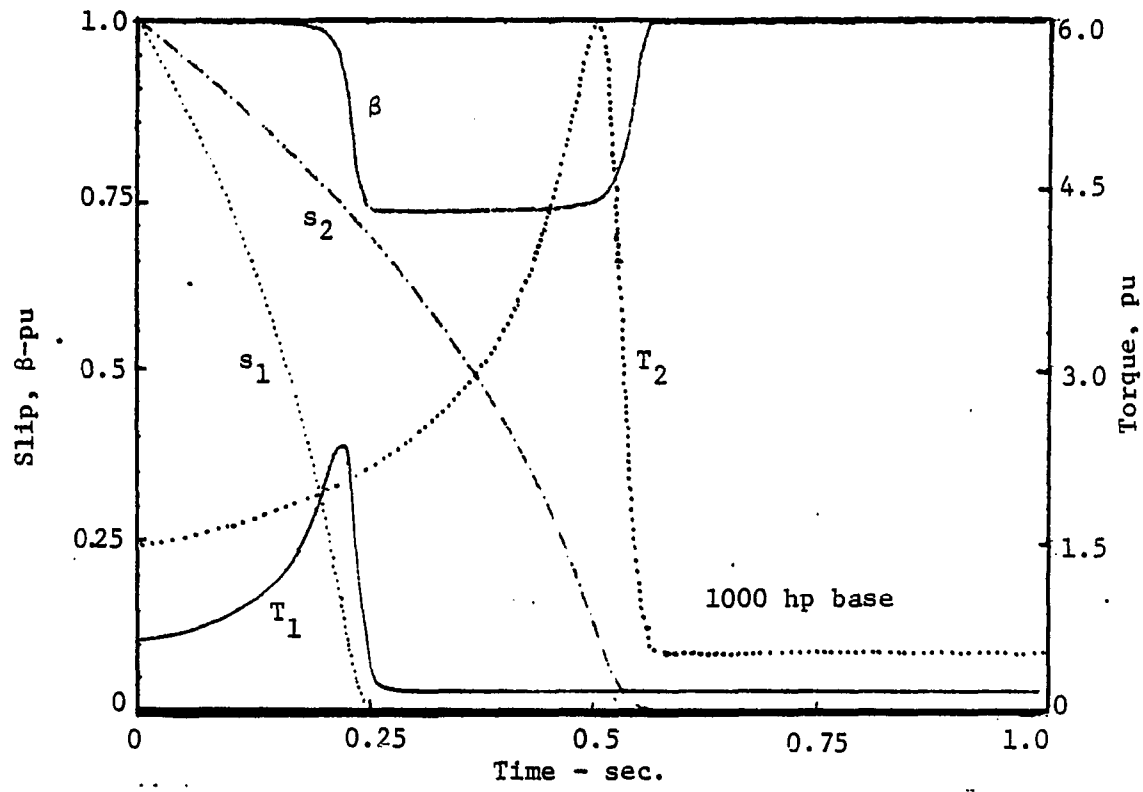

Figure 3.10. 1000 hp/2500 hp. Rotor resistances of both machines doubled

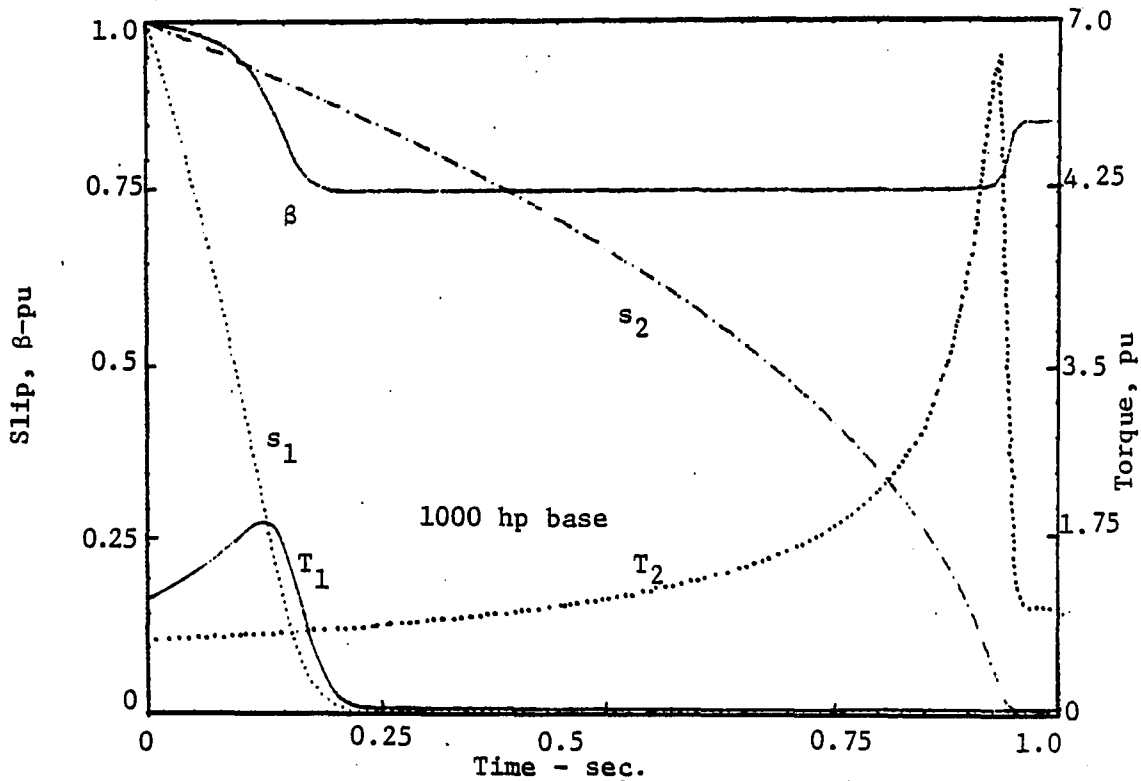

Figure 3.11. 1000 hp/2500 hp. Rotor resistance of first machine five times as high

higher starting torque, and the lower value of β has changed. It will be shown later in this chapter how the β values vary with rotor resistance.

The beta coefficient variation may be approximated by either a trapezoidal or rectangular shape, as illustrated in Figure 3.12. The choice of approximation depends on the degree of simplification desired. The error in using the rectangular form is least for low slip machines. These machines are often more important from a practical point of view because of their higher starting currents. In Figure 3.12c, the minimum value of the coefficient, β_2, may be derived as s_1 approaches 0 in the expression for beta given in equation 3.14. In the process of deriving the limit, it is seen that β_2 is independent of the slip of the second machine s_2. After simplification, this gives

$$\beta_2 = \frac{(r_{s1}+r_{r1})^2 + (r_{s2}+r_{r2})^2 \frac{x_1}{x_2} + x_1(x_1+x_2)}{(r_{s1}+r_{r1}+r_{s2}+r_{r2})^2 + (x_1+x_2)^2} \quad . \qquad (3.14)$$

The final value of the reactance coefficient, β_3, may be derived by taking the limit as $s_2 \to s_1 \to 0$. This gives

$$\beta_3 = \frac{(r_{r1}+r_{r2})^2[(r_{s1}+r_{r1})^2 x_2 + (r_{s2}+r_{r2})^2 x_1 + x_1 x_2 (x_1+x_2)]}{(r_{r1}^2 x_2 + r_{r2}^2 x_1)[(r_{s1}+r_{r1}+r_{s2}+r_{r2})^2 + (x_1+x_2)^2]} \quad . \qquad (3.15)$$

The expression for β_3 gives a value very close to 1.0 for most practical machines. The model may be simplified by setting β_3 to 1.0 with very little error. The procedure to calculate β_1 using the limit approach will become more complicated as the number of machines increases. However, another approach will be adopted which involves much less computational effort.

Considering the two machine case of Figure 3.4, the total current

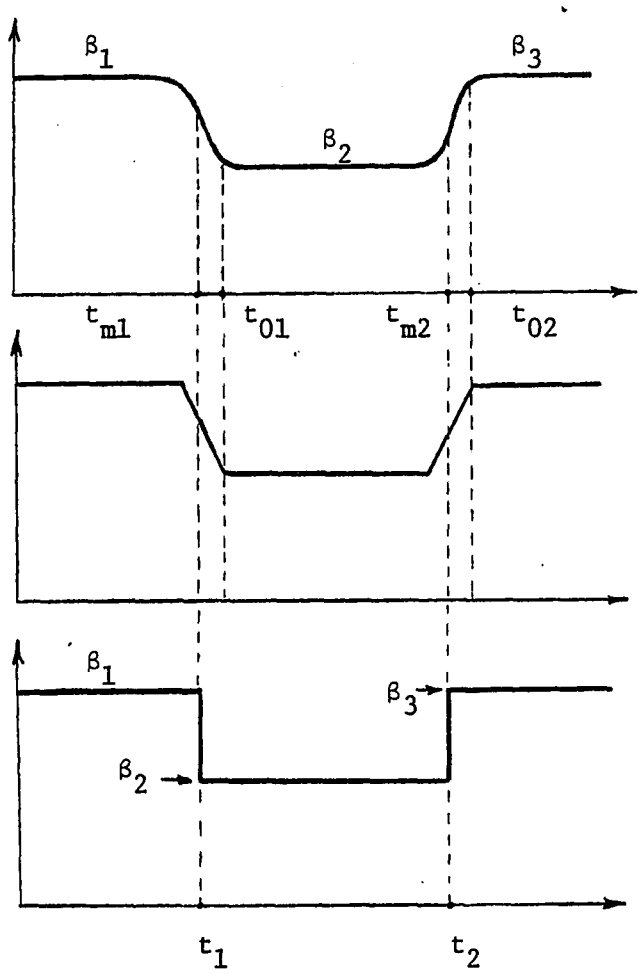

Figure 3.12. Reactance coefficient approximation

drawn by both machine 1 and 2 remains substantially constant during the starting period until the first machine reaches maximum torque. At this point, the current drops sharply. This is the same instant that the leakage reactance coefficient β changes from 1.0 to β_2. In view of this correspondence between the current changes and the β variation, the value of β_2 was derived in terms of the current ratio.

$$K = \frac{|I_2|}{|I_1 + I_2|} \quad . \tag{3.15}$$

This current ratio is a constant for any pair of machines since I_1 and I_2 are taken at their starting values with $s_1 = s_2 = 1$. K will be a function of the equivalent circuit constants of the two machines only. After some simplification, it can be shown that

$$K = \frac{|I_2|}{|I_1+I_2|} = \frac{(r_{s1}+r_{r1})^2 + x_1^2}{(r_{s1}+r_{r1})^2 + (r_{s1}+r_{r1})(r_{s2}+r_{r2}) + x_1^2 + x_1x_2} \tag{3.16}$$

If the same current ratio is derived using the equivalent circuit of the model of Figure 3.4, it can be seen that

$$\frac{|I_2|}{|I_1+I_2|} = \frac{\sqrt{4R^2 + x^2}}{\sqrt{R^2 + (1 + \frac{1}{S})^2 + \frac{x^2}{\beta^2}}} \tag{3.17}$$

$$\beta_2 = K \frac{x}{\sqrt{x^2 + R^2[4 - K^2(1 - \frac{1}{S})2]}} \quad . \tag{3.18}$$

Except for machine pairs having similar inertia constants, the equivalent slip S is not near zero at the time t_1, and the radical in the denominator is approximately equal to x. The exception is of little

consequence since, for such a case, the β coefficient is practically constant throughout the starting time of both machines and equal to one.

Therefore, the β_2 value can be approximated as

$$\beta_2 = \frac{|I_2|}{|I_1 + I_2|} = K \quad . \tag{3.19}$$

Although this value is extremely close to the β value found by equation 3.8, it assumes that the machine number one current falls to zero when it reaches its operating point. We can improve this approximation by including the value of the operating current of machine number one into the expression. The machine number one slip will not go to exactly zero, but reaches some steady state value. At this slip, the motor will draw current of a magnitude that depends on its loading condition. The new expression for β_2 is

$$\beta_2 = \frac{|I_2 + i_1|}{|I_1 + I_2|} \tag{3.20}$$

where i_1 is the steady state operating current of machine number one.

To calculate times t_1 and t_2 of Figure 3.12, we will use the equations which were developed in the previous chapter to calculate the run-up time for each individual motor. When the two machines have widely different inertia constants, the resulting variation of the reactance coefficient reflects that. Also, if two other motors with equal inertia constants are considered, then it would be expected that the run-up times t_1 and t_2 will not be very different. This is

verified in Figures 3.7 and 3.8 where the β variation all but disappeared. Neglecting the variation in the leakage reactance of the model will introduce little error in the case of machines of equal or nearly equal run-up times.

Case II: Nonsimultaneous starting

Deriving the model of two motors starting at different times presents no problem since β_2 and β_3 as given by equations 3.14 and 3.15 are functions of equivalent circuit parameters only. These two values of the reactance coefficient will remain unchanged regardless of different starting times. The value of t_1 and t_2 in Figure 3.12 must, however, be adjusted to take into account the time lag Δt in starting. Thus, if machine number one is delayed, then t_1, as obtained from the run-up time equations developed in Chapter II, must be increased to $t_1 + \Delta t$. Similarly, the run-up time for machine number two must be increased to $t_2 + \Delta t$ if it is the motor whose starting time is delayed. This can be verified by inspection of Figure 3.13 where the 1000 hp motor is delayed by 0.3 sec., and of Figure 3.14 where the 2500 hp motor is similarly delayed. In comparison with the base case of Figure 3.9 where $t_2 - t_1$ is 0.53 seconds, the interval is 0.23 seconds in Figure 3.13 and 0.83 seconds in Figure 3.14. The magnitude of β_2 will remain the same for all three cases of Figures 3.9, 3.13 and 3.14.

Summary

A model based on the equivalent circuit with variable electrical parameters has been developed to represent two three-phase induction

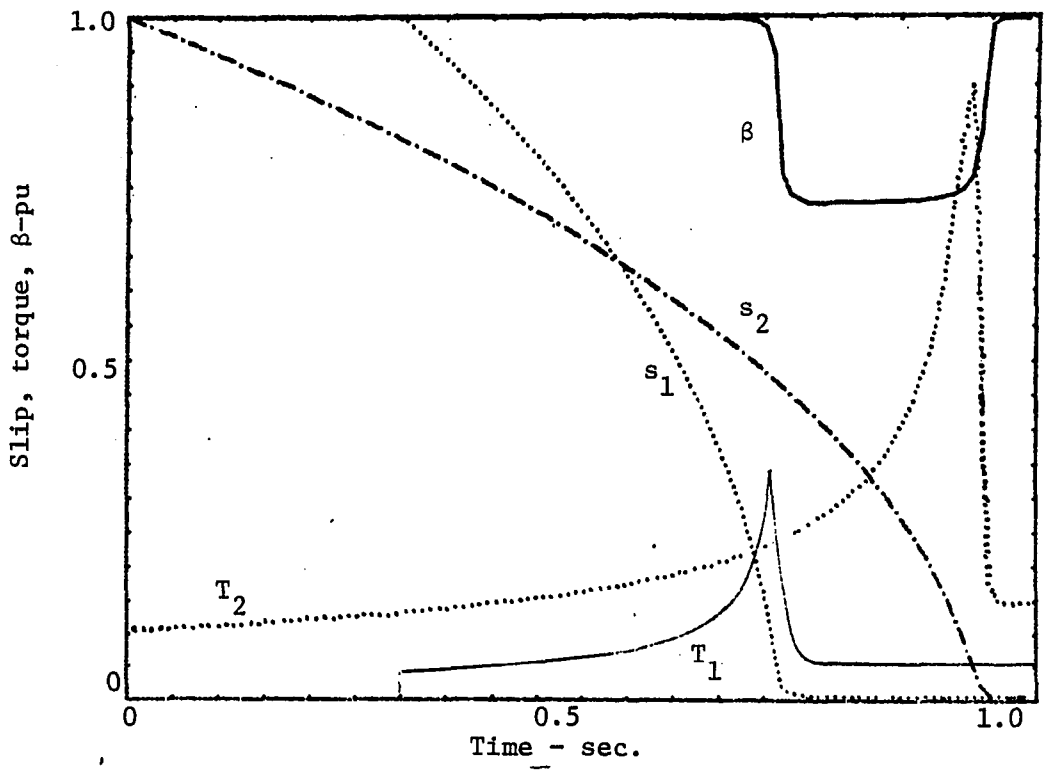

Figure 3.13. 1000 hp/2500 hp. No load. 1000 hp motor starts 0.3 sec. late

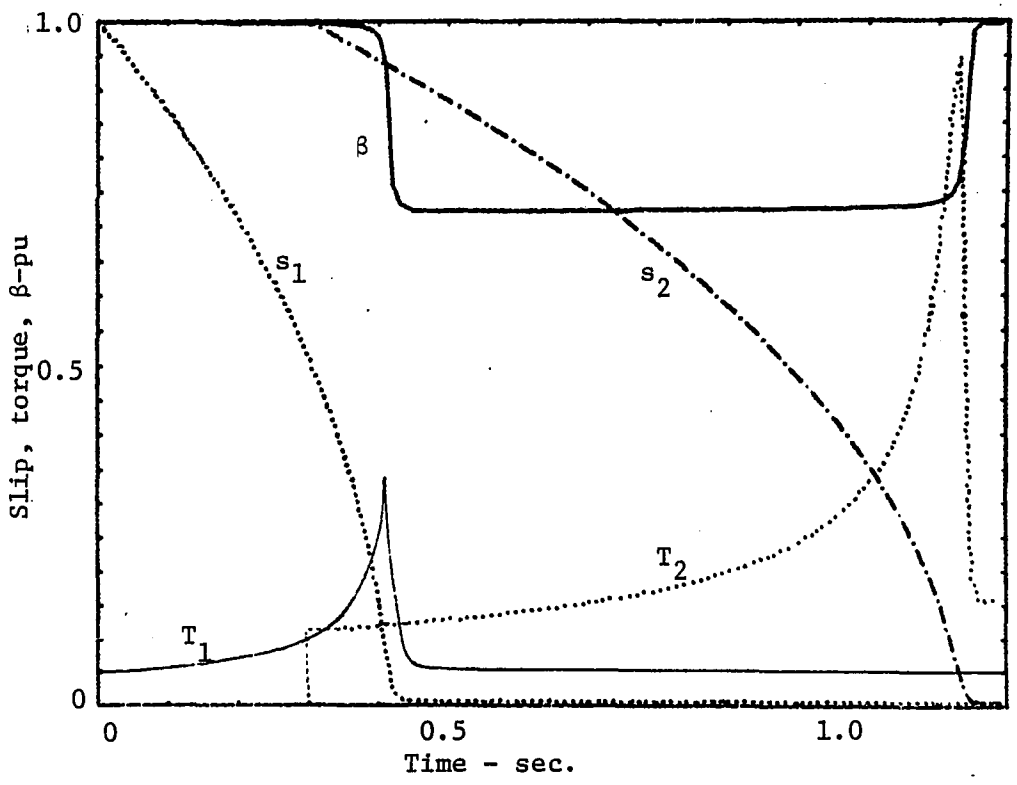

Figure 3.14. 1000 hp/2500 hp. No load. 2500 hp motor starts 0.3 sec. late

motors connected to the same bus. The model uses the concept of a variable leakage reactance, an equivalent slip, and an equivalent inertia constant. In the next chapter, this method of equivalency will be expanded for a group of several three-phase induction motors to determine an equivalent single representation of such a group.

CHAPTER IV. SINGLE EQUIVALENT REPRESENTATION OF A GROUP OF INDUCTION MOTORS

In the previous chapter, a single equivalent model of two parallel induction motors was developed. In practical power systems, there are often a number of induction motors which are supplied from a common bus. Thus, the procedure used for the case of a two motor group needs to be extended to obtain the parameters of a single equivalent model of more than two induction motors supplied from the same bus. This single equivalent model of a group of induction machines will be valid over the whole speed range (i.e., standstill to the full load condition).

The method which was developed to calculate the single equivalent model parameters is presented here.

Single Equivalent Model Electrical Parameters of a Group of Induction Motors

The standstill equivalent circuits of the individual machines are simplified by moving the magnetizing reactances to the terminals of the machines as shown in Figure 4.1a. If one first assumes that no deep bar rotor effects are present, then the resistance value of each machine R_i (i.e., subscript i denotes the ith machine) is simply the series combination of the stator winding resistance and the rotor resistance. The electrical parameters of the single equivalent model are obtained by making the circuits in Figures 4.1a and 4.1b electrically equivalent. The n machine equivalent model parameters are determined by

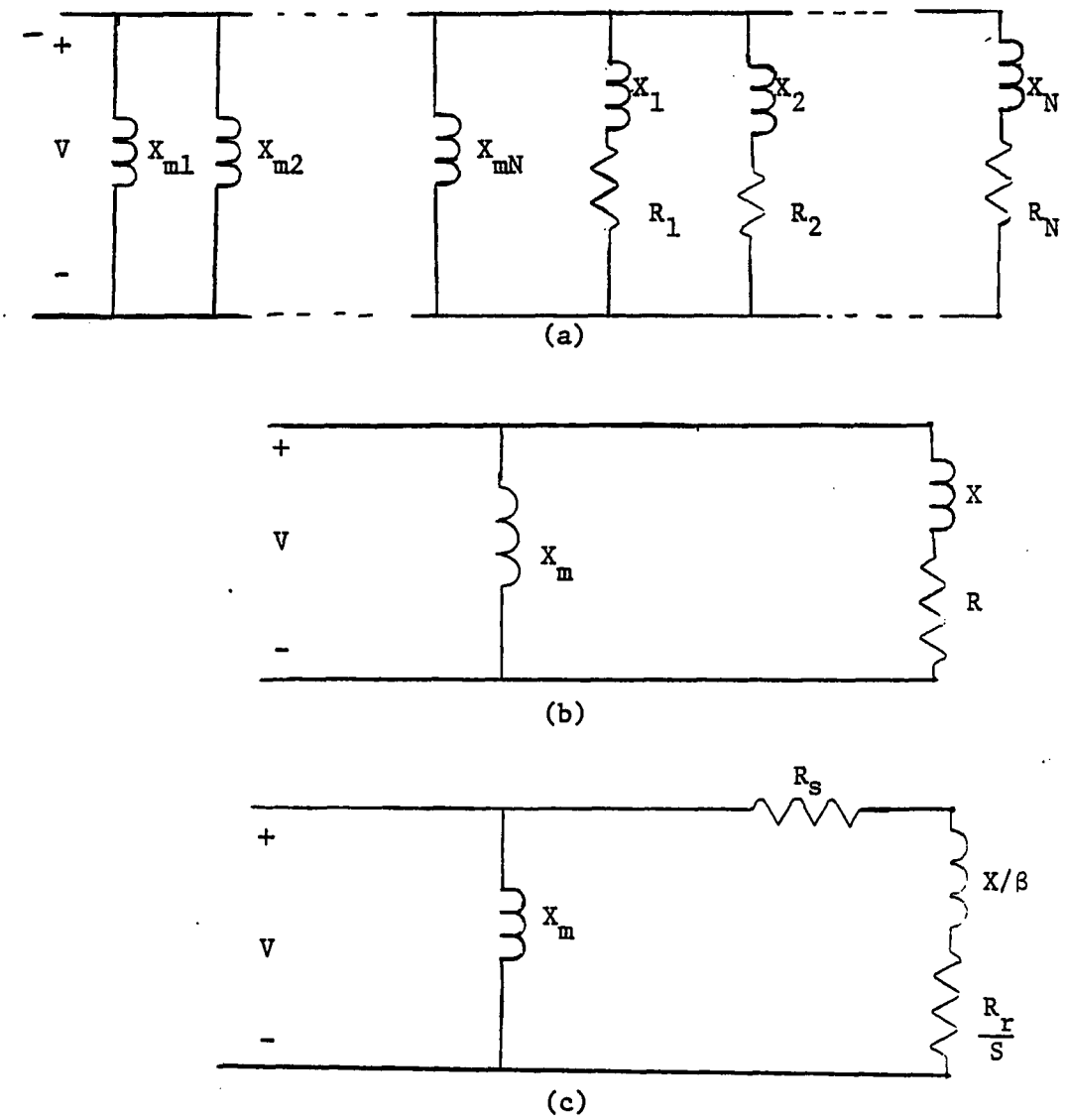

Figure 4.1. N-machine reduction to a single equivalent machine

$$(R + jX) = \left(\frac{1}{R_1 + jX_1} + \frac{1}{R_2 + jX_2} + \ldots + \frac{1}{R_n + jX_n}\right)^{-1} \qquad (4.1)$$

$$X_m = \left(\frac{1}{X_{m1}} + \frac{1}{X_{m2}} + \ldots + \frac{1}{X_{mn}}\right)^{-1} \qquad (4.2)$$

Then the equivalent resistance R is separated into an equivalent stator and rotor resistance by weighting the stator and the rotor resistances of the individual machines using the machine power rating as given by equations 4.3 and 4.4.

$$R = R_s + R_r \qquad (4.3)$$

$$\frac{R_r}{R_s} = \frac{\sum_{i=1}^{n} \frac{R_{ri}}{R_{si}} (VA_i)}{\sum_{i=1}^{n} (VA_i)} \qquad (4.4)$$

The resulting circuit is shown in Figure 4.1c.

Single Equivalent Model Including Deep Bar Effects

In order to include the deep bar effects, a linear relationship between the rotor resistance and slip is assumed resulting in a variable rotor resistance [3]

$$R_{rdb} = R_r(1 + K_{db}S) \qquad (4.5)$$

where:

K_{db} = deep bar effect linear constant, and

S = slip of the equivalent motor.

K_{db} may be found by calculating the equivalent locked rotor resistance using equations 4.1, 4.3 and 4.4 with the locked rotor ($s_i = 1$) resistance values of the individual motors.

$$K_{db} = \frac{R_{rLR}}{R_r} - 1 \tag{4.6}$$

where:

R_{rLR} = equivalent locked rotor resistance.

Figure 4.2 is the final single equivalent model of n parallel induction machines.

Analysis of the Leakage Reactance Coefficient for a Group of Induction Motors

For the case of two machines, an approximate method to obtain the magnitude of the leakage reactance coefficient was proposed. This method can be extended to be applicable to a group of induction machines. Consider the case of three machines. As one machine after another approaches steady-state speed, the resulting reactance coefficient can be approximated by the stepped function of Figure 4.3. The required times for each of the three machines to accelerate to the speed at its maximum torque are designated on the graph of Figure 4.3 as t_1, t_2, and t_3. These periods of time can be calculated from the run-up time expressions developed in Chapter II. The magnitudes of leakage reactance coefficient β_1, β_2 and β_3 are computed from the appropriate current ratios the same as for the two machine case.

Thus,

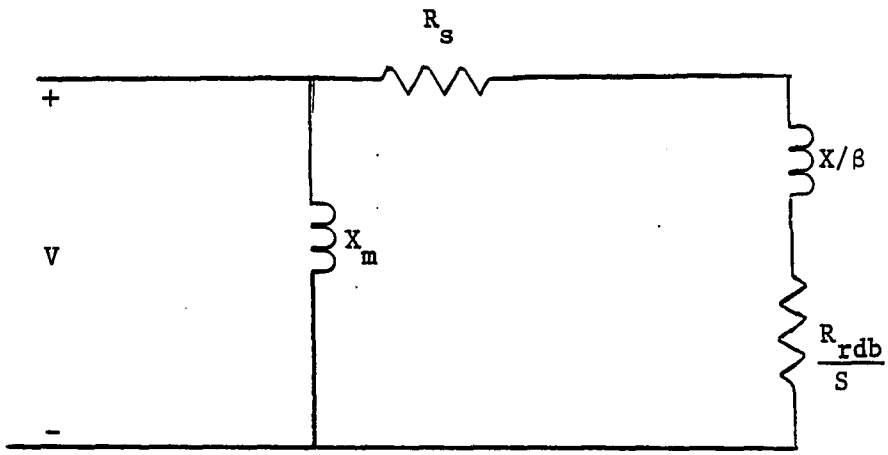

Figure 4.2. N-machine reduction to a single equivalent machine including deep bar effects

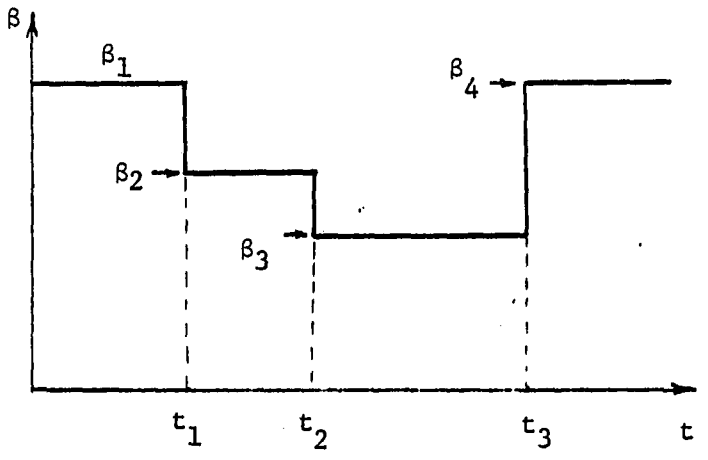

Figure 4.3. Three machine reactance coefficient

$$\beta_1 = \frac{\left|\sum_{m=1}^{3} I_m\right|}{\left|\sum_{m=1}^{3} I_m\right|} = 1 \tag{4.7}$$

$$\beta_2 = \frac{|I_2 + I_3 + i_1|}{|I_1 + I_2 + I_3|} \tag{4.8}$$

$$\beta_3 = \frac{|I_3 + i_1 + i_2|}{|I_1 + I_2 + I_3|} \tag{4.9}$$

$$\beta_4 = 1 \quad .$$

In the above equations, I_m is defined to be the current of the mth machine at the instant of start when $s_m = 1$. i_m is the steady-state current of the mth machine.

Therefore, for the case of n machines, the leakage reactance coefficient will be a multi-stepped function, as shown in Figure 4.4, and the magnitude at each step can be found by

$$\beta_m = \frac{\left|\sum_{i=m}^{n} I_i + \sum_{i=1}^{m-1} i_i\right|}{\left|\sum_{i=1}^{n} I_i\right|} \qquad m = 2, 3, \ldots, n \tag{4.10}$$

$$\beta_1 = \beta_{n+1} = 1 \quad . \tag{4.11}$$

Mechanical considerations of the single equivalent model

The equivalent model mechanical parameters are modeled by the following equations [8]

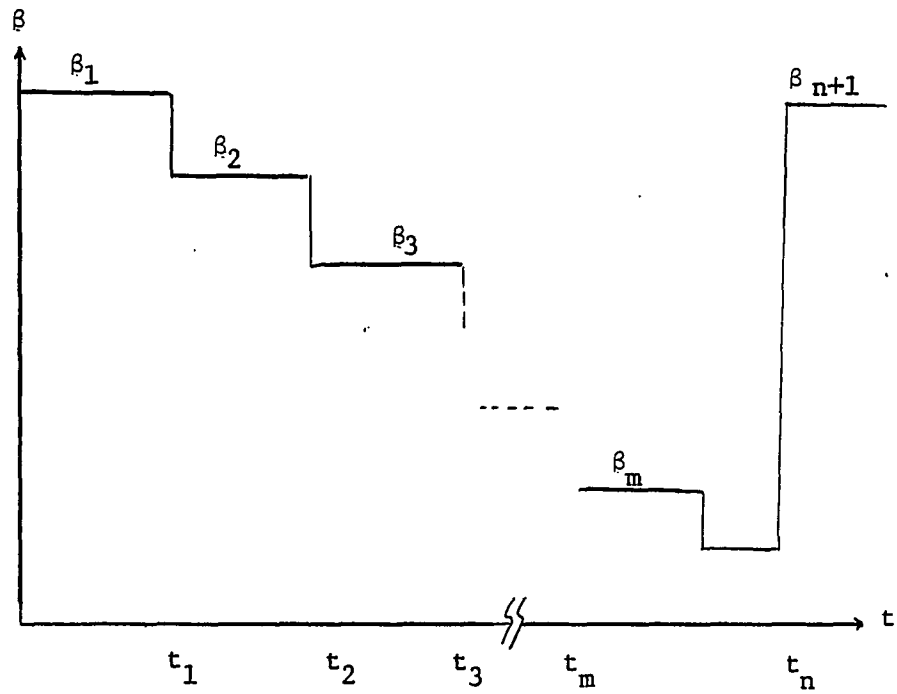

Figure 4.4. N machines leakage reactance coefficient β

$$H = \frac{\sum_{i=1}^{n} H_i (VA_i)}{\sum_{i=1}^{n} (VA_i)} \tag{4.12}$$

where:

H_i = inertia constant (sec) of ith machine;

VA_i = volt amper rating of ith machine; and

H = equivalent inertia constant (sec).

The mechanical torque load of the equivalent model is assumed to have an exponential form

$$T_m = T_0 \, \omega^{\alpha} \tag{4.13}$$

where:

T_m = mechanical torque on the motor shaft in per unit;

T_0 = load torque at synchronous speed;

ω = motor speed in per unit of synchronous speed; and

α = speed exponent for mechanical torque model.

The equivalent mechanical load parameters T_0 and α can be calculated by using equations 4.14 and 4.15:

$$T_0 = \sum_{i=1}^{n} T_{0i} \tag{4.14}$$

$$\alpha = \log_{\omega} \left[\frac{\sum_{i=1}^{n} T_{0i} \, \omega_i^{1+\alpha_i}}{T_0} \right] - 1 \, . \tag{4.15}$$

Criteria for Grouping Similar Motors

In this chapter, a method of combining a group of induction motors has been presented. However, in studies involving motor load

representation for large networks, substantial computational effort could be saved by dividing n number of motors into m similar subgroups of motors. The equivalent model for each subgroup can be determined using the technique which was developed in this chapter, with the equivalent model of each subgroup of induction motors having a constant leakage reactance. All similar subgroups of motors are then combined using the same method which was previously explained to obtain the single equivalent model for the group of n induction motors. This single equivalent model of the group of n motors will then have a variable leakage reactance with m-1 different calculated values instead of n-1 values.

The main criteria used to determine the similarity for any group of motors are the individual motors' run-up times. Therefore, any number of induction motors, regardless of their sizes and ratings, which have the same or nearly the same run-up time, can be put in the same similar subgroup. The equivalent parameters of the similar subgroup model can be found without detailed calculation of the variable leakage reactance coefficient because the coefficient would have little or no variation with respect to time.

In addition to run-up time, another criterion for establishing similar motor groups is the ratio of the motors' ratings. The reason to include the ratio of motor ratings as a criterion for grouping similar motors is as follows. When two motors have vastly different ratings, the characteristics of the bigger machine (i.e., current, power and reactive power) will dominate that of the smaller machine, as a result of which the smaller machine will have negligible effect on the equivalent group.

In practical studies, it is difficult to have two or any number of motors with exactly the same run-up times. Therefore, a criterion called similarity parameter will be defined and used to recognize similar motors. The similarity parameter is defined as follows:

$$sp = \frac{\text{percent difference in motors' run-up times}}{\text{ratio of motors' ratings}} .$$

The percent difference between run-up times of two motors is defined with the smaller of the two run-up times in the denominator. The ratio of motors' ratings in the above equation is always taken as the ratio greater than or equal to one.

In order to calculate the percent errors resulting from grouping two machines in a similar subgroup, a number of possible combinations were simulated. Each machine's run-up time was varied from 2 to 50 percent of a typical 100 hp motor run-up time. Then, the errors in the current envelopes compared to the vector summation of the currents obtained from the separate simulation of the two motors were calculated. Table 4.1 shows the error in the inrush current envelope for different run-up times and ratings and the calculated values of the similarity parameter.

A study case showed that for an assumed maximum error tolerance of 2.5% in the inrush current envelope, the similarity parameter maximum limit will be 0.033. Therefore, in order to divide a group of motors into similar subgroups using 2.5% as the maximum error, the similarity parameters should be calculated for all machine combinations and compared against the similarity parameter maximum limit of 0.033. Those combinations of machines with a similarity parameter less than 0.033 can be placed in the same similar subgroup.

Table 4.1. Current vs. time errors and similarity parameter values

Motor rating ratio[b]	Percent run-up time difference between pairs of motors[a]						
	2	4	6	8	10	20	50
1	0.98 / 0.02	1.92 / 0.04	2.38 / 0.06	3.70 / 0.08	4.36 / 0.10	12.50 / 0.20	16.00 / 0.50
2	0.65 / 0.01	1.28 / 0.02	1.88 / 0.03	2.46 / 0.04	3.03 / 0.05	5.55 / 0.10	11.11 / 0.25
3	0.49 / 0.006	0.96 / 0.013	1.40 / 0.02	1.80 / 0.025	2.27 / 0.033	4.16 / 0.067	8.33 / 0.167
5	0.32 / 0.004	0.64 / 0.008	0.94 / 0.012	1.23 / 0.016	1.52 / 0.02	2.78 / 0.04	5.56 / 0.10
6	0.28 / 0.003	0.55 / 0.006	0.81 / 0.01	1.06 / 0.132	1.30 / 0.165	2.38 / 0.033	4.76 / 0.833
8	0.22 / 0.002	0.43 / 0.005	0.63 / 0.0075	0.82 / 0.01	1.01 / 0.0125	1.85 / 0.025	3.70 / 0.0625
10	0.18 / 0.002	0.35 / 0.004	0.51 / 0.006	0.67 / 0.008	0.83 / 0.01	1.52 / 0.02	3.03 / 0.05
20	0.09 / 0.001	0.18 / 0.002	0.27 / 0.003	0.35 / 0.004	0.43 / 0.005	0.79 / 0.01	1.59 / 0.025
25	0.08 / 0.001	0.15 / 0.002	0.23 / 0.003	0.30 / 0.004	0.36 / 0.005	0.67 / 0.008	1.33 / 0.02

[a]Each entry in Table 4.1 has the format of

$$\frac{\text{Error in current vs. time curve in percent}}{\text{Similarity parameters (sp) values}}$$

[b]The base motor parameters used are typical parameters for a 100 hp motor.

Summary

In this chapter, a method of obtaining the electrical parameters for a single equivalent model was proposed. This method was extended to include the deep bar rotor effects of induction machines. This single equivalent model has a variable leakage reactance coefficient β. An algorithm to obtain approximate values of the variable leakage reactance coefficient was proposed. Expressions to obtain the equivalent mechanical parameters for the single equivalent model were also given in this chapter. In the last portion of this chapter, the criteria which are needed to divide a group of motors into similar subgroups were established.

CHAPTER V. MODEL VERIFICATION AND APPLICATION

In order to verify the proposed single equivalent model for a group of induction motors, both digital simulation and experimental methods were used. In this chapter, a series of simulation results will be presented.

These simulation studies include:

(1) Starting a group of induction machines.

(2) Similar motor grouping.

(3) Proposed model comparison with other models.

(4) Applications.

Starting a Group of Induction Machines

This part of the simulation studies has been subdivided into three categories:

(a) simultaneous starting;

(b) nonsimultaneous starting; and

(c) mixture of running and starting.

Verification of the single equivalent model for simultaneous starting

The starting current-time variation was obtained by digital computer for different pairs of machines and also for different combinations of three machines. Figure 5.1 shows the system configuration under study. In each case, the equivalent model parameters were computed as outlined in previous chapters and the equation of motion 2.21 was integrated by the fourth order Runge-Kutta method. The current computed for the model

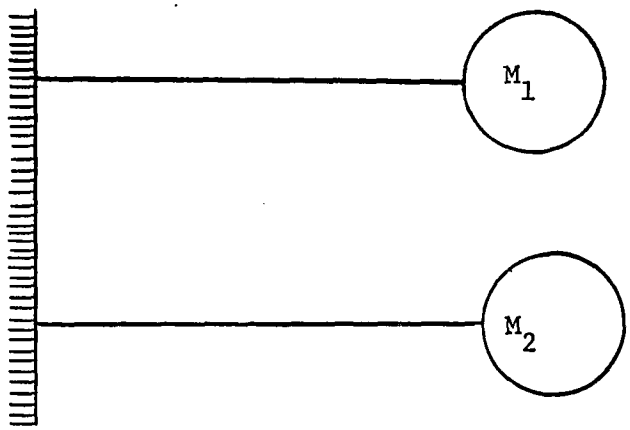

(a)

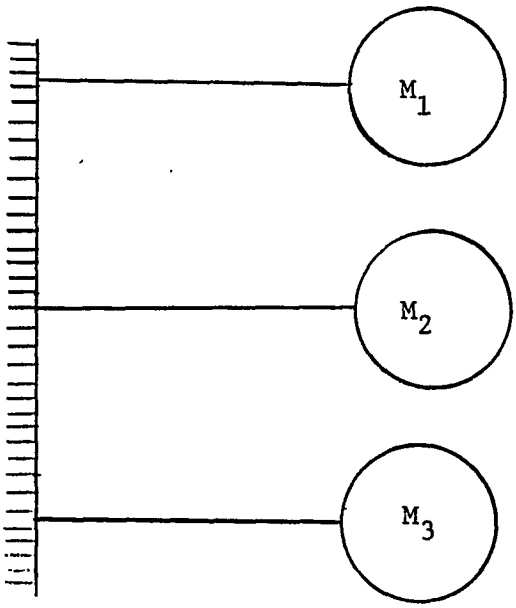

(b)

Figure 5.1. Parallel induction machines supplied from an infinite bus voltage

was then compared with that obtained by the vector summation of the separate motor currents calculated for each motor using the individual motor equivalent circuit and the same equation of motion. Table 5.1 shows all the parameters for each machine under study.

Figures 5.2 and 5.3 show this comparison for different pairs of machines, and the overall results show good agreement. Figures 5.4 and 5.5 show the current-time variation for combinations of three machines. These curves illustrate the accuracy of the single equivalent model.

Verification of the single equivalent model for nonsimultaneous starting

In this case, a typical 100 hp motor started 0.3 sec after a 1000 hp motor. Figure 5.6 shows the current time variation for a combination of these two machines with nonsimultaneous starting. The simulation results as shown in Figure 5.6 indicate a good agreement between the proposed model and the simulation of individual motors.

Verification of the model for a motor group including a mixture of running and starting motors

The dynamic single equivalent model for a group of motors has been shown to be valid for the cases of all motors starting at the same time, two or more motors starting at different times such that some of the motors have not reached steady-state before additional motors are switched on, and all motors initially at steady-state. This section presents the results of another case not previously considered, but one which will occur often in dynamic studies.

Table 5.1. Machine parameters[a]

Motor	hp	R_s	R_r	X	X_m	H
1	7.5	0.296	0.255	1.266	21.24	0.0025
2	10	0.377	0.312	1.1	14.655	0.003
3	20	0.2	0.175	1.5	12.5	0.012
4	300	0.005	0.0045	0.05	0.9	0.04
5	100	0.015	0.015	0.16	2.7	0.13
6	500	0.0024	0.0025	0.032	0.6	0.9
7	1000	0.0011	0.0011	0.016	0.35	1.7
8	2500	0.0004	0.0004	0.0064	0.132	8.75

[a]All parameters are on a 100 hp base.

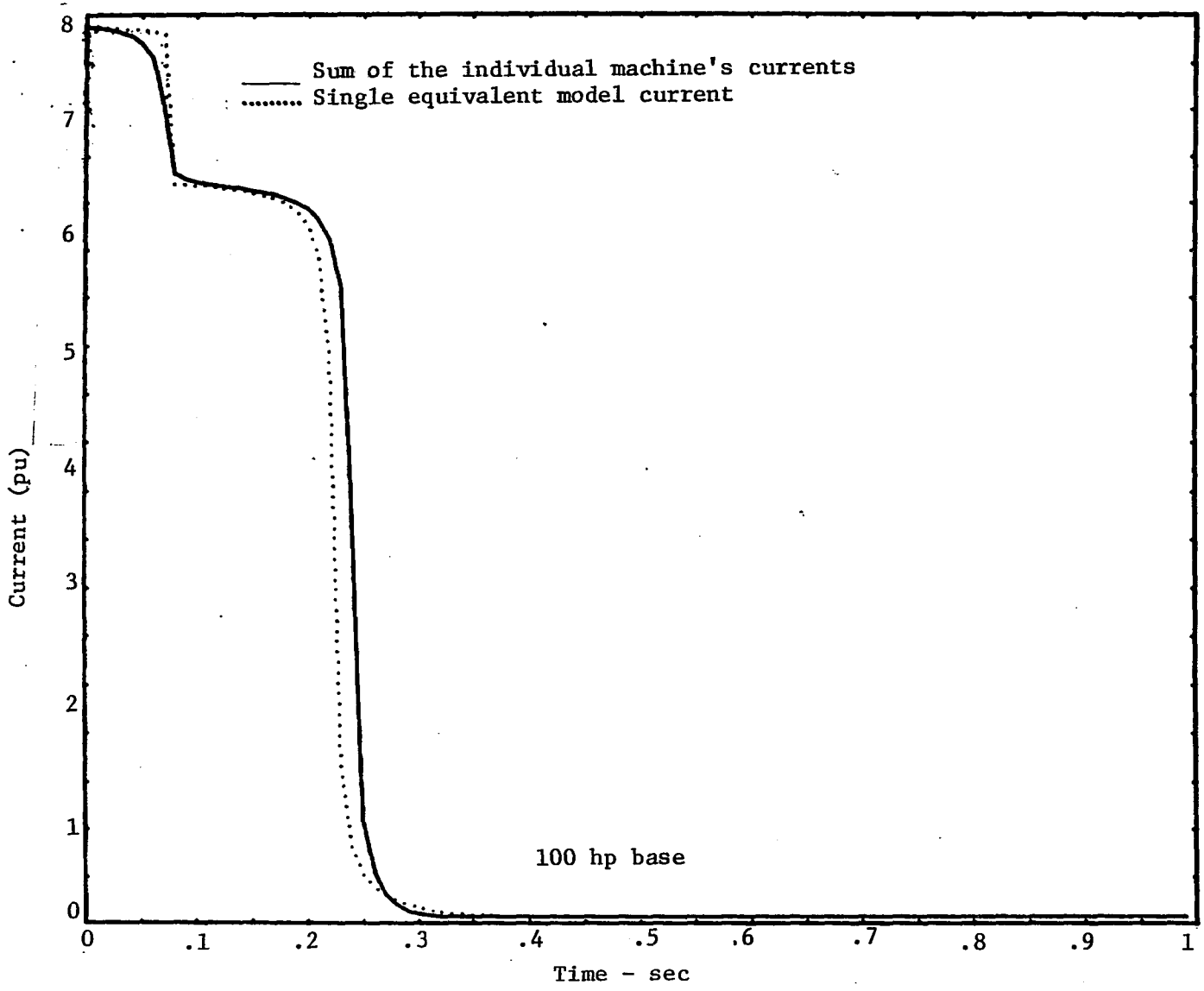

Fig. 5.2. Starting current comparison 20 hp/100 hp. Currents in per unit on 100 hp base

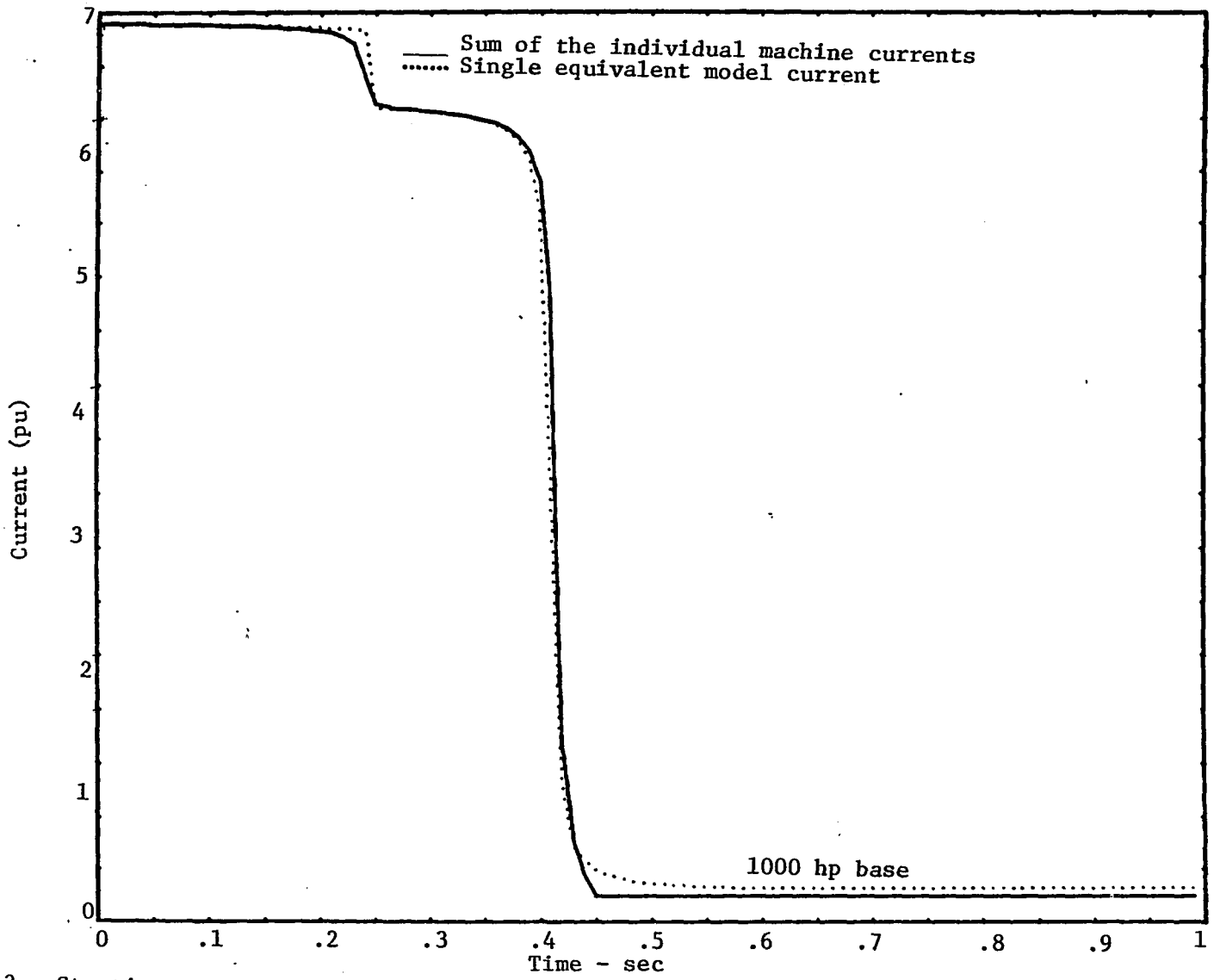

Figure 5.3. Starting currents 100 hp/1000 hp

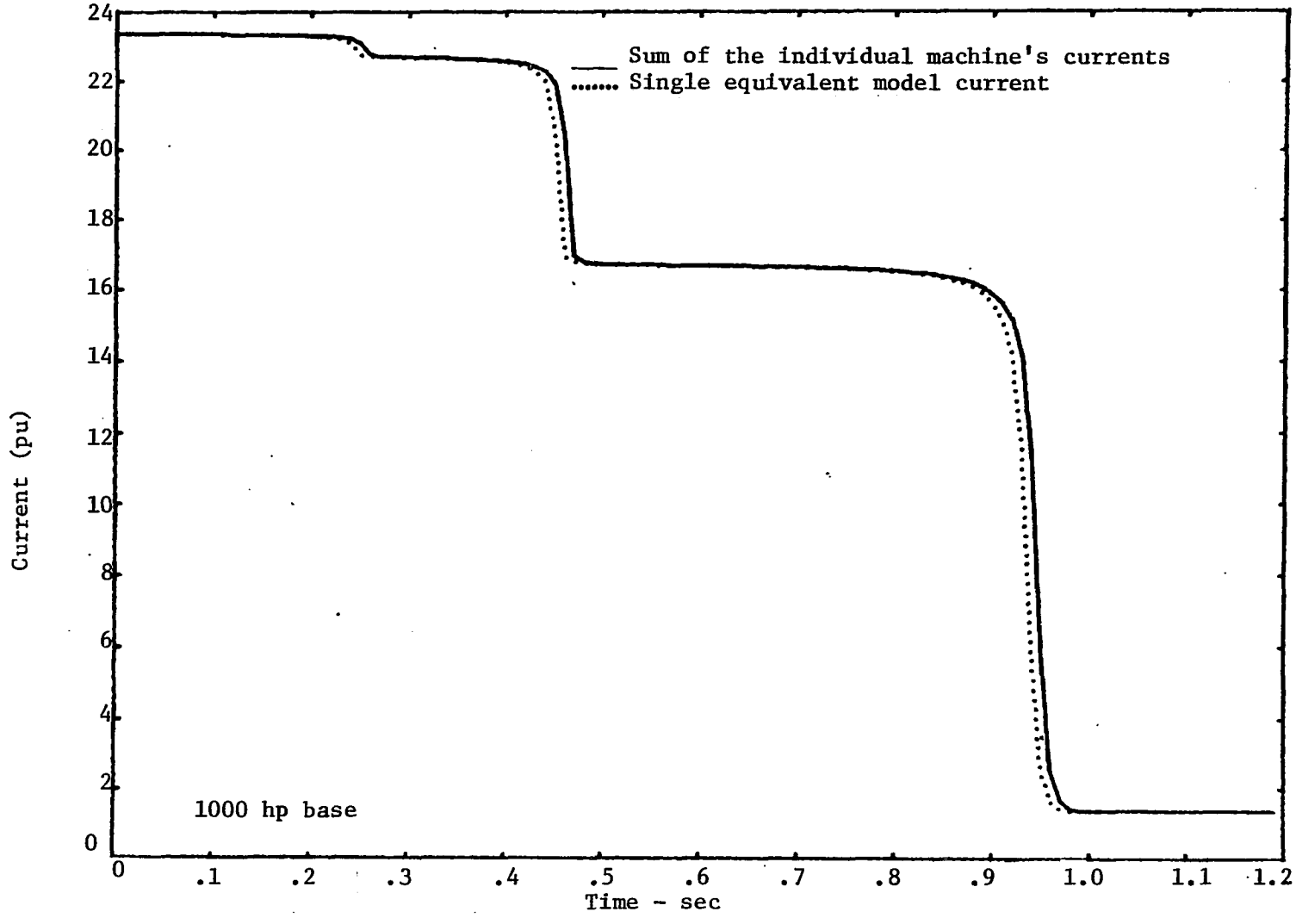

Figure 5.4. Starting current 100/1000/2500 hp

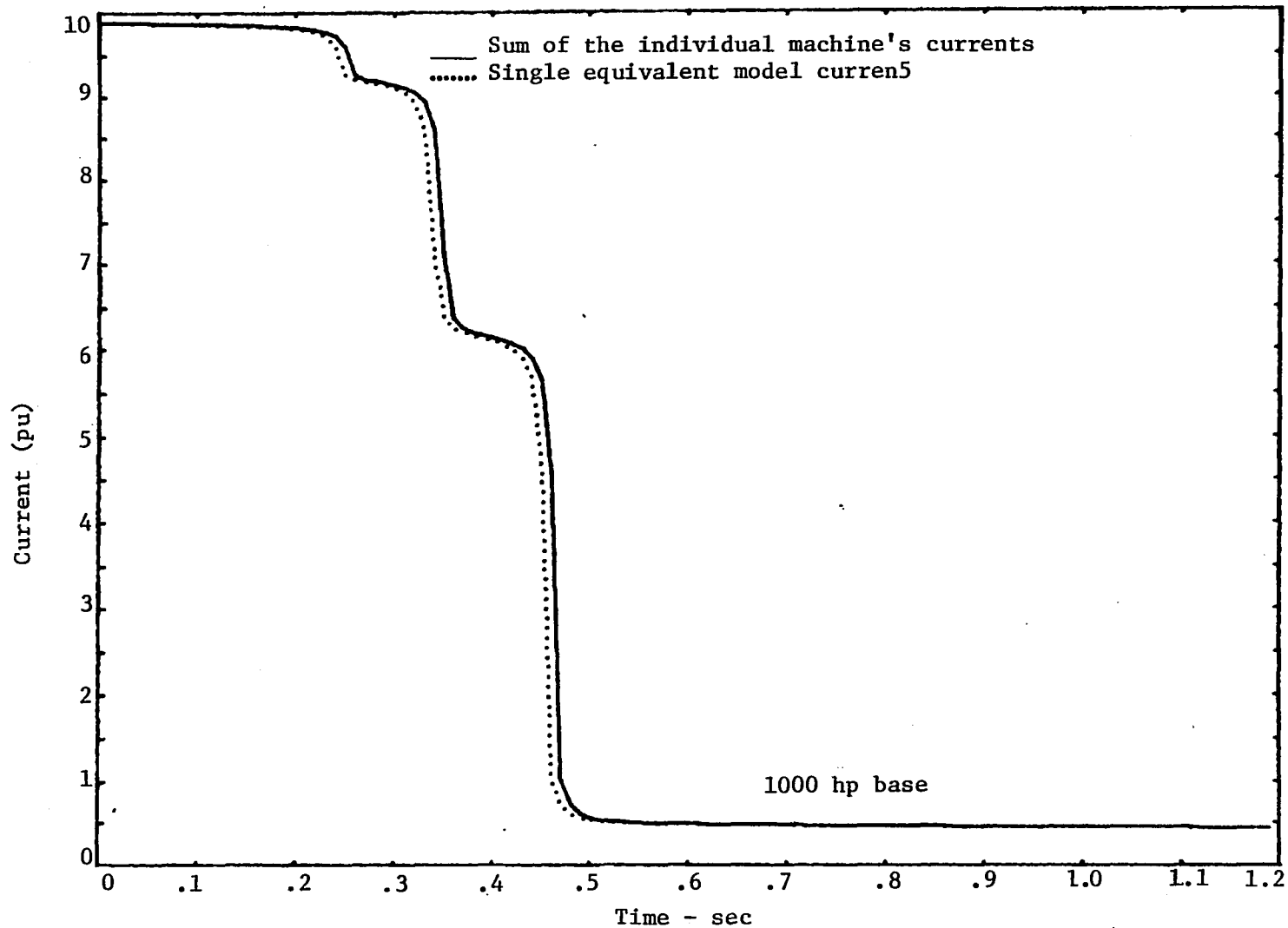

Figure 5.5. Starting current 100/500/1000 hp

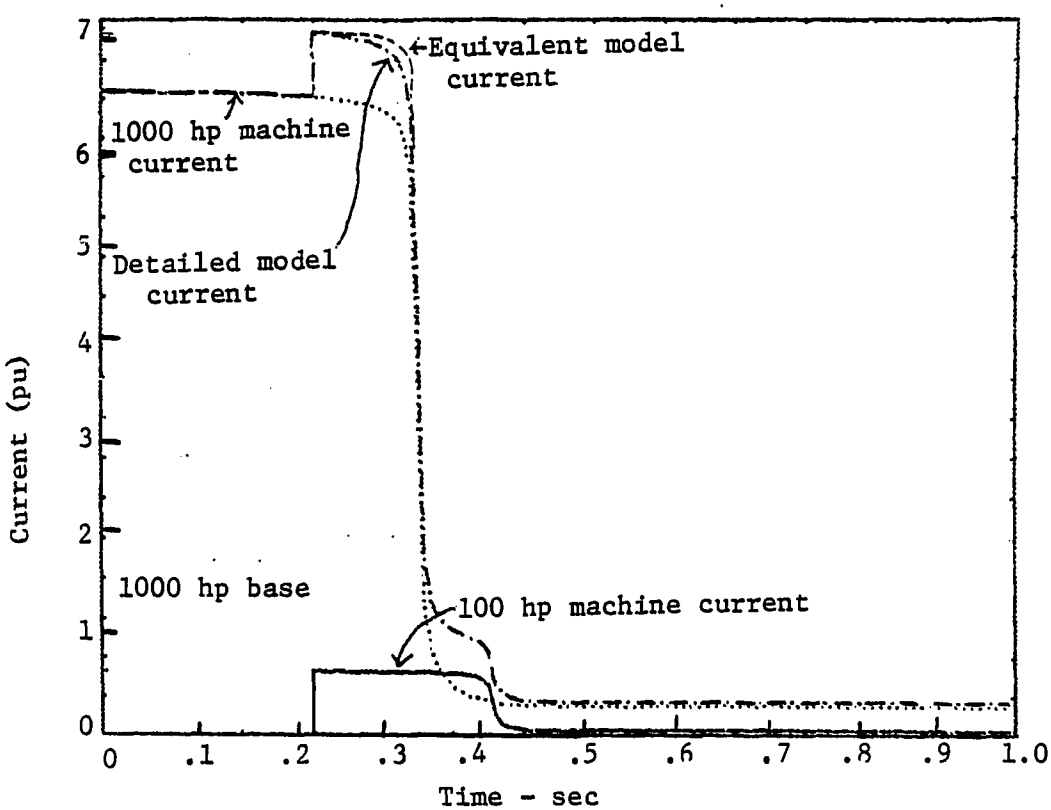

Figure 5.6. Starting current with different starting times (100 hp started 0.3 sec after 1000 hp motor)

Normally, most of the motors in a system will be running under steady-state conditions with some motors being switched on and off. The case presented here considers starting motors with other motors initially operating at steady-state.

The specific system simulated used three motors specified in Table 5.1. A 2500 hp motor was initially at steady-state and 100 and 1000 hp motors were started at the same time. A plot of the current versus time is shown in Figure 5.7 for both the single equivalent model simulation and the vector summation of the three individual machines. The plots are extremely close, thus verifying the model for this case.

Simulation Verification of the Single Equivalent Model for Grouping Similar Motors

A 19-motor group was identified with parameters shown in Table 5.1. The similarity parameter (sp) values were determined as developed in Chapter IV for each pair of motor groups with the closest run-up times as indicated in Figure 5.8a. For the combinations where the sp value was less than 0.033, the motors were combined into similar subgroups. This resulted in three subgroups shown in Figure 5.8b. To obtain the single equivalent model parameters, these three similar subgroups were combined using the technique which was developed in Chapter IV. A starting simulation was done on the single equivalent motor. Starting current resulting from this simulation was compared to the summation of the starting currents for all 19 motors, as shown in Figure 5.9. The difference in the results from the two methods was small.

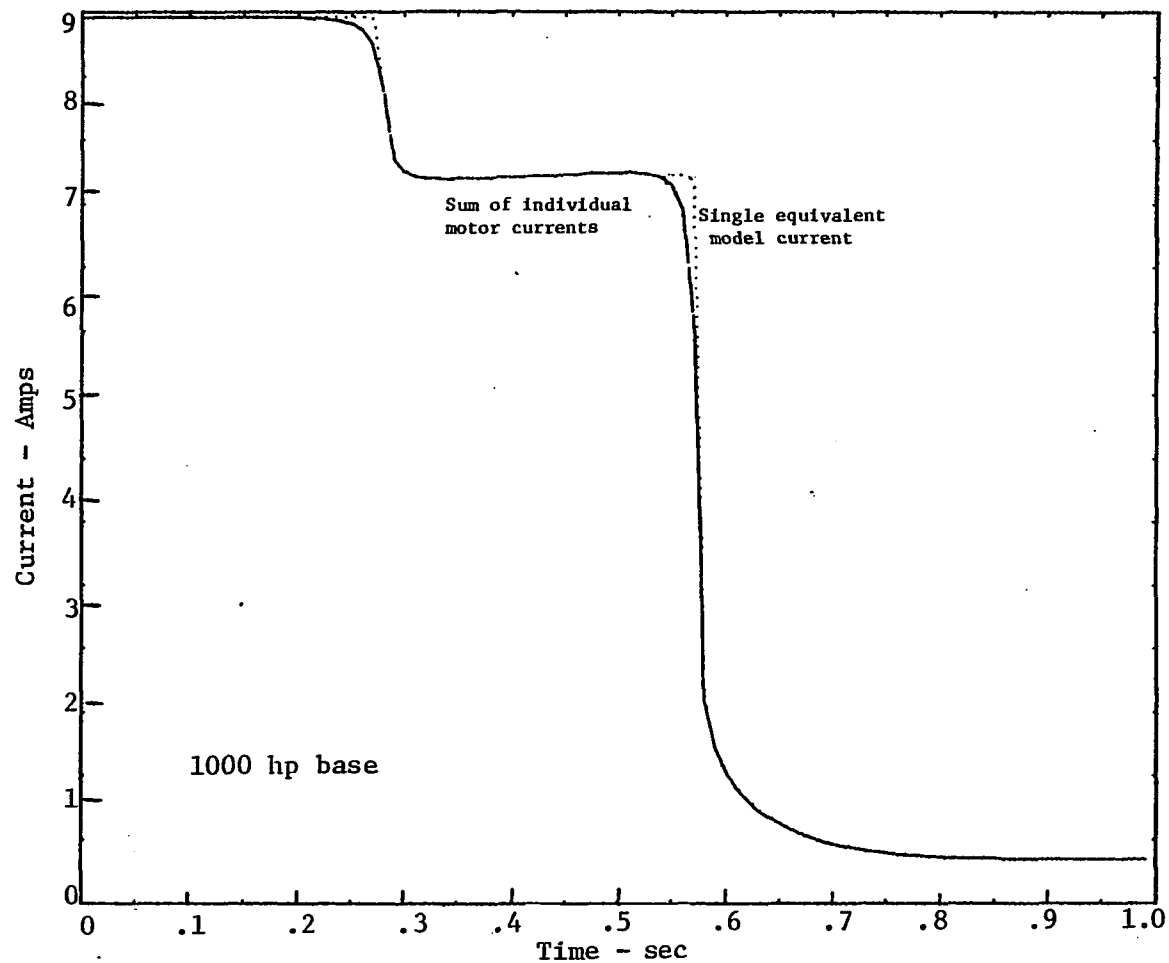

Figure 5.7. 2500 hp motor at steady-state while 100 hp and 1000 hp start

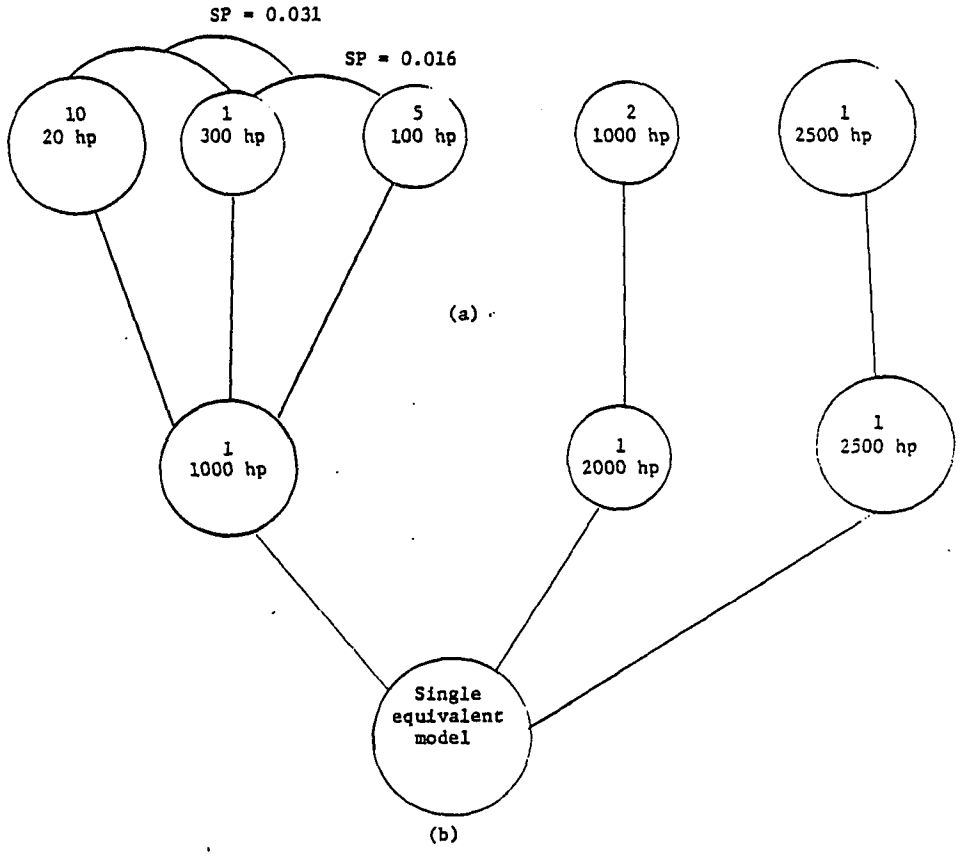

Figure 5.8. Similar motor groups
(a) Initial grouping
(b) Final grouping

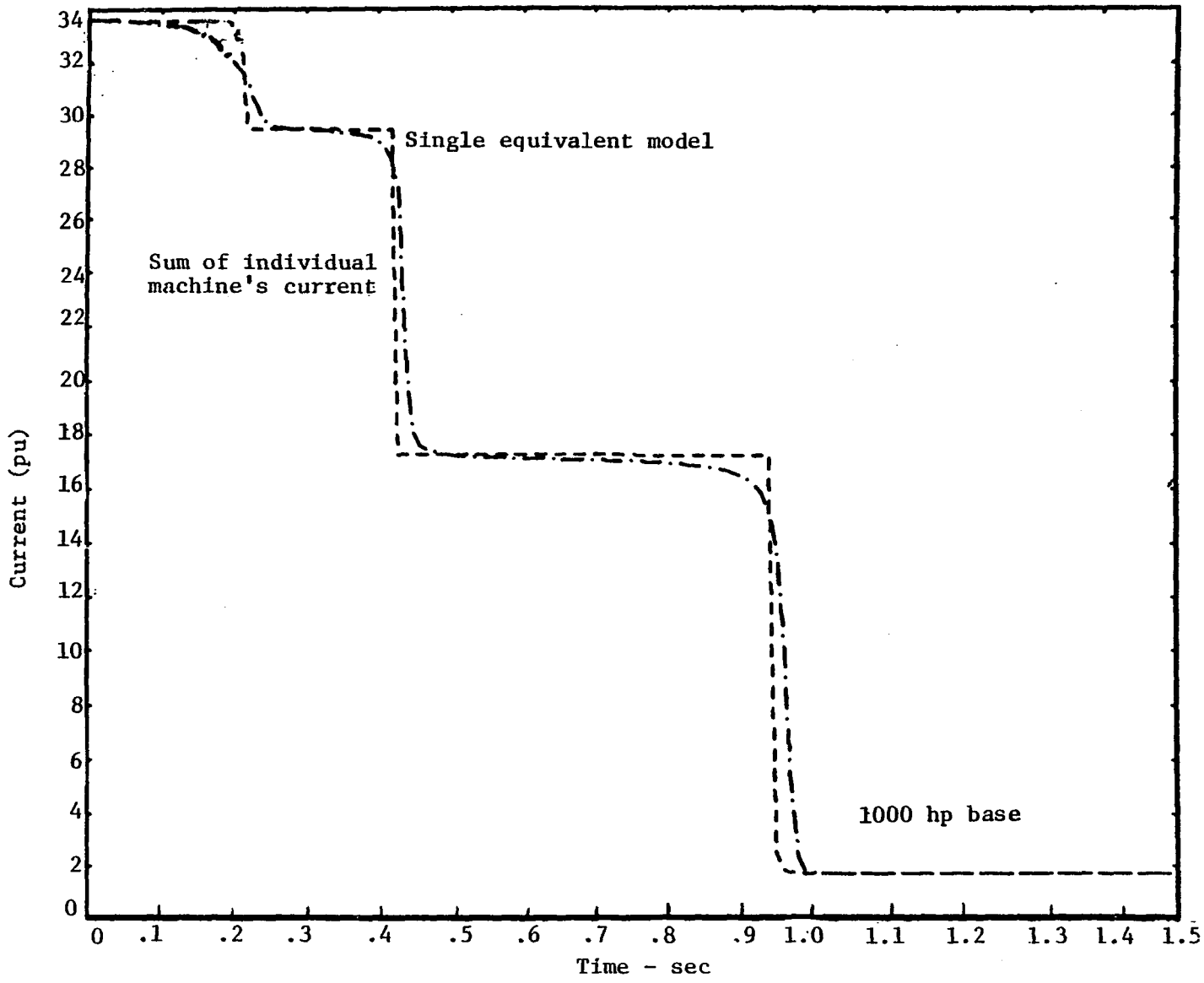

Figure 5.9. Nineteen motor group reduced to three similar subgroups

Single Equivalent Model Comparison with Other Models

The load representation in typical system studies is a static load model where the load is represented as a constant MVA, constant current, constant impedance or some combination of the three. As an alternative, part of load may also be modeled in detail as an induction or synchronous motor. In this part of the comparison, a number of induction machines of different sizes and ratings were chosen with the parameters given in Table 5.1. These induction motor loads were simulated for a simultaneous start-up using the equivalent circuit of each induction motor. Superposition of currents, input apparent power, input reactive power and torques of this simulation will be referred to as the detailed load model. The following comparisons are made to illustrate the differences among several models.

First, a single equivalent dynamic load model found in the literature is compared against the detailed model.

Second, the proposed single equivalent model is compared against the detailed model.

Finally, the proposed model will be compared with experimental results.

Comparison of the detailed model against an existing model

There are not any models available describing the behavior of the load which include starting transients. Berg's model [4] is the closest model which could be applied, but as can be seen in Figure 5.10, it fails to accurately predict the starting transient of the group of motors.

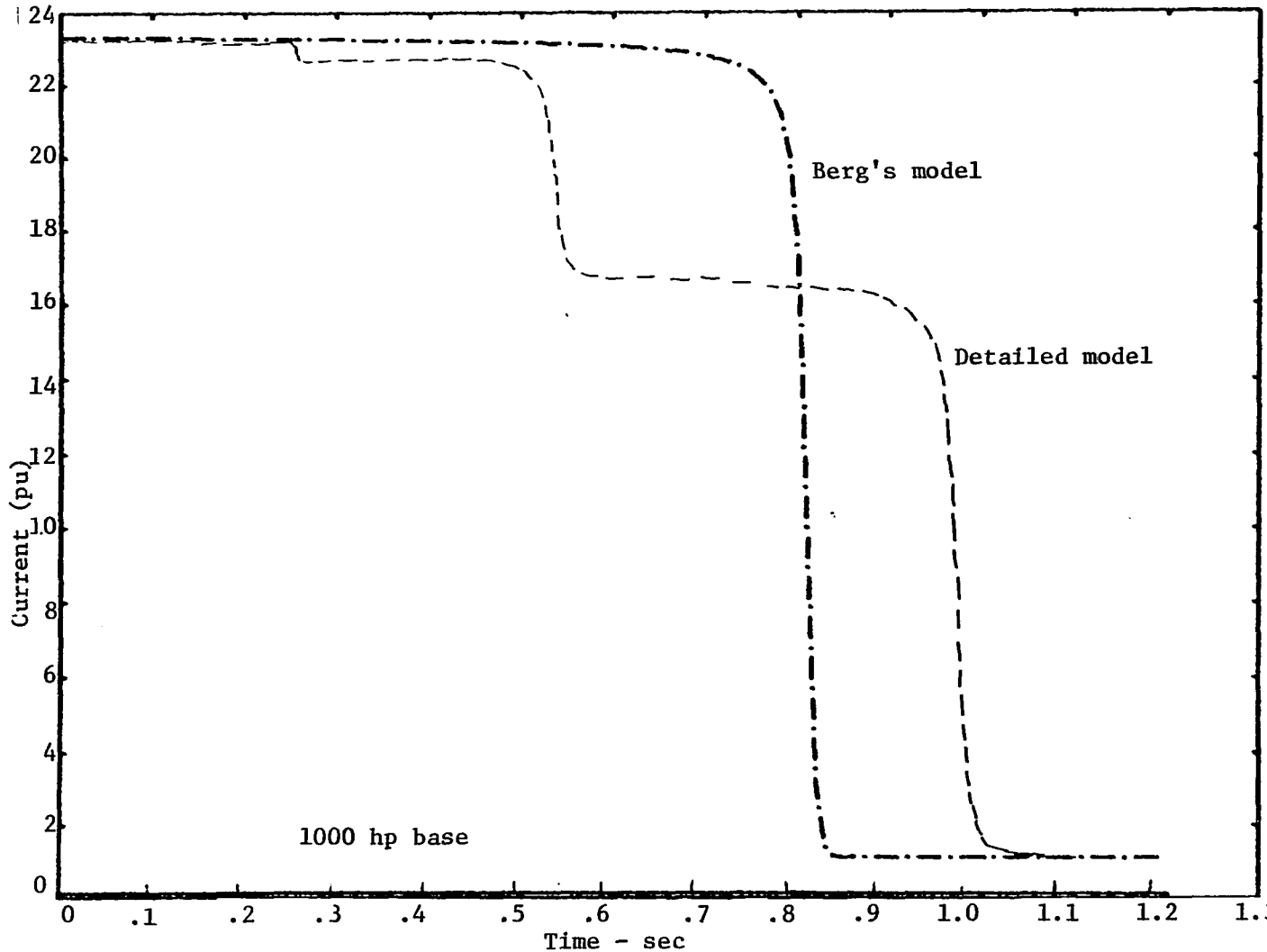

Figure 5.10. Characteristics of Berg's model
(a) Current vs. time

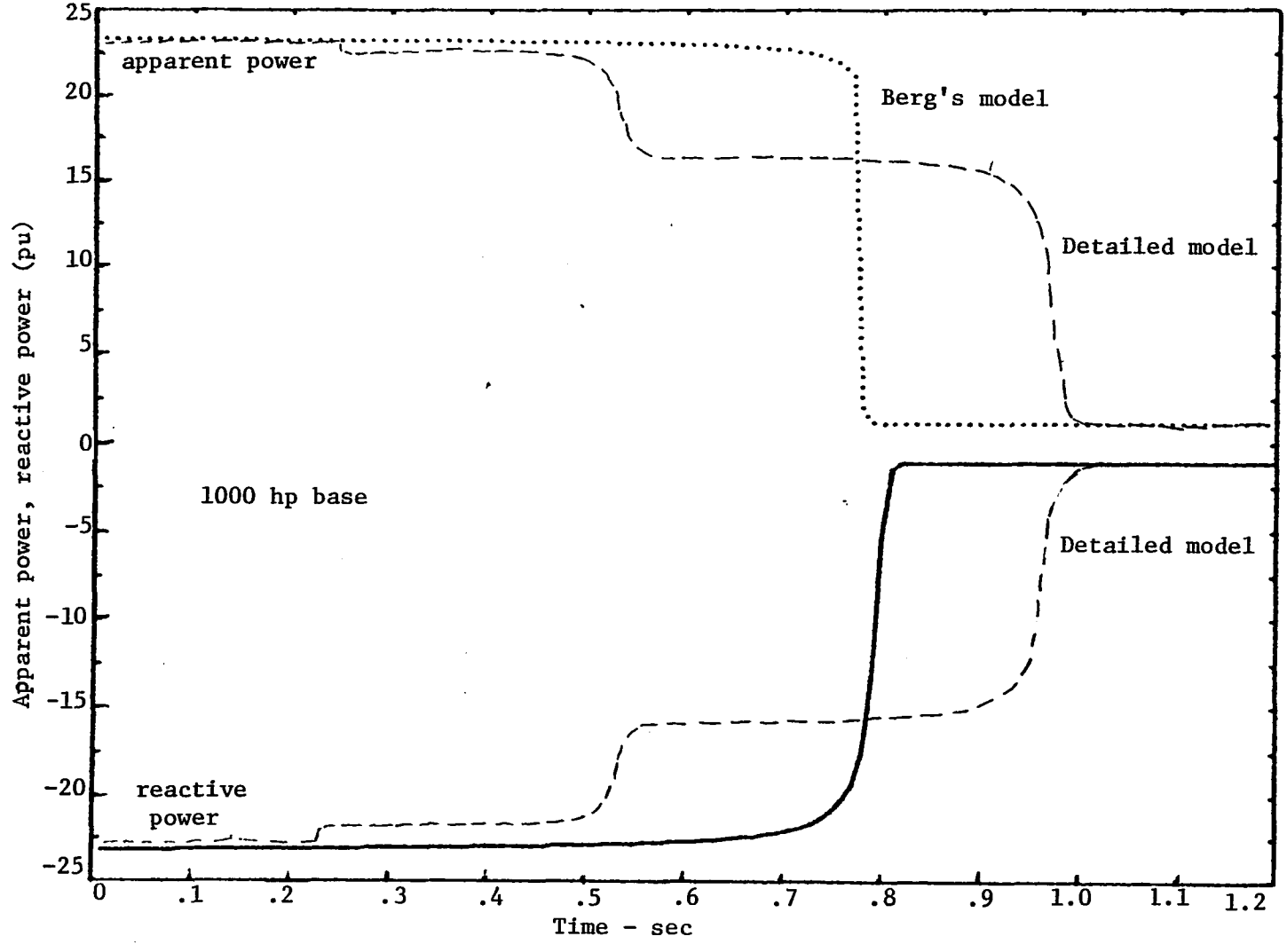

Figure 5.10. (Continued)
(b) Apparent power and reactive power vs. time

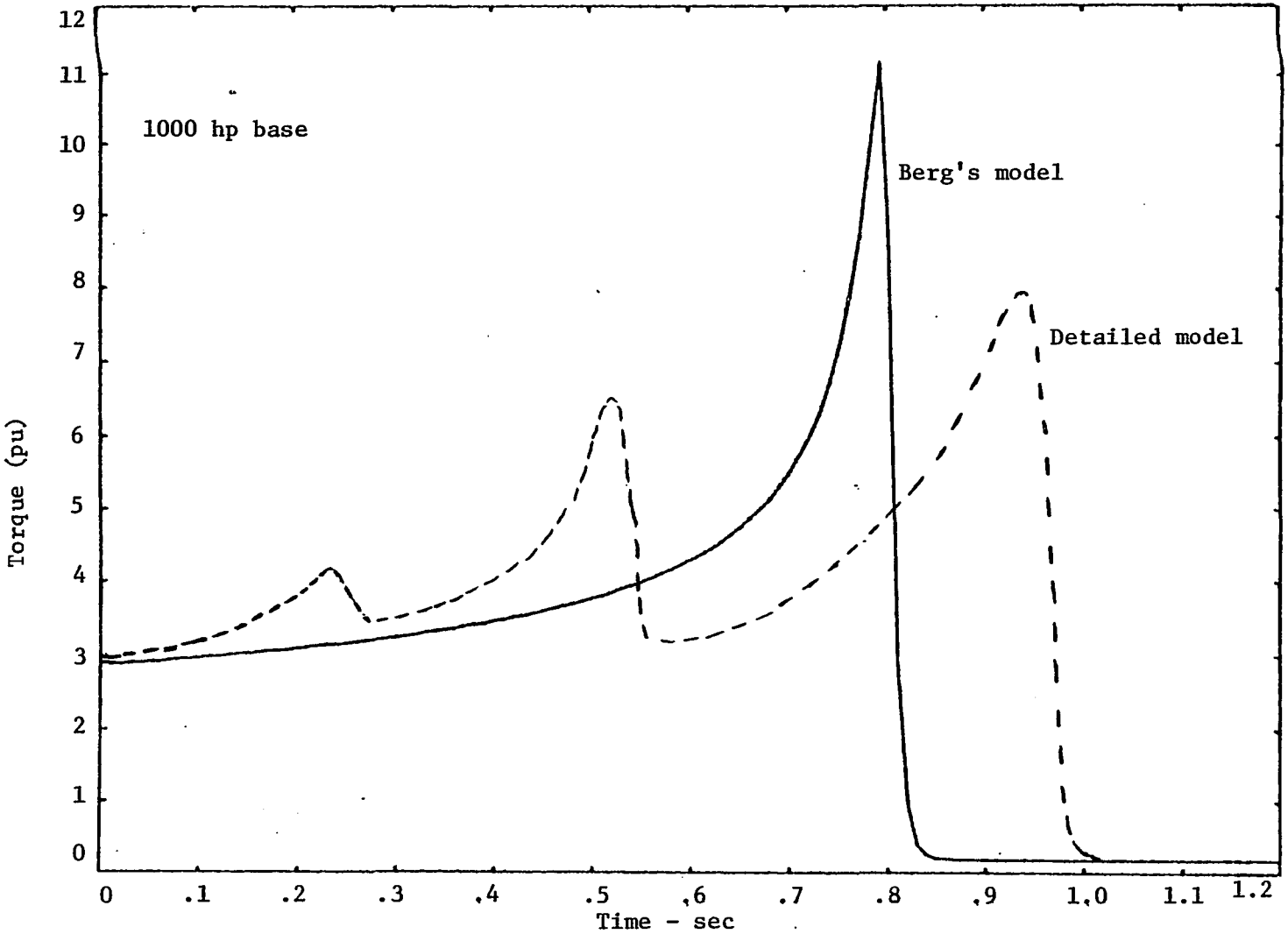

Figure 5.10. (Continued)
(c) Torque vs. time

There are two distinct differences in Berg's model [4] for starting transients: (1) the variation in the magnitude of the current is not predicted; and (2) the run-up time of his equivalent model is much less than the actual detailed model. Figures 5.10a, b, and c show results obtained from both models and the differences are clearly illustrated.

Comparison of the detailed model against the proposed single equivalent model

The same combination of three machines as in the previous case with Berg's model was simulated using the proposed equivalent model. The results from the detailed model agree quite well with the proposed equivalent model, as seen in Figures 5.11a, b, and c. This has also been illustrated with other results discussed earlier in this chapter.

Comparison between the single equivalent model and experimental results

Two induction machines of 7.5 hp and 10 hp ratings with parameters given in Table 5.1 were chosen. These two machines normally have nearly the same run-up times. It was more desirable to compare the proposed equivalent model with machines having different run-up times. Therefore, the 10 hp machine was coupled to the shaft of a dc motor in order to increase the machine's inertia constant. This resulted in a longer run-up time for that machine.

The combined inertia constant of the 10 hp induction machine and the coupled dc machine was found by measuring the mechanical load time constant τ_L which describes the rate at which the two coupled machines coast when the armature circuit is opened on the dc motor.

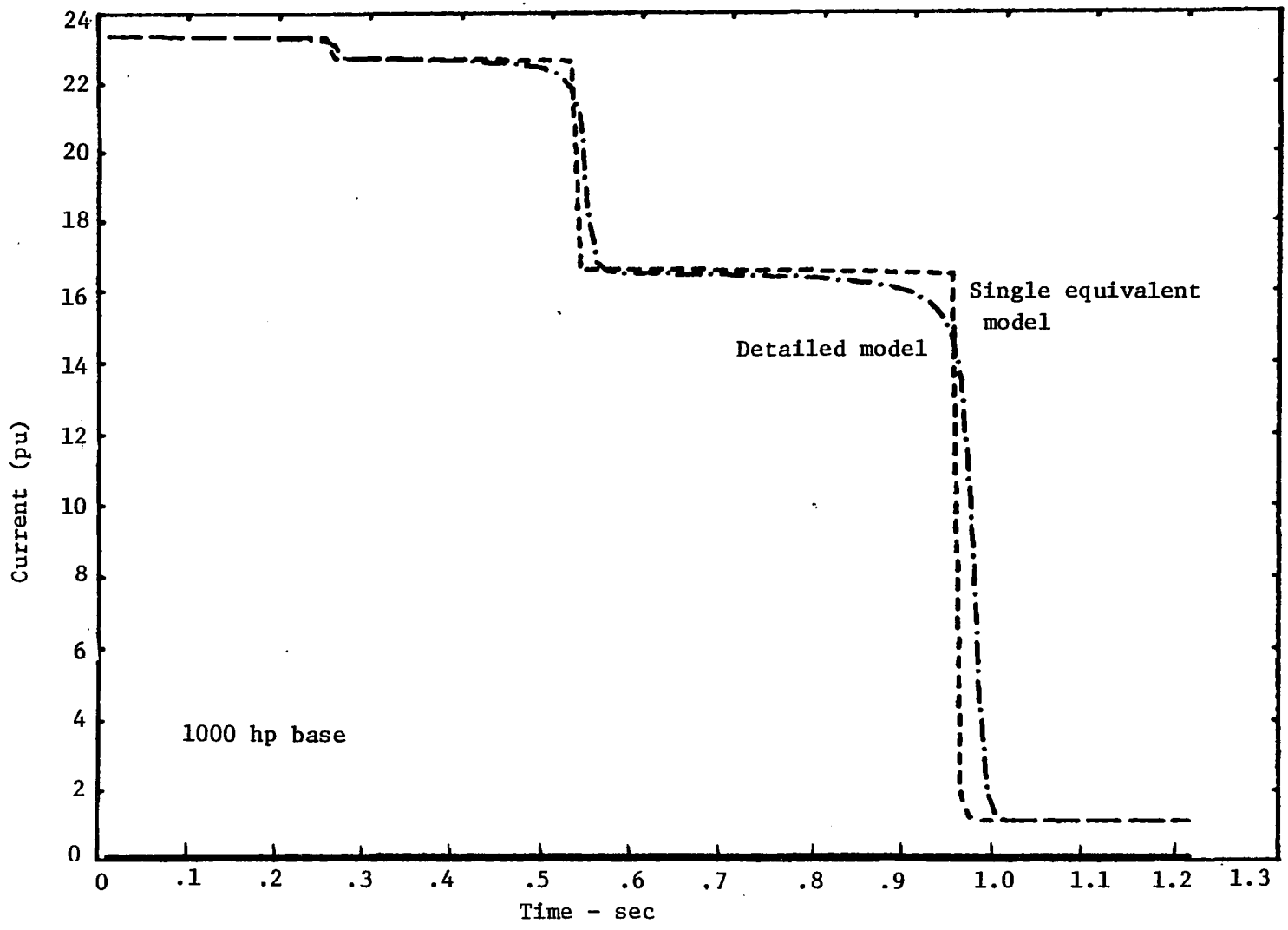

Figure 5.11. Characteristics of single equivalent model compared with the detailed model
(a) Current vs. time

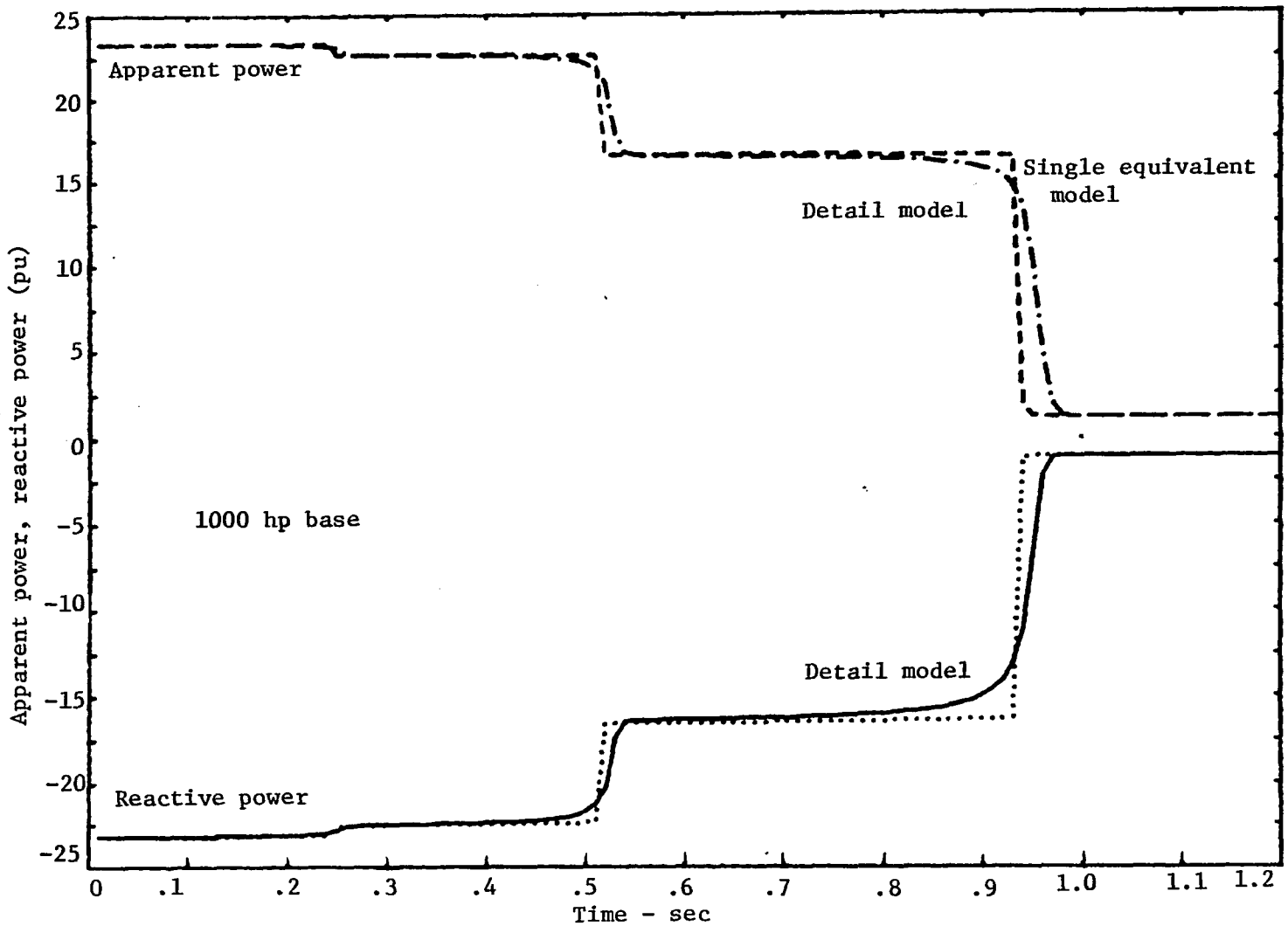

Table 5.11. (Continued)
(b) Apparent power and reactive power vs. time

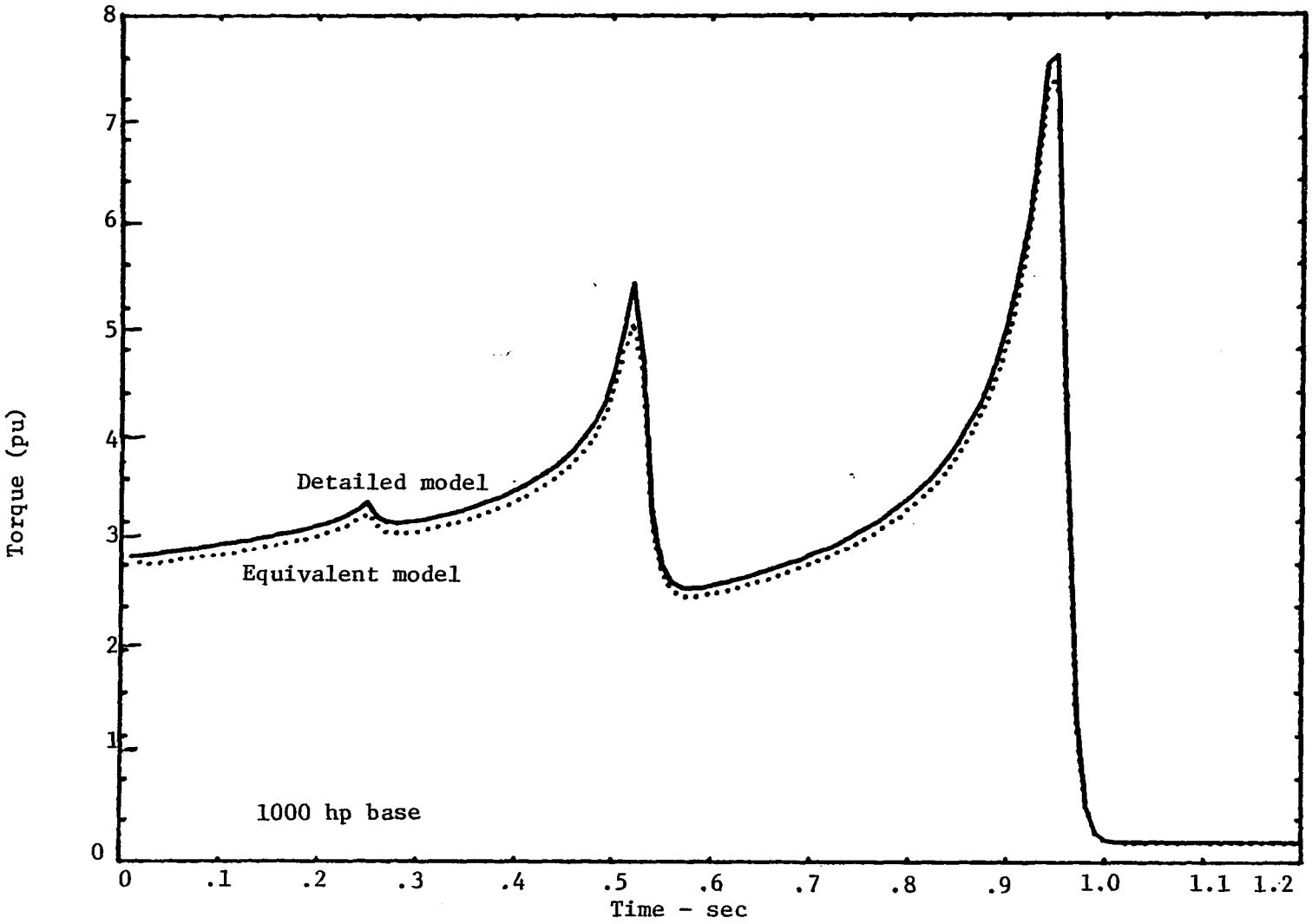

Figure 5.11. (Continued)
(c) Torque vs. time

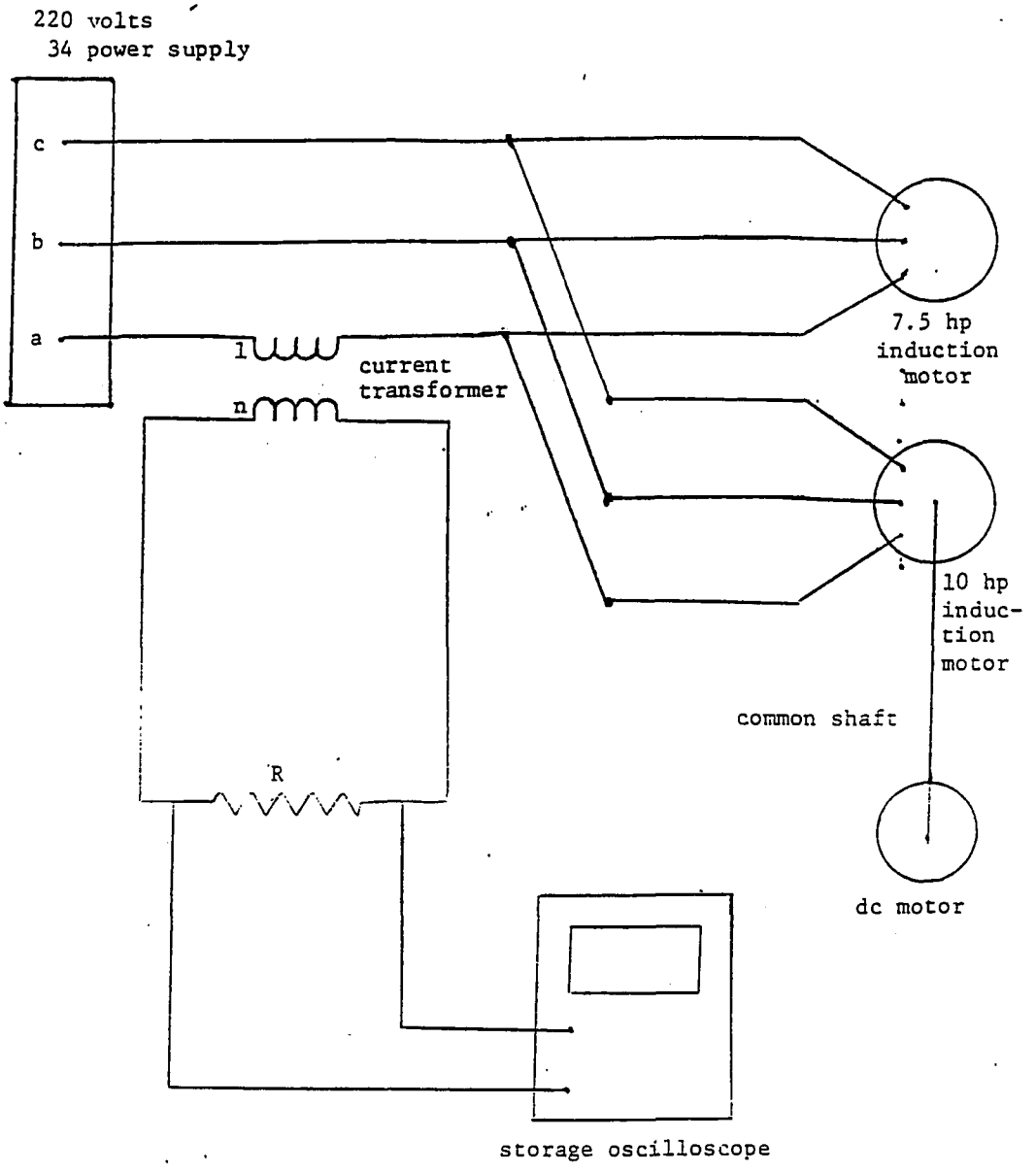

Fig. 5.11. (Continued)
(d) Experimental set-up

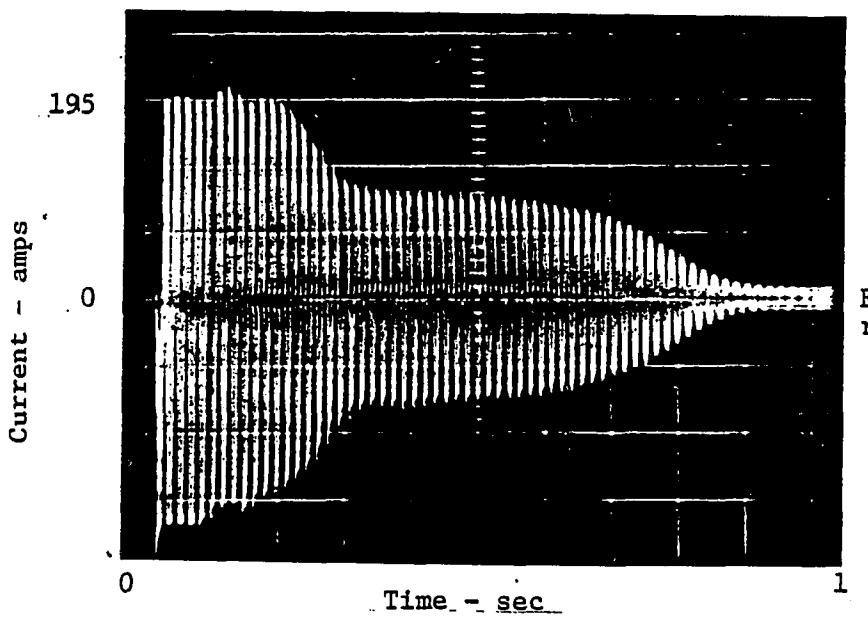

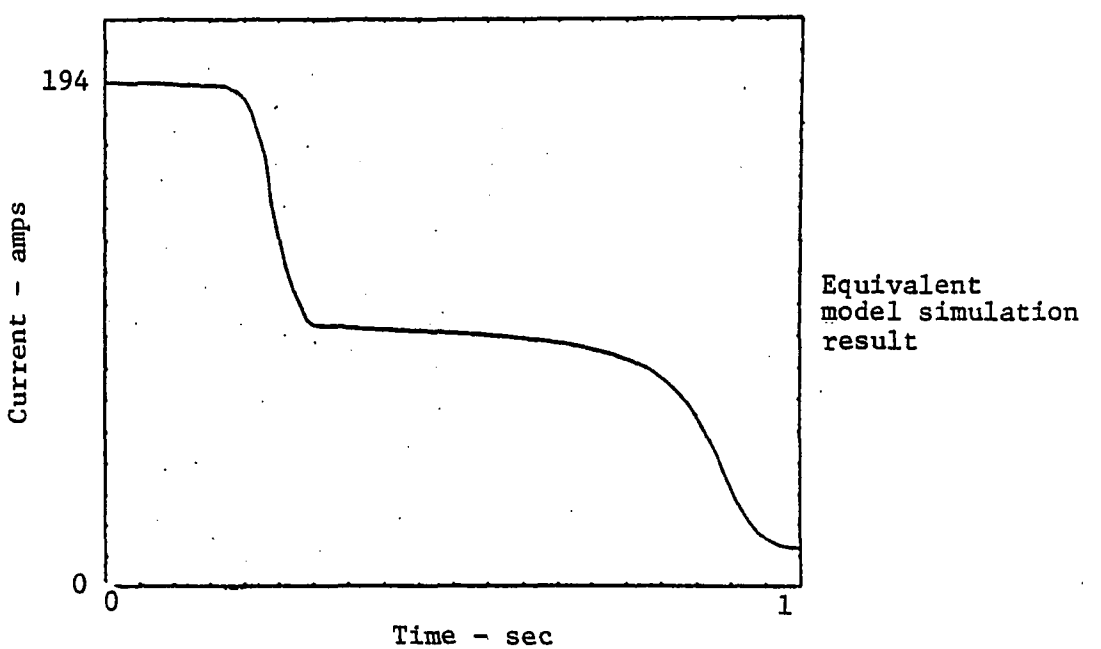

Figure 5.11. (Continued)
(e) Experimental current vs. time; simulation current vs. time

The inertia constant of the 7.5 hp induction machine was found as follows. First, the inertia constant of the 7.5 hp induction machine combined with a dc motor was found. Second, the inertia constant of the dc machine alone was obtained. The difference between these two values was the inertia constant of the 7.5 hp induction machine.

The equivalent circuit parameters were determined experimentally for the two laboratory induction motors. Then the parameters of the single equivalent model of these two machines were calculated using the expressions developed in Chapter 3.

The diagram of the laboratory experimental set-up is shown in Fig. 5.11d. This was a balanced three-phase system and only one of the phase currents was monitored. A current transformer was placed in the circuit of phase "a" to decrease the current through resistance R and to electrically isolate the storage oscilloscope. This resistance R had a very low value to minimize the effects on the motor performance.

The voltage across the resistor R was observed on the oscilloscope for the simultaneous starting of both motors and then photographed. This voltage waveform is proportional to the current in phase a. The scaling factor is $\frac{n}{R}$.

$$I_{\text{phase a}} = \frac{n}{R} V$$

where n is the turns ratio of the current transformer.

Then, the single equivalnet model was simulated for simultaneous start-up to obtain current vs. time data for comparison with the experimental results. In all other results presented in this chapter,

the current values are rms quantities. However, for comparison with the experimental current waveform, the peak current values were obtained to make the curves easier to compare.

Fig. 5.11e shows the current vs. time curves for both the experimental results and the simulation of the single equivalent model of the two machines. The results agree well.

Single Equivalent Model Application and Comparison

Transient stability study

A system with typical parameters (WSCC) was chosen to illustrate the application of the proposed single equivalent model in a transient stability study. The simulation results were obtained using two different models, the proposed single equivalent model and the constant impedance model. The system consists of nine buses, three generators and three loads. Figure 5.12 is a one line impedance diagram for the system under study. The prefault normal load flow solution is also given in Figure 5.12. Generator data for the three synchronous machines are given in Table 5.2a. The generators were represented by the full two axis model and IEEE Type 1 exciters. Exciter data are given in Table 5.2b, and induction machine parameters are given in Table 5.2c.

This system is large enough to be nontrivial and permits the illustration of a number of dynamic concepts and results. Two sets of studies were conducted.

First, all the loads were assumed to be constant impedance.

Second, 30 percent of the load at bus number five was induction machines and the other 70 percent was constant impedance. In both

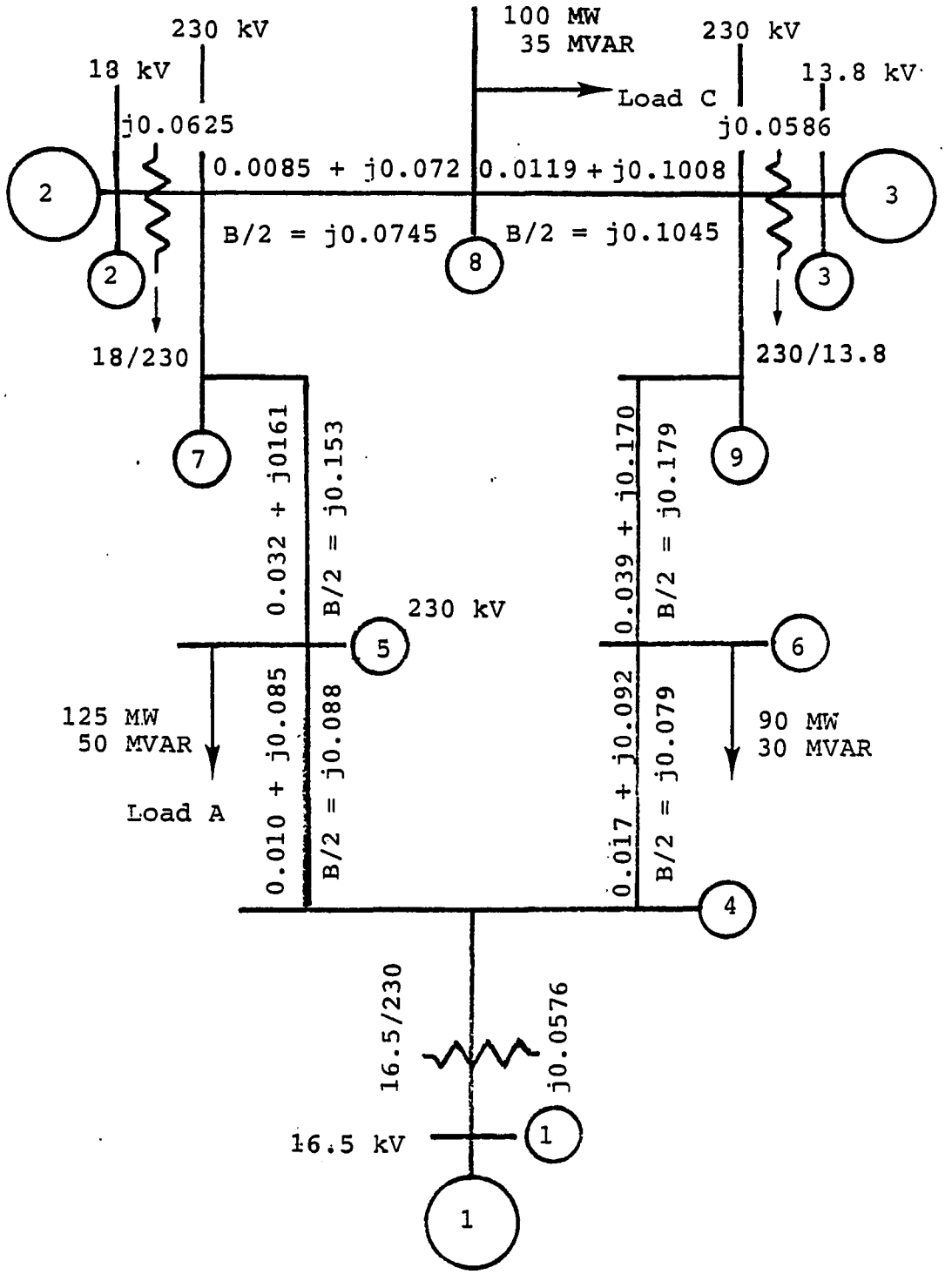

Fig. 5.12. The WSCC 9-bus test system

Table 5.2a. Generator data

Generator	1	2	3
Rated MVA[a]	247.5	192.0	128.0
kV	16.5	18.0	13.8
Power factor	1.0	0.85	0.85
Type	hydro	steam	steam
Speed	180 r/min	36000 r/min	36000 r/min
x_d	0.1460	0.8958	1.3125
x'_d	0.0608	0.1198	0.1813
x_q	0.0969	0.8645	1.2578
x'_q	0.0969	0.1969	0.25
x_ℓ (leakage)	0.0336	0.0521	0.0742
τ'_{d0}	8.96	6.00	5.89
τ'_{q0}	0	0.535	0.600
Stored energy at rated speed	2364 MW·s	640 MW·s	301 MW·s

[a]Reactance values are in pu on a 100-MVA base. All time constants are in s.

Table 5.2b. Exciter data

A_{ex}	B_{ex}	K_A	K_E	K_F	τ_R	τ_F	τ_E	τ_A
0.0013	1.4015	25	-0.0516	0.093	0.06	0.350	0.579	0.2

Table 5.2c. Single equivalent model parameters[a]

R_s	R_r	X	X_m	H	T_o	α	S
0.7774	0.5630	8.982	232.1715	0.0105	0.0183	1.96	0.01109

[a]All the single equivalent parameters are given on 100 MVA base.

cases, a three phase fault was placed on bus number seven. The load behavior at bus number five was monitored in both cases. Figures 5.13, 5.14, 5.15, and 5.16 show power, reactive power, voltages and generator rotor angles, respectively, for both cases one and two.

Figure 5.13 shows the real power consumed at bus number five for the two different load models. It can be seen that during the fault, the induction motor load at bus number five consumes more power than in the case of 100 percent constant impedance. This is because of the decrease in the motors' speeds due to the voltage drop during the fault. In the case of constant impedance, little variation of power during the fault can be seen. The post fault results are also quite different. As it was explained previously, the machines' speeds will decrease during the fault. Once the fault is cleared and the voltage has recovered, the machines will accelerate until their speeds reach the prefault steady-state value. Therefore, in that period of time, the machine load will consume considerably more power than it does in the prefault steady-state condition.

This pattern and reasoning are also consistent for the reactive power drawn by the load as observed from the curves shown in Figure 5.14.

The voltage at bus number five for both cases is shown in Figure 5.15. For the case with induction machine load, the voltage continues to drop during the fault because the machines' speeds will decrease, causing them to draw more current during the fault. In the constant impedance case, the voltage remained nearly constant during the fault.

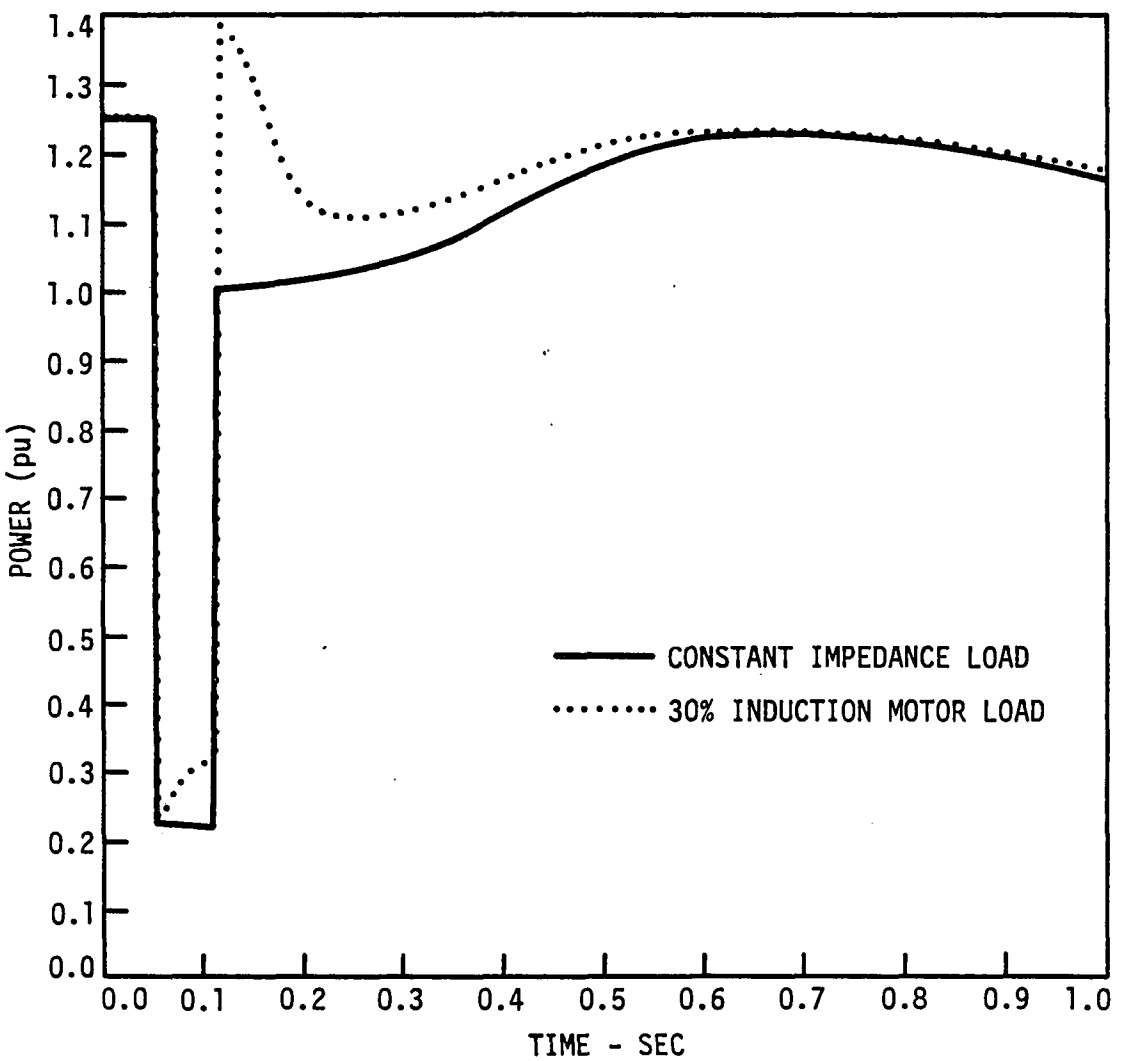

Figure 5.13. Real power comparison for transient stability study

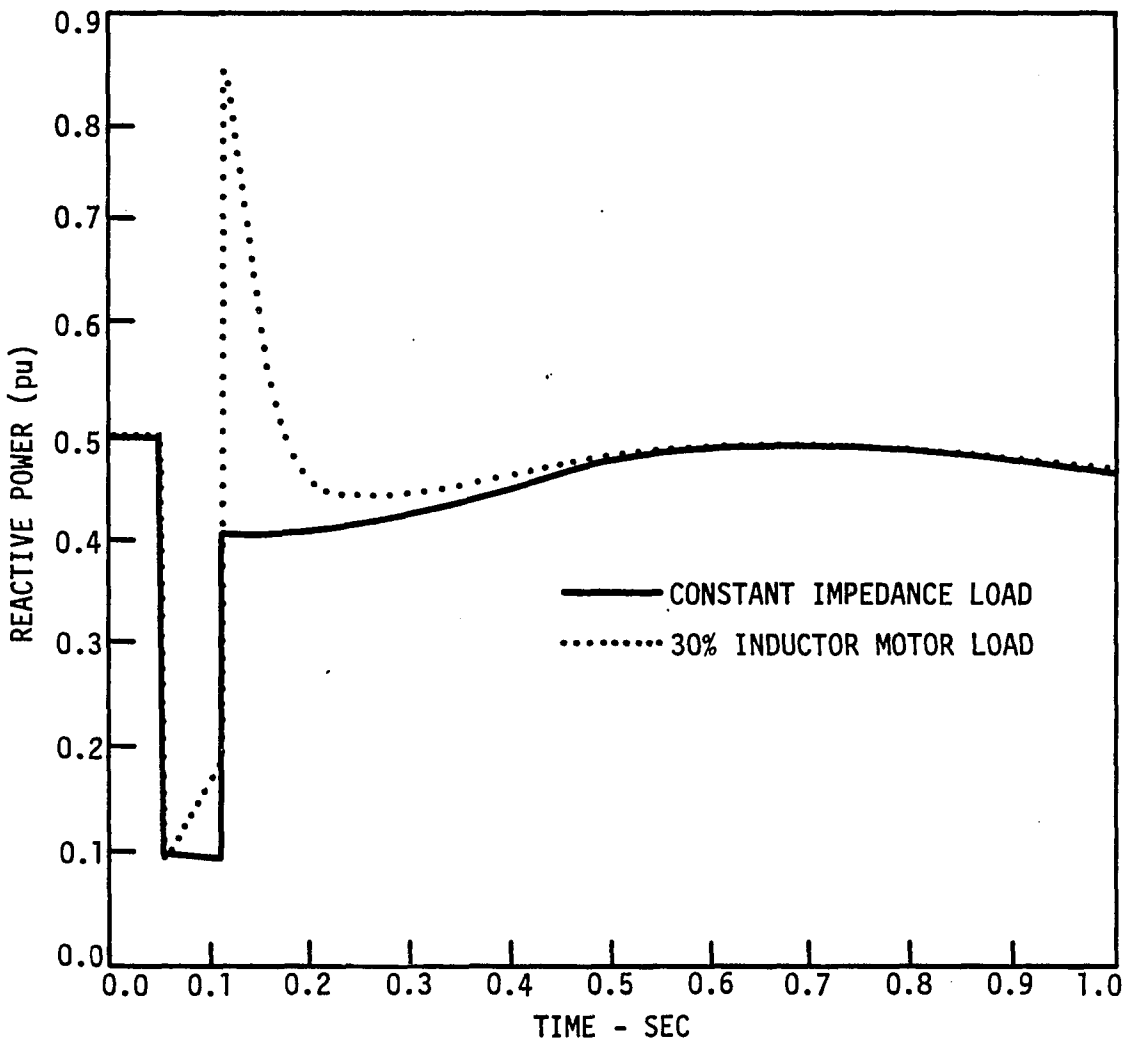

Figure 5.14. Reactive power comparison for transient stability study

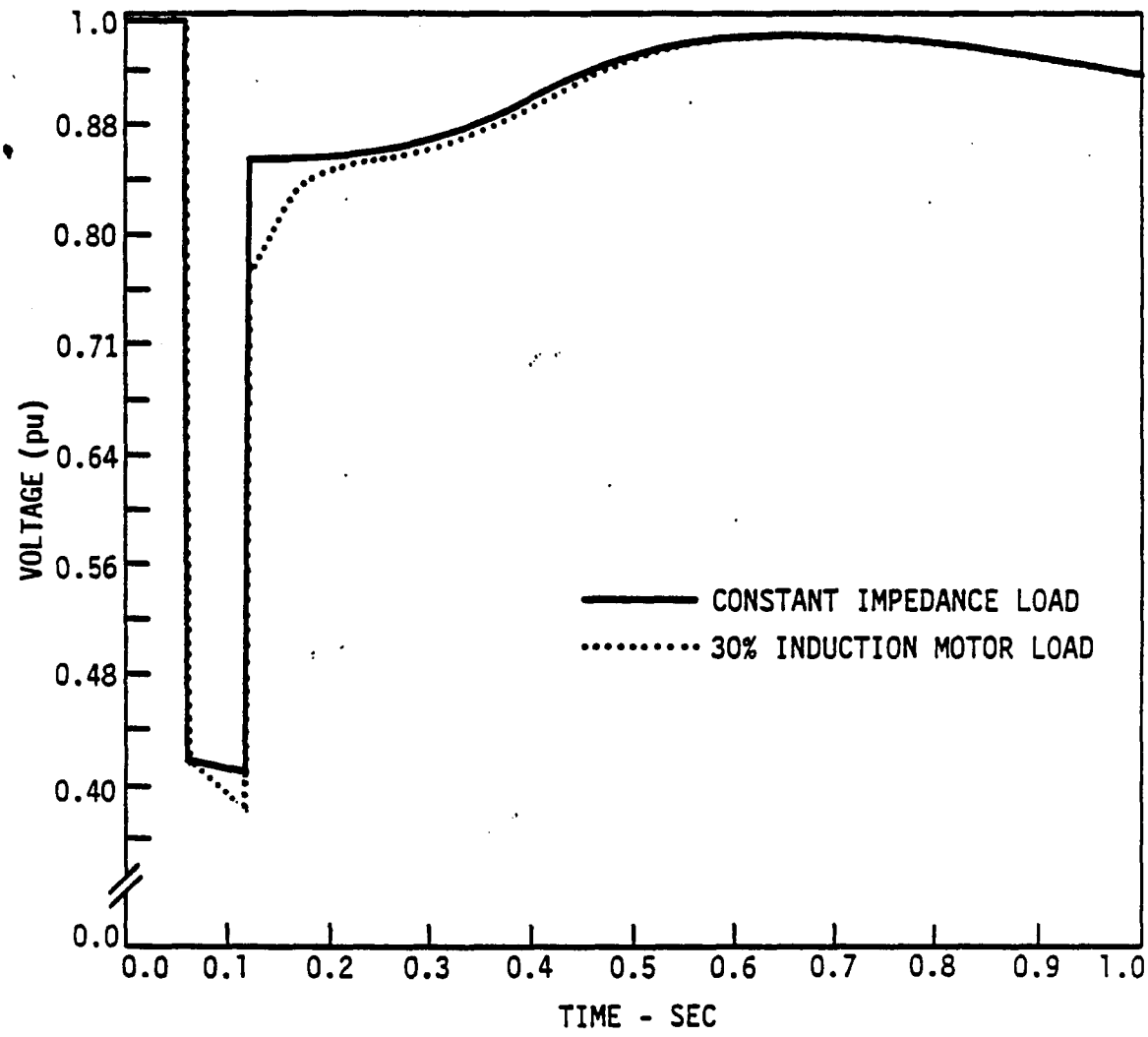

Figure 5.15. Bus voltage comparison for transient stability study

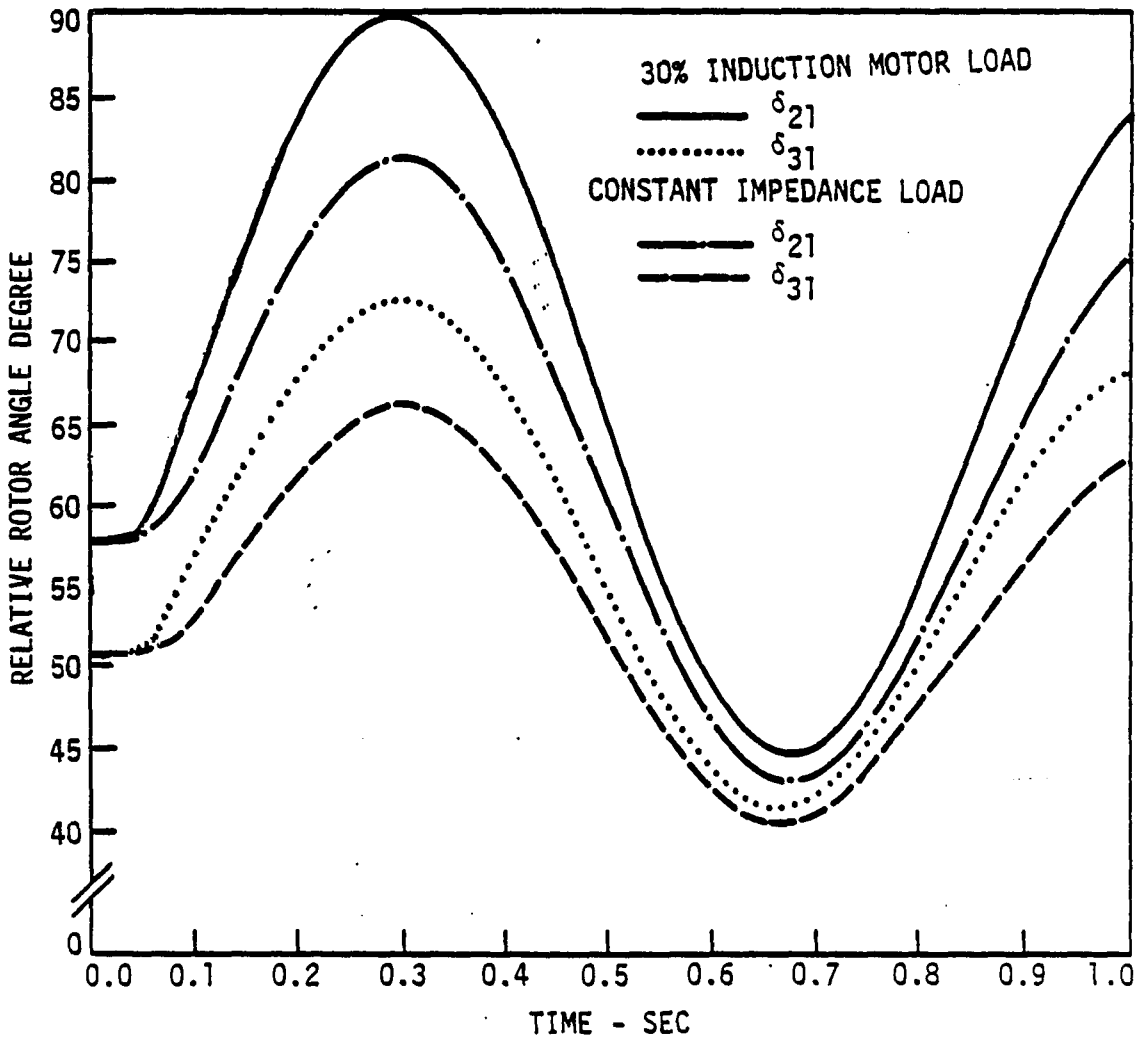

Figure 5.16. Relative rotor angle comparison for transient stability study

Figure 5.16 shows the rotor angles of generators 2 and 3 with respect to generator 1 for both cases. There are some differences, most notably in the peak amplitude of the swing angles. This illustrates that the proposed single equivalent induction motor model could be used in transient stability studies to evaluate the effects of induction motor load.

Application of model for voltage dip studies

Another application of the single equivalent model is the investigation of voltage dip on distribution systems. To verify the validity of the single equivalent model for such applications, the voltage on the system shown in Figure 5.17 was dropped to 65 percent of rated value and held at that level. Figure 5.18 shows real and reactive power for both the single equivalent model and the vector summation of the three individual motors. It can be seen that these plots are extremely close. Therefore, the single equivalent model can be successfully utilized to investigate voltage dip types of studies.

Summary

In this chapter, simulation results were presented to demonstrate the validity and application of the single equivalent model of a group of induction motors. The results obtained from utilizing the proposed model for starting, running, and mixtures of running and starting groups of induction motors were shown to have good agreement with the results obtained from the vector summation of the individual motors' simulation results.

Results obtained from dividing motors into similar subgroups showed that the proposed similarity parameter can be successfully used as the criteria for defining similar subgroups. A study case of 19 machines demonstrated how a larger group of motors can successfully be divided into a much smaller number of similar subgroups.

Experimental data obtained in a machinery laboratory were also presented as part of the verification of the proposed model. Finally, applications of the single equivalent model were illustrated for voltage dip and transient stability studies.

From the result comparisons, it can be concluded that the proposed single equivalent model can accurately predict the dynamic performance of a group of induction motors and can be incorporated into typical power system simulation studies.

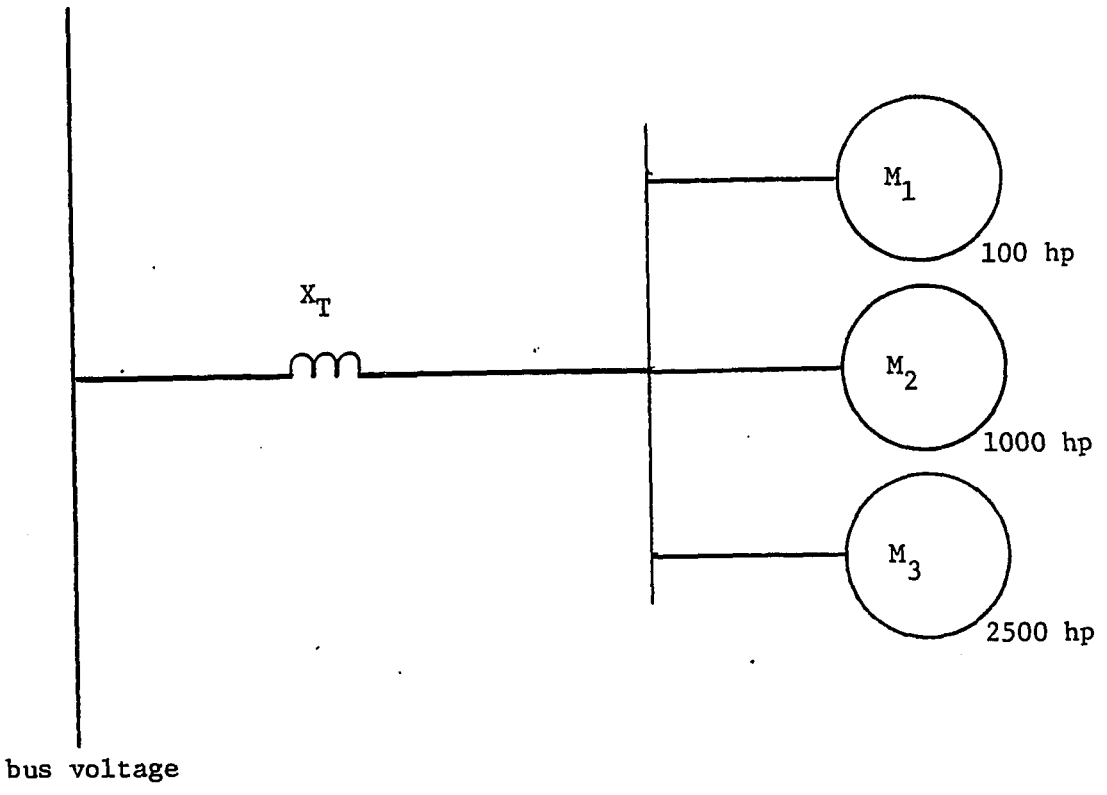

Figure 5.17. The system for voltage dip study

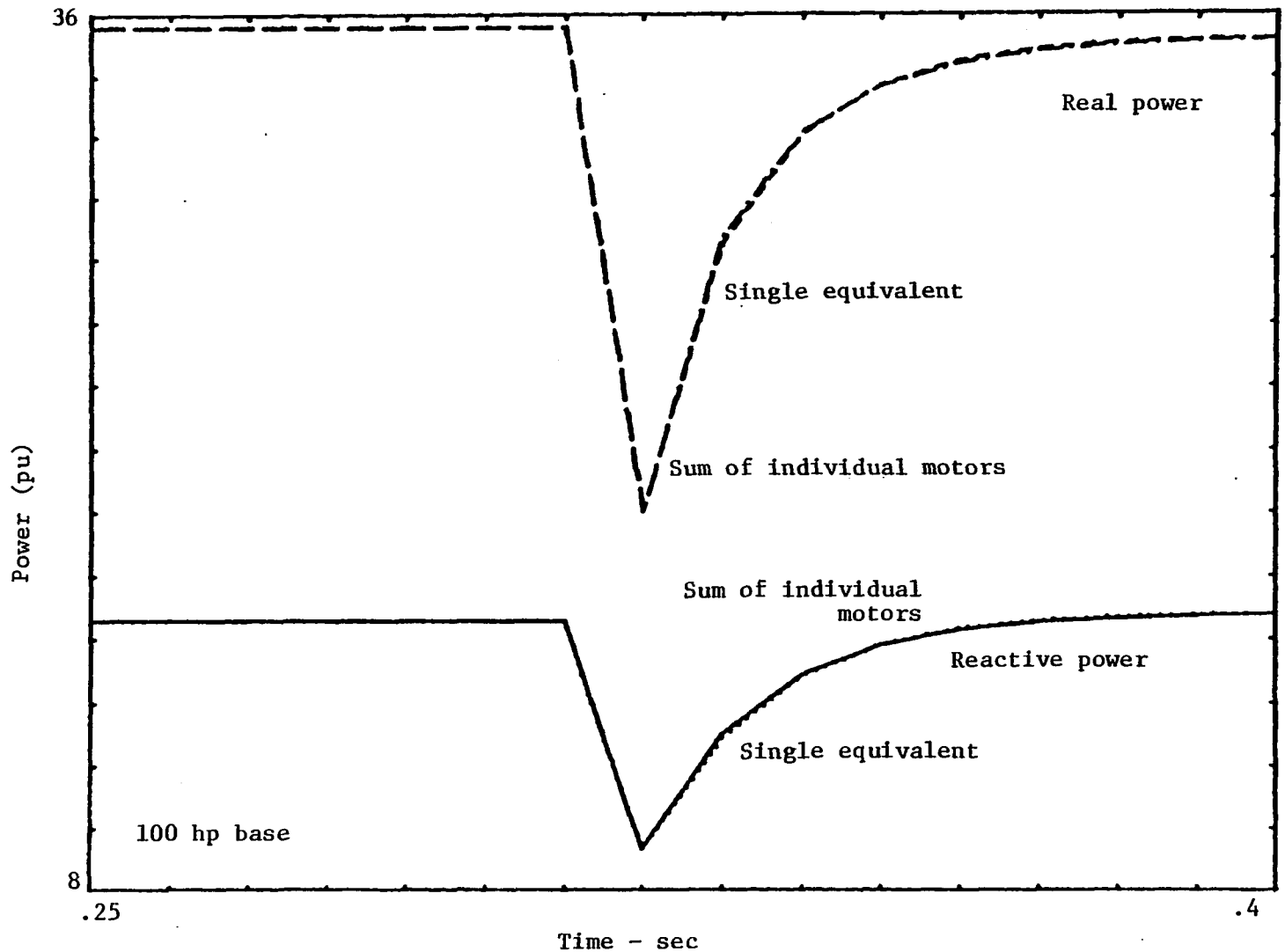

Figure 5.18. Three motor group, 100, 1000, 2500 hp; 65% voltage dip at t = 0.12 sec

CHAPTER VI. CONCLUSION

Recent economic pressures have encouraged the electric utility industry to design and operate their systems closer to the predicted thermal and stability limits. The evaluation of the reliability of the system depends on the accuracy of these predicted limits. In order to more accurately determine where the limits are, the need for the improvement of load modeling techniques has increased. Recently, the loads in the United States have been analyzed and classified by Arthur D. Little [10]. It was pointed out that induction motor loads constitute about 66% of the industrial, commercial and residential loads. Therefore, one of the main areas of load model improvement is developing techniques for including the dynamic behavior of the induction motor portion of the load.

In studies involving motor loads for large networks, detailed representation of each motor is not practical. Even in dealing with proposed simplified motor models, the mathematical equations and computational requirement become prohibitive. Further reduction of the computational requirements is necessary to practically represent a group of induction motors.

In this research, a method of finding a single equivalent representation of a group of induction motors has been developed. The model was developed in order to have a dynamic induction motor load model valid over the whole speed range (zero to full load speed), and, especially, to be able to predict the starting transients of a group of induction motors. The load model is based upon the induction motor

equivalent circuit and has been extended to include deep-bar rotor effects as well as stator resistance effects of induction machines.

The single equivalent model parameters are determined directly from the individual motors' equivalent circuit parameters. The proposed single equivalent model representing a large number of induction motors is similar to the well-known induction machine equivalent circuit model. The proposed single equivalent model contains a variable leakage reactance which is determined prior to the simulation from the individual equivalent circuit of each motor in the group.

The model is shown to accurately predict the dynamic response of a group of induction motors for both running, starting or a combination of running and starting conditions. The effect of voltage dips on the response of a group of motors is shown to agree well when the reduced model is compared to the vector summation of the responses from the individual motors. This model can be incorporated as a load model in power system studies such as load flow, transient stability, and distribution voltage dip analysis.

BIBLIOGRAPHY

1. Abdel-Hakim, M. M. and Berg, G. J. "Dynamic single-unit representation of induction motor groups." IEEE Transactions PAS-95, 1976, 155-161.

2. Akhtar, M. Y. "Frequency dependent dynamic representation of induction motor loads." Proceedings IEE 115, 1968, 802-812.

3. Arnold, C. P. and Pacheco, E. J. P. "Modeling induction motor start-up in a multi-machine transient stability program." A79 492-0, IEEE-PES summer meeting, 1979.

4. Berg, G. J. and Subramaniam, P. "Induction motor load representation." A79 472-2, IEEE-PES summer meeting, 1979.

5. Brereton, D. S.; Lewis, G. G. and Young, C. C. "Representation of induction motor loads during power system stability studies." AIEE Transactions PAS-76, 1957, 451-461.

6. Concordia, C. and Ihaia, S. "Load representation in power system stability studies." 81 DM 346-6, IEEE-PES Summer meeting, 1981.

7. Hanania, J. I.; Mahmoud, A. A.; Day, A. L. and Roohparvar, F. "Induction motor group representation by variable speed-dependent reactance model." Proceedings of the Midwest Power Symposium, University of Illinois at Urbana-Champaign, October 1981.

8. Iliceto, F. and Capasso, A. "Dynamic equivalents of asynchronous motor loads in system stability studies." IEEE Transactions PAS-84, 1974, 1650-1657.

9. Krause, P. C. and Thomas, C. H. "Simulation of symmetrical induction machinery." IEEE Transactions PAS-84, 1965, 1038-1053.

10. Little, Arthur D. Inc. "Energy efficiency and electric motors." Publication PB 259-129, National Technical Information Service, U.S. Department of Commerce, Springfield, Virginia, 1976.

11. Maginnis, F. G. and Schultz, N. R. "Transient performance of induction motors." AIEE Transactions 63, 1944, 641-646.

12. Mahmoud, A. A.; Calabrese, C. and Harley, R. G. "Induction motor transient performance prediction in a distribution network." A78 536-5, IEEE-PES summer meeting, 1978.

13. Mauricio, W. and Semlyer, P. "Effect of load characteristics on dynamic stabilities of power systems." T72 019-3, IEEE-PES winter meeting, 1971.

14. Roohparvar, F.; Mahmoud, A. A.; and Hanania, J. I. "Multi-machine modeling of a group of 3-phase induction motors." Proceedings IEEE International Conference on Electrical Energy, April 1981, 24-31.

15. Sabir, S. A. Y. and Lec, D. C. "Dynamic load models derived from data acquired during system transients." 82 WM 146-9, IEEE-PES, winter meeting, 1982.

16. Slater, R. D.; Wood, W. S.; Flynn, F. P. and Simpson, R. "Digital computation of induction motor transient torque patterns." Proceedings IEEE, 113, No. 5, 1966, 819-822.

17. Sastry, K. P. R. and Burridge, R. E. "Investigation of a reduced order model for induction machine dynamic studies." IEEE Transactions PAS-95, 1976, 962-969.

18. Stanley, H. C. "An analysis of the induction machine." AIEE Transactions 57, 1938, 751-757.

ACKNOWLEDGMENTS

The author wishes to express his appreciation to all of whom assisted in the development and completion of the author's dissertation. The author owes much gratitude to his major professor, Dr. A. A. Mahmoud, whose gracious insight initiated the dissertation topic and whose encouragement and patient guidance made possible the completion of the study.

A member on the author's committee, Dr. Al Day, deserves the author's highest praise for his diligence throughout the past three years, especially for his comprehension and expertise of the research topic. The many hours spent reviewing the research by Dr. Day, and the resulting feedback and knowledgeable suggestions were the critical guideline for the research. Thanks must also be extended to Dr. Day's kind and patient wife, Dixie.

The contributions by other members of the author's committee, Dr. D. Musil, Dr. R. Post, and Dr. A. Abian, were invaluable.

A special acknowledgment is necessary to my elder brother, Mr. Farzin Roohparvar, who greatly assisted in the computer programming and in the mathematical simulations which were imperative to the research. Thanks are also due to the typist, Mrs. Carolyn Taylor, for the completion of the research.

APPENDIX A. NEWTON'S METHOD

Newton's method is one of the most powerful methods for finding a root of a function. There are other techniques that will accomplish this task, but Newton's method, when it works, converges to the root of the function very rapidly. There are at least two common ways of introducing Newton's method. The most common way is to consider the technique graphically. Suppose $f(x)$ is differentiable on $[c,d]$ and $f'(x) \neq 0$ for all $x \varepsilon [c,d]$.

The idea is to provide an initial value $x_1 \varepsilon [c,d]$ as a starting value and update this value until either

(1) x_n approximates T (as shown in Figure A.1) with error $< \varepsilon$;

(2) x_n does not lie in $[c,d]$; or

(3) the number of iterations exceeds a preassigned value and we terminate the procedure because of apparent lack of convergence.

Let x_n be an approximation of T. If x_n is not sufficient close to T, update x_n to x_{n+1}, where x_{n+1} is the unique real number such that $(x_{n+1},0)$ lies on the tangent line through $(x_n,f(x_n))$. The equation of this line is given by

$$y - f(x_n) = f'(x_n)(x-x_n) \quad .$$

Thus, if $y = 0$,

$$x-x_n = -f(x_n)/f'(x_n)$$

and so

$$x_{n+1} = x_n - f(x_n)/f'(x_n) \quad .$$

A second method of looking at Newton's method is an intuitive approach based on the Taylor Polynomial.

Suppose f is twice differentiable on [c,d] and $f'(x) \neq 0$ for all $x \in [c,d]$.

Consider the second degree polynomial for f(x), expanded around x_n,

$$f(x) = f(x_n) + (x-x_n)\, f'(x_n) + \frac{(x-x_n)^2}{2} f''(x_n) \quad .$$

Assuming $(x-x_n)$ is very small, $(x-x_n)^2$ is even smaller and the second order term can be neglected. Since f(x) = 0, we have

$$0 = f(x_n) = -\,(x-x_n)f'(x_n) \quad .$$

Solving for x, we get

$$x_{n+1} = x_n - f(x_n)/f'(x_n) \quad .$$

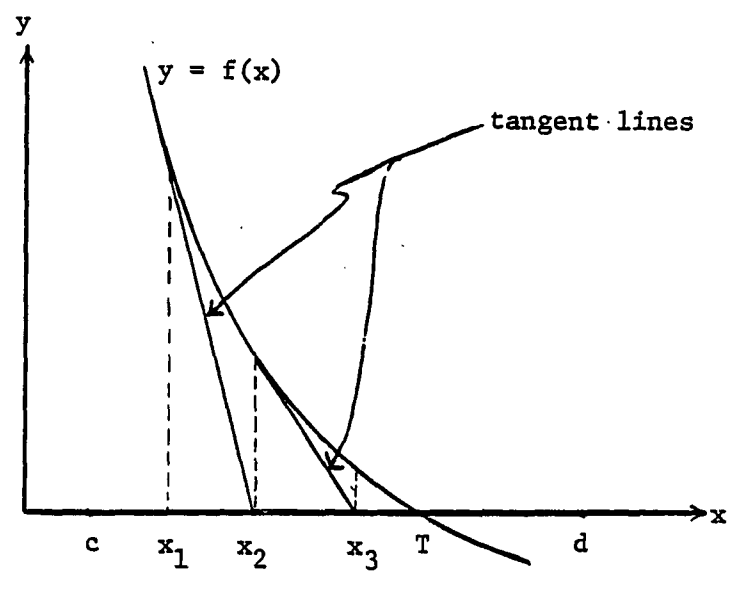

Figure A.1. Convergence process of Newton's method

APPENDIX B. MECHANICAL BASES AND PER UNIT EQUATIONS

Since power is the product of torque and speed, base torque can be taken as rated three-phase power divided by rated mechanical speed. Defining S_b as the rated power per phase and ω_b as the rated speed in electrical radians per second, the expression for base torque in terms of S_b and ω_b is:

$$T_b = \frac{P}{2} \frac{3S_b}{\omega_b} \tag{B.1}$$

where P is the number of poles of the machine.

If T_m is the mechanical load torque, the dimensional equation for rotor acceleration is

$$\frac{2}{P} J \frac{d\omega_r}{dt} = T_e - T_m \tag{B.2}$$

where J is the moment of inertia and ω_r is the rotor speed in electrical radians/sec. Since the kinetic energy of a rotating body is

$$W = \frac{1}{2} J\omega_m^2 \tag{B.3}$$

the stored energy at rated speed is

$$W_R = \frac{1}{2} J \left(\frac{2}{P} \omega_b\right)^2 \tag{B.4}$$

because the mechanical speed is $\omega_m = \frac{2}{P} \omega_b$.

Solving equation B.4 for J and substituting into equation B.2 gives

$$\frac{2W_R}{\frac{2}{P} \omega_b^2} \frac{d\omega_r}{dt} = T_e - T_m \quad . \tag{B.5}$$

When equation B.5 is divided by equation B.1, the relationship between rotor acceleration and per unit torque is found to be

$$\frac{2W_R}{\omega_b 3S_b}\frac{d\omega_r}{dt} = T_e - T_m \quad . \tag{B.6}$$

where T_e and T_m are now in per unit.

The inertia constant H has been defined to be the ratio of inertially stored energy to rated three-phase volt amperes, or

$$H = \frac{W_R}{3S_b} \tag{B.7}$$

and equation B.6 is rewritten to be

$$\frac{2H}{\omega_b}\frac{d\omega_r}{dt} = T_e - T_m \tag{B.8}$$

where H and t are in seconds, ω_r and ω_b are in radians/sec., and torque is in per unit.

APPENDIX C. MATHEMATICAL LIMITS OF THE SPEED OF THE EQUIVALENT MACHINE

Recalling equation 3.7 and taking its limit as S_1 and S_2, approach to zero will result in

$$\lim_{(s_1=s_2=s)\to 0} S = \lim_{s\to 0} \frac{R_r}{A(s_1,s_2) - R_s} \tag{C.1}$$

$$= \lim_{s\to 0} \frac{R_r}{\frac{(r_{s1}+\frac{r_{r1}}{s}+r_{s2}+\frac{r_{r2}}{s})(r_{s1}+\frac{r_{r1}}{s})(r_{s2}+\frac{r_{r2}}{s})+x_2^2(r_{s1}+\frac{r_{r1}}{s})+x_1^2(r_{s2}+\frac{r_{r2}}{s})}{(r_{s1}+\frac{r_{r1}}{s}+r_{s2}+\frac{r_{r2}}{s})^2+(x_1+x_2)^2} - R_s}$$

$$= \lim_{s\to 0} \frac{R_r}{\frac{(sr_{s1}+r_{r1}+sr_{s2}+r_{r2})(sr_{s1}+r_{r1})(sr_{s2}+r_{r2})+s^2[x_2^2(sr_{s1}+r_{r1})+x_1^2(sr_{s2}+r_{r2})]}{s(sr_{s1}+r_{r1}+sr_{s2}+r_{r2})^2+s^3(x_1+x_2)^2} - R_s}$$

$$= \lim_{s\to 0} \frac{sR_r(sr_{s1}+r_{r1}+sr_{s2}+r_{r2})^2}{(sr_{s1}+r_{r1}+sr_{s2}+r_{r2})(sr_{s1}+r_{r1})(sr_{s2}+r_{r2})+s^2[x_2^2(sr_{s1}+r_{r1})+x_1^2(sr_{s2}+r_{r2})]}$$

$$+ s^3(x_1+x_2)^2$$

$$-sR_s(sr_{s1}+r_{r1}+sr_{s2}+r_{r2})^2+s^3(x_1+x_2)^2$$

$$= \frac{0}{(r_{r1}+r_{r2})(r_{r1})(r_{r2})} = 0 \quad .$$

Therefore, it is shown that

$$\lim_{(s_1=s_2)\to 0} S = 0 \quad . \tag{C.2}$$

The equivalent speed ω in a per unit system is

$$\omega = 1 - S \quad . \tag{C.3}$$

The expressions for ω_1 and ω_2 are given in equations C.4 and C.5.

$$\omega_1 = 1 - s_1 \tag{C.4}$$

$$\omega_2 = 1 - s_2 \quad . \tag{C.5}$$

Taking the limit of equation C.4 will result as

$$\lim_{s_1 \to 0} \omega_1 = \lim_{s_1 \to 0} (1-s_1) = 1 \quad . \tag{C.6}$$

Also, taking the limit of equation C.5 will yield

$$\lim_{s_2 \to 0} \omega_2 = \lim_{s_2 \to 0} (1-s_2) = 1 \quad . \tag{C.7}$$

Finally, taking the limit of equation C.3 will result as

$$\lim_{S \to 0} \omega = \lim_{S \to 0} (1-S) \tag{C.8}$$

$$\lim_{S \to 0} \omega = 1 \quad .$$

Therefore, it has been shown that as individual machines' speeds approach zero, so does the speed of the single equivalent model.

APPENDIX D. TRANSFORMATION TO o.d.q. AXIS QUANTITIES

The relation between the various coil flux linkages, self and mutual inductances, and coil current is given as:

$$\begin{bmatrix} \lambda_{as} \\ \lambda_{bs} \\ \lambda_{cs} \\ \hline \lambda_{ar} \\ \lambda_{br} \\ \lambda_{cr} \end{bmatrix} = \left[\begin{array}{ccc|ccc} L_s & -L_{sm} & -L_{sm} & L_{as-ar} & L_{as-br} & L_{as-cr} \\ -L_{sm} & L_s & -L_{sm} & L_{bs-ar} & L_{bs-br} & L_{bs-cr} \\ -L_{sm} & -L_{sm} & L_s & L_{cs-ar} & L_{cs-br} & L_{cs-cr} \\ \hline L_{ar-as} & L_{ar-bs} & L_{ar-cs} & L_r & -L_{mr} & -L_{mr} \\ L_{br-as} & L_{br-bs} & L_{br-cs} & -L_{mr} & L_r & -L_{mr} \\ L_{cr-as} & L_{cr-bs} & L_{cr-cs} & -L_{mr} & -L_{mr} & L_r \end{array}\right] \begin{bmatrix} i_{as} \\ i_{bs} \\ i_{cs} \\ \hline i_{ar} \\ i_{br} \\ i_{cr} \end{bmatrix} \qquad (D.1)$$

where the subscript "s" denotes stator quantities and "r" rotor quantities; a, b, or c denotes the three stator or rotor phases; and L_s equals stator self-inductance, which is constant for all the three identical stator phases.

L_{sm} = mutual inductance between stator phases, a positive constant

L_r = rotor self-inductance, which is constant for all three identical rotor phases

L_{rm} = mutual inductance between rotor phases, a positive constant.

All mutual inductances between stator and rotor phases ($L_{is} - L_{jr}$) in the above matrix are variables, and their magnitudes depend on the position of the rotor with respect to the stator. In general, these mutual inductances are given by equation D.2:

$$L_{is-jr} = L_{jr-is} = L_{sr} \cos \alpha_{is-jr} \quad . \tag{D.2}$$

L_{sr} is constant and α_{is-jr} is the angle between stator winding i and rotor winding j in general for any rotor position θ_r.

Matrix D.1 may also be represented by matrix D.3.

$$\begin{bmatrix} \lambda_{abcs} \\ \hline \lambda_{abcr} \end{bmatrix} = \left[\begin{array}{c|c} L_1 & L_2 \\ \hline L_3 & L_4 \end{array}\right] \begin{bmatrix} i_{abcs} \\ \hline i_{abcr} \end{bmatrix} \tag{D.3}$$

Stator and rotor phase voltages can be written as follows:

$$\left[\begin{array}{c} V_{as} \\ V_{bs} \\ V_{cs} \\ \hline V_{ar} \\ V_{br} \\ V_{cr} \end{array}\right] = \left[\begin{array}{ccc|ccc} r_s & 0 & 0 & 0 & 0 & 0 \\ 0 & r_s & 0 & 0 & 0 & 0 \\ 0 & 0 & r_s & 0 & 0 & 0 \\ \hline 0 & 0 & 0 & r_r & 0 & 0 \\ 0 & 0 & 0 & 0 & r_r & 0 \\ 0 & 0 & 0 & 0 & 0 & r_r \end{array}\right] \left[\begin{array}{c} i_{as} \\ i_{bs} \\ i_{cs} \\ \hline i_{ar} \\ i_{br} \\ i_{cr} \end{array}\right] + \left[\begin{array}{c} P\lambda_{as} \\ P\lambda_{bs} \\ P\lambda_{cs} \\ P\lambda_{ar} \\ P\lambda_{br} \\ P\lambda_{cr} \end{array}\right] \tag{D.4a}$$

where P is the $\frac{d}{dt}$ operator.

Equation D.4a could be written in a compact matrix.

$$\begin{bmatrix} V_{abcs} \\ \hline V_{abcr} \end{bmatrix} = \left[\begin{array}{c|c} r_s U_3 & 0 \\ \hline 0 & r_r U_3 \end{array}\right] \begin{bmatrix} i_{abcs} \\ \hline i_{abcr} \end{bmatrix} + \begin{bmatrix} P\lambda_{abcs} \\ \hline P\lambda_{abcr} \end{bmatrix} \tag{D.4b}$$

$[U_3]$ is a 3 by 3 unity matrix, and [0] is a null matrix.

Transformation to o.d.q. Axis Quantities

Simplification of a, b and c phase equations for flux linkage D.1 and voltage D.4a can be achieved by transformation of variables from abc quantities to o.d.q. axis quantities. This is accomplished by using the orthogonal version of Park's transformation. This transformation transforms all variables onto the direct (d) and quadrature (q) axes as in equation 1.4, and the o axis, which is stationary. The most commonly used reference frames are known as the synchronously rotating reference frame, the rotor reference frame, the stationary or stator reference frame, and the arbitrary reference frame.

In the synchronously rotating reference frame, the d and q axes rotate at synchronous speed. The d and q axes are fixed to the rotor in the rotor reference frame. In the stationary reference frame, the d and q axes are stationary, and thus fixed to a constant position on the stator. The arbitrary reference frame is an intermediate step which is useful because of its generality. In Figures D.1 and D.2, the angles θ and β are defined as the angles between the d axis and the A phase magnetic axis of the stator and rotor, respectively.

Park's Transformation

Transformation from the abc phase quantities to the arbitrary reference frame o.d.q. axis quantities is accomplished by equation D.5.

For stator quantities,

$$[F_{odqs}] = [P_{\theta}][F_{abcs}] \quad . \qquad (D.5a)$$

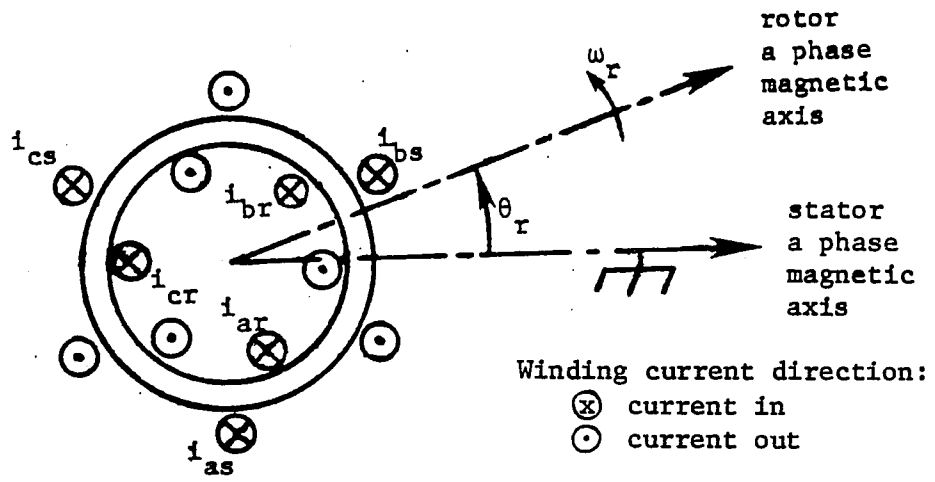

Figure D.1. General three-phase induction motor

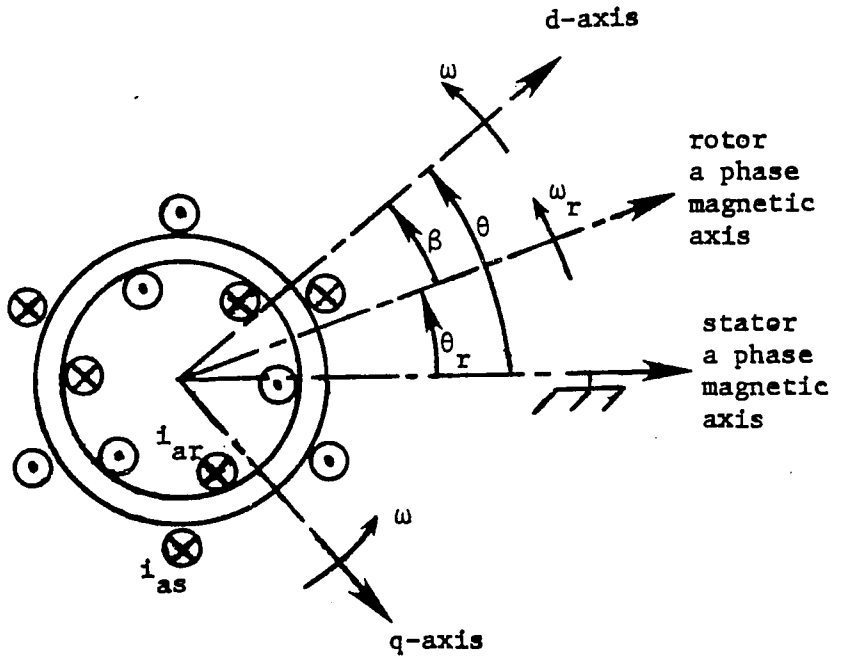

Figure D.2. Motor with magnetic axes and arbitrary d and q axes shown

For rotor quantities,

$$[F_{odqr}] = [P_\beta][F_{abcr}] \tag{D.5b}$$

where

$$[P_\theta] = \sqrt{\frac{2}{3}} \begin{bmatrix} \sqrt{\frac{1}{2}} & \sqrt{\frac{1}{2}} & \sqrt{\frac{1}{2}} \\ \cos\theta & \cos(\theta-120) & \cos(\theta+120) \\ \sin\theta & \sin(\theta-120) & \sin(\theta+120) \end{bmatrix}$$

$$[P_\beta] = \sqrt{\frac{2}{3}} \begin{bmatrix} \sqrt{\frac{1}{2}} & \sqrt{\frac{1}{2}} & \sqrt{\frac{1}{2}} \\ \cos\beta & \cos(\beta-120) & \cos(\beta+120) \\ \sin\beta & \cos(\beta-120) & \sin(\beta+120) \end{bmatrix} \tag{D.6}$$

$[F_{abc}]$ is the set of three-phase quantities: current, voltage, or flux linkage. $[F_{odq}]$ is the corresponding set of axis quantities. Because of the orthogonality of the transformation, it follows that

$$[P_\theta]^{-1} = [P_\theta]^T, \quad [P_\beta]^{-1} = [P_\beta]^T . \tag{D.7}$$

Transformation of Equations

Equation D.8 describes a general system of three-phase voltages.

$$\begin{bmatrix} v_a \\ v_b \\ v_c \end{bmatrix} = \begin{bmatrix} R & 0 & 0 \\ 0 & R & 0 \\ 0 & 0 & 0 \end{bmatrix} \begin{bmatrix} i_a \\ i_b \\ i_c \end{bmatrix} + \begin{bmatrix} P\lambda_a \\ P\lambda_b \\ P\lambda_c \end{bmatrix} \tag{D.8}$$

In matrix notation, equation D.8 becomes

$$[v_{abc}] = [R_{abc}][i_{abc}] + [P\lambda_{abc}] \ . \tag{D.9}$$

In order to obtain the o.d.q. axis voltages, equation D.9 is multiplied by $[P_\theta]$.

$$[P_\theta][v_{abc}] = [P_\theta][R_{abc}][P_\theta]^{-1}[P_\theta][i_{abc}] + [P_\theta][P\lambda_{abc}] \ . \tag{D.10}$$

Equation D.10 can be rewritten as

$$[v_{odq}] = [P_\theta][R_{abc}][P_\theta]^{-1}[i_{odq}] + [P_\theta][P\lambda_{abc}] \ . \tag{D.11}$$

If the o.d.q. axis resistance is defined as

$$[R_{odq}] = [P_\theta][R_{abc}][P_\theta]^{-1} \ , \tag{D.12}$$

where:

$$[R_{odq}] = [P_\theta] \begin{bmatrix} R & 0 & 0 \\ 0 & R & 0 \\ 0 & 0 & R \end{bmatrix} [P_\theta]^{-1} = \begin{bmatrix} R & 0 & 0 \\ 0 & R & 0 \\ 0 & 0 & R \end{bmatrix}$$

equation D.11 becomes

$$[V_{odq}] = [R_{odq}][i_{odq}] + [P_\theta][P\lambda_{abc}] \quad . \tag{D.13}$$

Equation D.12 is known as a similarity transformation.

The derivative of equation D.5 is

$$[PF_{odq}] = [PP_\theta][F_{abc}] + [P_\theta][PF_{abc}] \tag{D.14}$$

$$[P_\theta][PF_{abc}] = [PF_{odq}] - [PP_\theta][F_{abc}] \quad .$$

Since $[F_{abc}] = [P_\theta]^{-1}[F_{odq}]$,

$$[P_\theta][PF_{abc}] = [PF_{odq}] - [PP_\theta][P_\theta]^{-1}[F_{odq}] \quad . \tag{D.15}$$

Using equation D.6,

$$[PP_\theta][P_\theta]^{-1} = \begin{bmatrix} 0 & 0 & 0 \\ 0 & 0 & -P\theta \\ 0 & P\theta & 0 \end{bmatrix} \tag{D.16}$$

Similarly, for rotor quantities,

$$[PP_\beta][P_\beta]^{-1} = \begin{bmatrix} 0 & 0 & 0 \\ 0 & 0 & -P\beta \\ 0 & P\beta & 0 \end{bmatrix} \tag{D.17}$$

By substituting the results of equations D.15 and D.16 into equation D.13, the o.d.q. axis voltages can be written in terms of o.d.q. variables only.

$$[V_{odq}] = [R_{odq}][i_{odq}] + [P\lambda_{odq}] + \begin{bmatrix} 0 \\ -\lambda_q P\theta \\ \lambda_d P\theta \end{bmatrix} \quad . \qquad (D.18)$$

APPENDIX E. DIGITAL COMPUTER PROGRAM FOR THE REDUCED ORDER MODEL

The simulated equations are given in equations E.1, E.2, E.3 and E.4. The step-by-step time solution of these equations is undertaken by first solving the electrical equations with the current value of rotor slip. The developed torque is then found from the rotor current. Equation E.4 is then solved over a time step of integration by a fourth order Runga-Kutta integration subroutine. A time step of 0.01 second was used in this study. The rotor speed is then used to find the slip for the next iteration. The digital program used to solve the reduced order model in this study is presented in Table E.1.

Table E.2 contains a list of computer variables and constants and the equivalent expressions used in the text. A simplified flow chart of the computer program is given in Figure E.1, and the equivalent circuit is shown in Figure E.2.

Equations E.1-E.4 are given below:

$$\bar{V}_{as} = [r_s + j\omega_b(M + L_s)]\ \bar{I}_{as} - j\omega_b M\ \bar{I}_{ar} \tag{E.1}$$

$$0 = -[\frac{r_r}{s} + j\omega_b(M + L_r)]\ \bar{I}_{ar} + j\omega_b M\ \bar{I}_{as} \tag{E.2}$$

$$T_e = \frac{r_r I_{ar}^2}{s} \tag{E.3}$$

$$\omega = \frac{\omega_b}{2H} \int (T_e - T_m)\ dt \quad . \tag{E.4}$$

Table E.1. Reduced order model digital program listing

```
C        MAIN PROGRAM
C        ------------
C        STARTING OF AN INDUCTION MOTOR WITH SINGLE CAGE ROTOR,SUPPLIED
C       FROM INF. BUS, THRU  ZC TIE-LINE IMPEDANCE.FIRST ORDER MODEL FOR
C      MACHINE   NEGLECTS  ELECTRICAL  TRANSIENTS.  EQUATIONS AND
C     SIGN CONVENTIONS FROM BOOK BY ADKINS AND HARLEY.
C - - - - - - - - - - - - - - - - - - - - - - - - - - - - - - - - - - -
C "REED"  READS IN AND PRINTS OUT DATA
C "COEFF"  FINDS VARIOUS A,B,C,D, ETC. COEFFICIENTS FOR MOTOR EQUNS.
C "INTEG"  IS NUMERICAL INTEGRATING ROUTINE WHICH IN TURN CALLS
C  "PLANT". "PLANT"CONTAINS DIFFERENTIAL EQUNS. AND "INTEG" RETURNS
C  NEW INTEGRATED VALUES TO "MAIN PROGRAM".
C "RITE"  PRINTS OUT COLUMNS OF INTEGRATION RESULTS
C    "MSTART" SETS INITIAL VALUES FOR STARTING THE MOTOR.
C    "NDIFF" IS THE NUMBER OF DIFFERENTIAL EQUNS TO SOLVE IN "XY".
C
     COMMON/BL1/SQ2,SQ3,DEG,RAY,XY(6),XDOT(6), ACF,WZ,PAI,SUD1,SUQ1
     COMMON/BL4/ T,DELT,LINES, L,N,TFINAL,NDIFF,II
     COMMON A(100,10),X(100),Y(100)
     II=0
     CALL REED
     READ(5,11) NUMRUN
 11  FORMAT( I2)
     DO 86 NRUN= 1,NUMRUN
     READ(5,12) FCAP
 12  FORMAT( F10.3 )
     CALL STEADY
     WRITE(6,60)
     CALL CAPACT(FCAP)
C DISTURBANCE  STARTS#####DISTURBANCE  STARTS######
     CALL MSTART
     WRITE(6,10)
 10  FORMAT('-',2X,'TIME',3X,'VTRMS',4X,              'SLIP',4X,
    2 'SPEED',3X,'TEM',6X,'TLM',4X,'TEM3',3X,'IMRMS',3X,'VFEED',
```

Table E.1 Continued

```
     3 5X,'BVA', 4X,'BPOW', 5X,'BPF',5X,'TVA',4X,'TPOW',5X,'TPF',/)
      CALL RITE
 84   CONTINUE
      CALL INTEG(T, DELT,NDIFF, XY, XDOT  )
      IF(L-N) 77,78,77
 78   L=0
      LINES= LINES+1
      IF( LINES-5) 38,37,37
 37   WRITE(6,60)
      LINES= 0
 38   CALL RITE
 77   L=L+1
      IF(T.GT. TFINAL ) GO TO 85
      GO TO 84
 85   CALL RITE
 86   CONTINUE
 60   FORMAT(2X,'-------------------------------------------------------
     2-------------------------------------------------------')
      DO 998 I=1,5
      DO 997 J=1,II
      Y(J)=A(J,I)
997   CONTINUE
      CALL GRAPH(II,X,Y,I,4,10.0,6.0,0.0,0.0,0.0,0.0,-10.0,
     +'T-SEC ;',' -P.U.;','          ;','IN PER UNIT;')
998   CONTINUE
      DO 996 J=1,II
      X(J)=A(J,3)
      Y(J)=A(J,4)
996   CONTINUE
      CALL GRAPH(II,X,Y,1,4,10.0,6.0,0.0,0.0,0.0,0.0,-10.0,
     +'SPEED-;','TORQUE;','LINE     ;','IN PER UNIT;')
      STOP
      END
C - - - - - - - - - - - - - - - - - - - - - - - - - - - - - - - - - - -
C
```

Table E.1 Continued

```
      SUBROUTINE REED
      REAL L1,L2,L3,LM,L11,L22,L33,LAMDA,LAMDAR,IMRMS,IMINST,LC
      COMMON/BL1/SQ2,SQ3,DEG,RAY,XY(6),XDOT(6), ACF,WZ,PAI,SUD1,SUQ1
      COMMON/BL4/ T,DELT,LINES, L,N,TFINAL,NDIFF,II
      COMMON/BL5/R1,X1,RM,XM,TX1,TXI1,T1,T11,POLES,F, PHASE,HM,
     2  LAMDA,LAMDAR,RC,XC,R2,X2,R3,X3,TLM,TEM,URMS,SPEED
      COMMON/BL6/ TACM,SLIP ,TL0,TL2
      COMMON A(100,10),X(100),Y(100)
      WRITE(6,103)
103   FORMAT('1', 45X, 'SYSTEM      DATA',/45X, '------------------' )
      READ(5,  100)R1,X1,RM,XM,R2,X2,TLM
      WRITE(6, 101)R1,X1,RM,XM,R2,X2,TLM
      READ(5,100)  POLES,F,PHASE, HM,LAMDA, RC,XC
      WRITE(6,102) POLES,F,PHASE, HM,LAMDA, RC,XC
100   FORMAT(8F9.4 )
101   FORMAT('0', 2X,'R1=',F6.4,8X,'X1=',F6.4,8X,'RM=',F6.4,8X,'XM=',
     2 F6.3,8X,'R2=',F6.4,8X,'X2=',F6.4,8X,'TLM=', F6.4 )
102   FORMAT(    2X,'POLES=',F4.1,9X,'F=',F6.1,8X,'PH=',F4.1,10X,'H=',
     2 F4.1,8X,'LAMDA=',F6.1,8X,'RC=',F6.4,9X,'XC=',F6.4 )
C
      READ(5,104) DELT,N,TFINAL,TL0,TL2
      WRITE(6,105) DELT,N,TFINAL,TL0, TL2
 104  FORMAT( F7.4, I3,3F10.4 )
 105  FORMAT( 2X,'DELT=',F6.4,8X,'N=',I2,10X,'TFINAL=',F4.1,7X,
     2'TL0=', F6.3,7X, 'TL2=', F7.4 )
      RETURN
      END
C - - - - - - - - - - - - - - - - - - - - - - - - - - - - - - - - - - -
C
      SUBROUTINE STEADY
      REAL L1,L2,L3,LM,L11,L22,L33,LAMDA,LAMDAR,IMRMS,IMINST,LC
      COMPLEX UBUS, UMOT,IMOT,ZC,ZMOT,ZMAG,ZLEAK,CMPLX,CAIL,ZL
      COMPLEX ZCIRC, ZCAP ,CVFEED
      COMMON/BL1/SQ2,SQ3,DEG,RAY,XY(6),XDOT(6), ACF,WZ,PAI,SUD1,SUQ1
      COMMON/BL4/ T,DELT,LINES, L,N,TFINAL,NDIFF,II
```

Table E.1 Continued

```
      COMMON A(100,10),X(100),Y(100)
      COMMON/BL5/R1,X1,RM,XM,TX1,TX11,T1,T11,POLES,F, PHASE,HM,
     2  LAMDA,LAMDAR,RC,XC,R2,X2,R3,X3,TLM,TEM,URMS,SPEED
      COMMON/BL6/ TACM,SLIP ,TL0,TL2
      COMMON/BL9/  UBUS, UMOT,IMOT,ZC,ZMOT,ZMAG,ZLEAK,RMOT,XLEAK,ZL
      SQ2= SQRT(2.0)
      SQ3= SQRT(3.0)
      PAI= 3.141593
      WZ= 2.0*PAI*F
      ACF= PAI*F/HM
      T=0.0
      LINES = 1
      L=1
      NDIFF= 1
      DO 300 J=1,6
      XY(J) =0.0
  300 XDOT(J)= 0.0
      TEM=0.0
      TACM= 0.0
      URMS= 1.0
      UMOT= CMPLX( 0.0,0.0)
      IMOT= CMPLX(0.0,0.0)
      UBUS= CMPLX( URMS, 0.0)
      ZC= CMPLX( RC,XC)
      ZMAG= CMPLX(0.0,XM)
      XLEAK= X1 +X2
      SLIP= 1.0
      T=0.0
      SPEED=0.0
      XY(1) = WZ*SPEED
      SLIP = 1.0 - SPEED
      RETURN
C- - - - - - - - - - - - - - - - - - - - - - - - - - - - - - - - - - - - - -
      ENTRY CAPACT(FCAP)
      RMOT= R1+ R2/SLIP
```

Table E.1 Continued

```
      ZLEAK= CMPLX( RMOT,XLEAK)
      ZMOT= ZMAG*ZLEAK/(ZMAG+ ZLEAK)
      ZCIRC= ZC +ZMOT
      XCAP = -AIMAG( ZCIRC)*FCAP
      XCAP = 0.001
      ZCAP= CMPLX( 0.0, XCAP)
      ZL= ZC + ZCAP
      ZCIRC = ZL+ ZMOT
      WRITE( 6,299) XCAP,FCAP, ZCIRC
299   FORMAT( '-', 3X,'TRANSMISSION LINE SERIES CAPACITIVE REACTANCE OF'
     2,F8.4,1X,'P.U. PER PHASE,EQUALS ',F4.2,1X, 'TIMES TOTAL CIRCUIT IN
     3DUCTANCE.' ,/,4X, 'TOTAL CIRCUIT IMPEDANCE = ',F8.4,1X,'+',1X,'J('
     4, 1X, F9.4,1X, ') P.U.' )
      RETURN
C- - - - - - - - - - - - -- - - - - - - -- - - - - - - - - - - -  -- -- - -
      ENTRY MSTART
      WRITE(6,250)
 250  FORMAT('-',40X,'STARTING PERFORMANCE OF A 3-PHASE INDUCTION MOTOR'
     2 )
      CALL PLANT( T, XY, XDOT )
      RETURN
C - - - - - - - - - - - - - - - - - - - - - - - - - - - - - - - - - - -
      ENTRY RITE
      AIMI= AIMAG(IMOT)
      RIM= REAL(IMOT)
      IMRMS= SQRT( RIM*RIM + AIMI*AIMI )
      RV= REAL(UMOT )
      AIV = AIMAG( UMOT )
      VRMS= SQRT( RV*RV + AIV*AIV )
      CVFEED = UBUS - IMOT*ZC
      ACVF = AIMAG( CVFEED )
      RCVF= REAL( CVFEED )
      VFEED = SQRT( RCVF*RCVF + ACVF*ACVF )
      TEM3 = TEM*3.0
C
```

Table E.1 Continued

```
      TVA= VRMS*IMRMS
      TPOW= RIM*RV + AIMI*AIV
      TPF= TPOW/TVA
      BVA= URMS*IMRMS
      BPOW= URMS*RIM
      BPF= BPOW/BVA
      WRITE(6,301)T,VRMS,SLIP,SPEED,TEM,TLM,TEM3,IMRMS,VFEED   ,
     2 BVA,BPOW,BPF,   TVA,TPOW,TPF
  301 FORMAT( F7.3,14F8.3)
      II=II+1
      X(II)=T
      A(II,1)=VRMS
      A(II,2)=SLIP
      A(II,3)=SPEED
      A(II,4)=TEM
      A(II,5)=IMRMS
      RETURN
      END
C  - - - - - - - - - - - - - - - - - - - - - - - - - - - - - - - - - - -
C
      SUBROUTINE PLANT( TDUM, V, YDOT )
      DIMENSION V(6),YDOT(6)
      REAL L1,L2,L3,LM,L11,L22,L33,LAMDA,LAMDAR,IMRMS,IMINST,LC
      COMPLEX UBUS, UMOT,IMOT,ZC,ZMOT,ZMAG,ZLEAK,CMPLX,CAIL,ZL
      COMMON/BL1/SQ2,SQ3,DEG,RAY,XY(6),XDOT(6), ACF,WZ,PAI,SUD1,SUQ1
      COMMON/BL4/ T,DELT,LINES, L,N,TFINAL,NDIFF,II
      COMMON A(100,10),X(100),Y(100)
      COMMON/BL5/R1,X1,RM,XM,TX1,TX11,T1,T11,POLES,F, PHASE,HM,
     2  LAMDA,LAMDAR,RC,XC,R2,X2,R3,X3,TLM,TEM,URMS,SPEED
      COMMON/BL6/ TACM,SLIP ,TL0,TL2
      COMMON/BL9/  UBUS, UMOT,IMOT,ZC,ZMOT,ZMAG,ZLEAK,RMOT,XLEAK,ZL
      RMOT= R1+ R2/SLIP
      ZLEAK= CMPLX( RMOT,XLEAK)
      ZMOT= ZMAG*ZLEAK/(ZMAG+ ZLEAK)
      IMOT= UBUS/(ZL+ ZMOT)
```

Table E.1 Continued

```
      UMOT= UBUS- IMOT*ZL
      CAIL = UMOT/ZLEAK
      RAIL = REAL(CAIL)
      AIAIL= AIMAG(CAIL)
      AILEAK= SQRT( RAIL*RAIL + AIAIL*AIAIL )
      TEM=  AILEAK*AILEAK*R2/SLIP
      SPEED= V(1)/WZ
      TLM = TL0 + TL2*SPEED*SPEED
      TACM=  TEM -TLM
      YDOT(1)= ACF*TACM
      SLIP = 1.0- SPEED
      RETURN
      END
C - - - - - - - - - - - - - - - - - - - - - - - - - - - - - - - - - - - -
C
      SUBROUTINE INTEG(T,DELT,N,X,YDOT  )                              MAIN0010
C     FIXED KUTTA MERSON OVERRIDING THE VARIABLE TIME STEP             MAIN0020
      DIMENSION  X(6), YDOT(6), XN(6)
      DIMENSION FK1(8), FK2(8), FK3(8), FK4(8),  FK5(8)
C     N IS LIMITED BY CORE STORAGE AND IS THE NUMBER OF DIFFERENTIAL EQNMAIN0050
      DELT2=DELT/2.                                                    MAIN0060
      DELT3=DELT/3.                                                    MAIN0070
      CALL PLANT(T, X , YDOT )                                         MAIN0080
      DO 10 M=1,N                                                      MAIN0090
      FK1(M)=DELT3*YDOT(M)                                             MAIN0100
      XN(M)=X(M)+FK1(M)                                                MAIN0110
 10   CONTINUE                                                         MAIN0120
      T3=T+DELT3                                                       MAIN0130
      CALL PLANT(T3, XN, YDOT )                                        MAIN0140
      DO 20M =1,N                                                      MAIN0150
      FK2(M)=DELT3*YDOT(M)                                             MAIN0160
      XN(M)=X(M)+(FK2(M)+FK1(M))/2.                                    MAIN0170
 20   CONTINUE                                                         MAIN0180
      CALL PLANT(T3, XN, YDOT )                                        MAIN0190
      DO 30 M=1,N                                                      MAIN0200
```

Table E.1 Continued

```
      FK3(M)=DELT3*YDOT(M)                                                    MAIN0210
      XN(M)=X(M)+(FK3(M) *9.+3.*FK1(M))/8.                                    MAIN0220
   30 CONTINUE                                                                MAIN0230
      T2=T+DELT2                                                              MAIN0240
      CALL PLANT(T2, XN, YDOT )                                               MAIN0250
      DO 40M=1,N                                                              MAIN0260
      FK4(M)=DELT3*YDOT(M)                                                    MAIN0270
      XN(M) = X(M) +( 3.*FK1(M) -9.*FK3(M) +12.*FK4(M) )/2.                   MAIN0280
   40 CONTINUE                                                                MAIN0290
      T=T+DELT                                                                MAIN0300
      CALL PLANT(T, XN, YDOT )                                                MAIN0310
      DO 50M=1,N                                                              MAIN0320
      FK5(M)=DELT3*YDOT(M)                                                    MAIN0330
   50 CONTINUE                                                                MAIN0340
      DO 60M=1,N                                                              MAIN0350
C                                                                             MAIN0370
      X(M)=X(M)+(FK1(M)+4.*FK4(M)+FK5(M))/2.                                  MAIN0380
   60 CONTINUE                                                                MAIN0390
      RETURN                                                                  MAIN0410
      END                                                                     MAIN0420
$ENTRY
  0.0      0.0       0.0        1.3      0.03     0.04       0.0
  4.0     60.0       3.0       1.0      -90.0     0.000      0.00
 0.025    2  2.2        0.0       0.0
 1
     0.0
//GO.FT14F001 DD DSNAME=&SM,UNIT=SCRTCH,DISP=(NEW,PASS),                      00000001
// SPACE=(800,(120,15)),DCB=(RECFM=VBS,LRECL=796,BLKSIZE=800)                 00000002
//SMPLTTR EXEC PLOT,PLOTTER=INCRMNTL,FORM=W                                   00000003
```

Table E.2. Equivalent parameters

Text	Computer Program
r_s	R1
r_r	R2
$\omega_b L_s$	X1
$\omega_b L_r$	X2
$\omega_b M$	XM
H	HM
$\overline{V}_{as}$	UMOT
$\overline{I}_{as}$	IMOT
$\overline{V}_{\infty}$	UBUS
S	SLIP
ω_b	WZ
ω_r/ω_b	SPEED
ω_r	XY(1) V(1)
$p\omega_r$	YDOT(1)
$\overline{I}_{ar}$	AILEAK

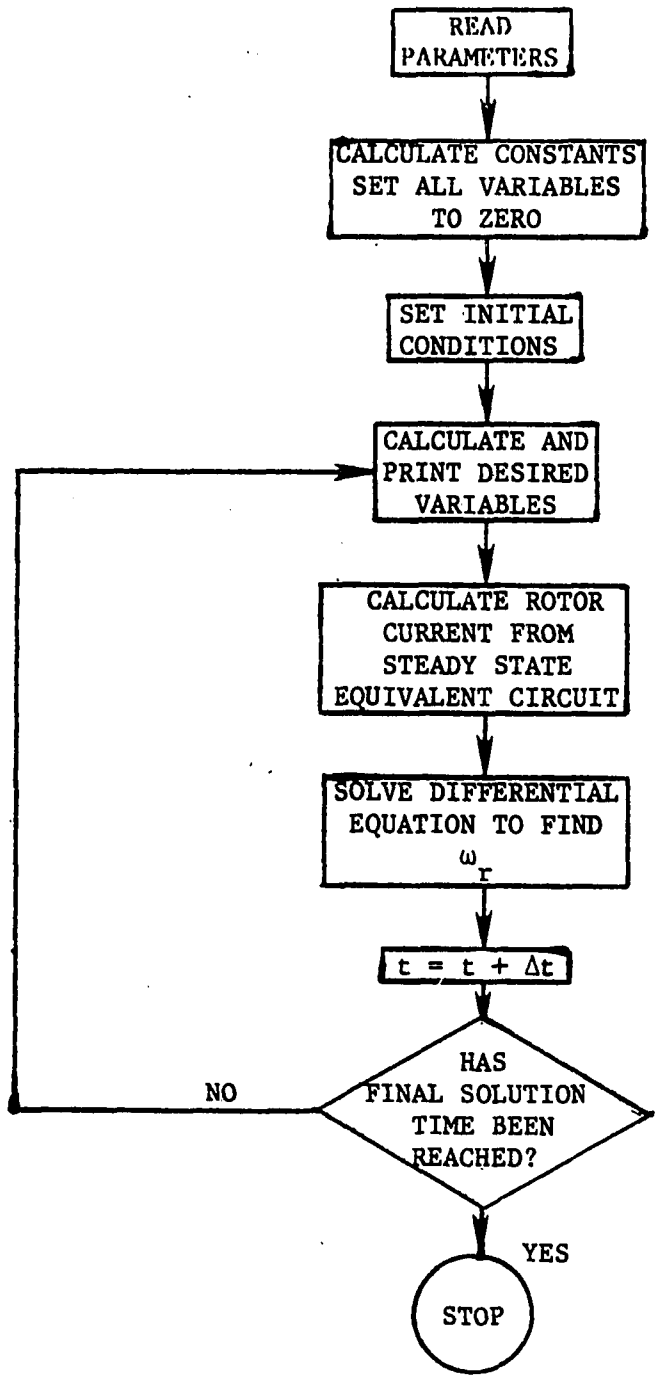

Figure E.1. Simplified flow chart of the reduced order model digital program

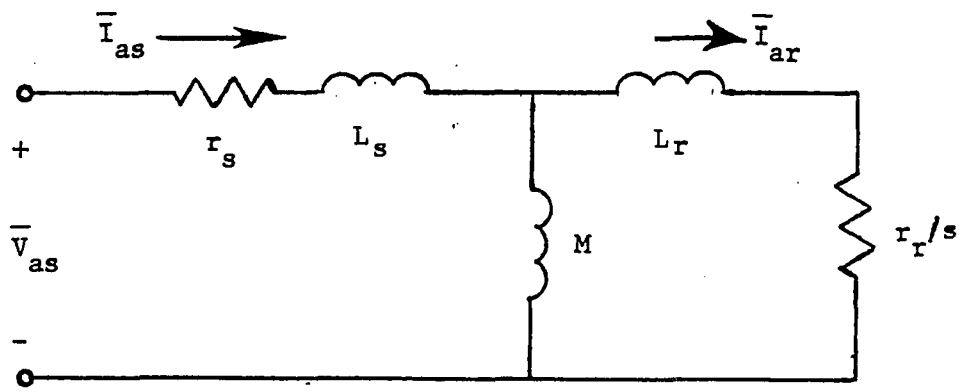

Figure E.2. The reduced order model equivalent circuit